Assessing the effectiveness of green stormwater infrastructure for addressing stormwater management goals at the watershed scale: application of the BACI design

Final Report to Chesapeake Bay Trust

Pooled Monitoring Program

Keith N. Eshleman, Ph.D.*[,1]
Trevor Frissell[2]
Briana Mentzer[3]
James Garlitz[3]

June 12, 2026

*Principal Investigator and corresponding author: e-mail: keshleman@umces.edu

[1]Professor, University of Maryland Center for Environmental Science, Appalachian Laboratory, 301 Braddock Road, Frostburg, MD 21532

[2]Formerly, Faculty Research Assistant, University of Maryland Center for Environmental Science, Appalachian Laboratory, 301 Braddock Road, Frostburg, MD 21532

[3]Senior Faculty Research Assistant, University of Maryland Center for Environmental Science, Appalachian Laboratory, 301 Braddock Road, Frostburg, MD 21532

Table of Contents

List of Acronyms and Abbreviations

A: area (watershed)
α: groundwater recession constant
BACI: before-after, control-impact
BF: baseflow (runoff)
BF_A: annual baseflow (depth)
BFC: baseflow coefficient
BFI_{max}: maximum baseflow index (parameter in RDF)
BMP: best management practice
C: concentration of a particular water quality constituent
CBT: Chesapeake Bay Trust
CFU: colony forming unit
C_i: concentration of a particular water quality constituent in the *i*th sample of an event
Cl: chloride
CMB: conductivity mass balance
C_n: concentration of a particular water quality constituent in "new" water
C_o: concentration of a particular water quality constituent in "old" water
CV: coefficient of variation
DON: dissolved organic nitrogen
DR: direct runoff
DRC: direct runoff coefficient
DPR: rainfall intensity, dual polarization product
D_S: disturbed surface area (of watershed)
E. coli: *Escherichia coli* (bacteria)
EL: event load of a particular water quality constituent
EMC: discharge-weighted event mean concentration of a particular water quality constituent
EPA: US Environmental Protection Agency
FBF: field bias factor (for areal rainfall estimation)
FIA: flow injection analysis
FIA-NO_3-N: nitrate nitrogen measured by flow injection analysis
G: gage height
GSI: green stormwater infrastructure
ha: hectares
HoCoG: Howard County (Maryland) Government
IC-NO_3-N: nitrate-N measured by ion chromatography
I_S: impervious surface area (of watershed)
ISA: impervious surface area
kg: kilograms
L: liters
LOADEST: load estimation model developed by USGS
mg: milligrams
mL: milliliters
N: nitrogen

NEXRAD: Next Generation Weather Rainfall
NH_4-N: ammonium nitrogen
NOAA: National Oceanographic and Atmospheric Administration
NO_2-N: nitrite nitrogen
NO_3-N: nitrate nitrogen
NSE: Nash-Sutcliffe efficiency (a goodness-of-fit criterion)
P: precipitation (depth) or phosphorous
P_E: design rainfall (depth)
PLBR: Plumtree Branch
PN: particulate nitrogen
PO_4-P: orthophosphate phosphorous
PP: particulate phosphorous
Q: stream discharge (units = volume per time)
Q_P: peak stream discharge
R: runoff (depth)
R_A: annual runoff (depth)
RDF: recursive digital filter
R_{Ei}: radar-estimated point rainfall (depth) for event *i*
R_{Gi}: gaged point rainfall (depth) for event *i*
SC: specific conductance (measure of conductivity)
SOC-P: soluble organic and colloidal phosphorous
SO_4: sulfate
t: time
TDN: total dissolved nitrogen
TDP: total dissolved phosphorous
TN: total nitrogen
TP: total phosphorous
TSS: total suspended solids
UCAR: University Corporation for Atmospheric Research
UMCES: University of Maryland Center for Environmental Science
USEPA: US Environmental Protection Agency
USGS: US Geological Survey
UTLP: unnamed tributary of the Little Patuxent River
WCT: Weather and Climate Toolkit

Executive Summary

The overarching objective of this research study was to monitor stormflow hydrology in a pair of contiguous, gaged research watersheds in suburban Baltimore, Maryland in order to quantify the integrated effectiveness of green stormwater infrastructure (GSI) in treating runoff from impervious surfaces. In the study design, one of the selected watersheds (the "treated" watershed) was considered "developing" since the monitoring occurred during a period in which suburban development was active, while the sister watershed (the "reference" watershed) was considered "developed" since most of the suburban development and land use change had occurred many decades prior to the study. The watersheds monitored during the study were: 1) Plumtree Branch (PLBR, the reference watershed): a 2.1 km^2 watershed that was mostly developed in the 1960s and 1970s and features the use of traditional gray stormwater infrastructure; and 2) an unnamed tributary to the Little Patuxent River (UTLP, the "treated" watershed): a 0.80 km^2 watershed that was partially developed in the 1990s and 2000s when more stringent stormwater management regulations were being put into effect in Maryland.

This report represents the culmination of two projects sponsored by Chesapeake Bay Trust (CBT). In terms of data collection, the first project involved stormflow and baseflow monitoring during two phases ("early" and "late") of active development and GSI implementation (2000 – 2003) in the UTLP watershed; results from that project were summarized by Eshleman (2023). The second project involved monitoring during the post-development phase (2023 – 2025) and this report was based on the integrated analysis of results from all three phases using methods appropriate for a "before-after, control-impact" (BACI) experimental design. Since the earlier project lacked a true "pre-development" period of data collection, data from the early phase of development (i.e., prior to the GSI being implemented) was used in its place for the statistical comparisons—particularly the development of linear regression models for predicting hydrologic and water quality metrics during the late and post phases of development and quantifying any "treatment effects" of GSI implementation.

During the two projects (5.5 years in duration), hydrologic metrics for 211 common discrete events at both watersheds were characterized using the field data and publicly-available radar rainfall data. This dataset includes detailed rainfall and runoff data for: 39 early phase events, 71 late phase events, 93 post phase events, and 8 snowmelt/rain-on-snow events; the snowmelt/rain-on-snow events were analyzed separately. Nearly one-quarter of the 211 common events characterized for hydrology were also characterized for water quality; overall, 1,903 streamwater samples (157 baseflow samples and 1,746 storm event samples) were collected and analyzed for 17 primary water quality constituents during the 5.5-year project. *E. coli* and total coliform bacteria levels were also characterized for 8 of the post phase events

(plus during baseflow conditions); a total of 157 discrete samples were subjected to microbial analysis.

We were able to develop statistically-significant BACI models for all six of the primary stormflow metrics (event areal rainfall; event runoff; event runoff coefficient; event peak runoff; event direct runoff coefficient; and event baseflow coefficient) using data for the early development phase. Despite the lack of data from a true "pre-development" period and the fact that a relatively small portion (~13%) of the watershed was disturbed during the most recent development, we were able to detect and quantify significant treatment effects of the GSI for five of the six metrics (all except areal rainfall). Importantly, the treatment results were numerically consistent—demonstrating very similar reductions (26 – 33%) between the post and early development phases for four of the five metrics; only event baseflow coefficient showed a statistically significant increase (52%) during the post development phase. The significant treatment effects were internally consistent and could be explained by hydrologic theory through use of a conceptual model. The results strongly support the interpretation that the primary treatment effect of the GSI is stormwater retention; in particular, the highly effective retention of stormflow produced from "new" impervious watershed surfaces by distributed GSI (i.e., bioretentions, dry wells) in the watershed was demonstrated. The fact that the reductions (~30%) are very close to the percentage change (38%) in the watershed area that was disturbed during the recent development also suggests that a very large percentage of the overland runoff produced by the new development is being retained by the GSI within the watershed. The impressive reduction in overland runoff from impervious surfaces can be explained by the fact that: 1) the bioretention cells were designed and built to infiltrate storms of much greater magnitude than those for which GSI in Maryland has historically been required to address; and 2) the bioretention outfalls were located at the edge of a protected forested floodplain, effectively buffering the stream from the effects of the outflows and providing an opportunity for re-infiltration and evapotranspiration.

We were also able to develop suitable BACI models for many of the water quality constituents (e.g., baseflow and stormflow concentrations and loads), but relatively few treatment effects of the GSI on water quality were detected. We did find significant treatment effects of the GSI on baseflow NO_3-N concentrations (positive effect, post phase only) and on the stormwater event load (*EL*) of NO_3-N (negative effect, late phase only), but no effects on stormflow NO_3-N event mean concentrations (*EMCs*) in either phase. These seemingly disparate results were reconciled using the same two-component mixing model that was used for chemical hydrograph separations. The results of the conceptual analysis strongly suggest a "new" source of NO_3-N in the UTLP watershed and the most likely candidates are 1) NO_3-N produced in the bioretentions and 2) lawn fertilizer N. We also found a statistically significant reduction in Cl for the late period using the BACI model (suggesting retention), but this effect also disappeared

during the post development period; the most likely reason is a source of watershed Cl from application of Cl-containing salts onto "new" roads, driveways, and sidewalks in the UTLP watershed.

As an alternative to the BACI design, we also estimated annualized loads for each of the 17 water quality constituents using statistical loading models that made use of the entire dataset for each watershed. A comparison of the relative (i.e., post phase to early phase) annualized loads between the two watersheds showed that NO_3-N, TN, and TDN loads increased at a higher rate at UTLP than at PLBR (where some of these loads actually decreased), but the opposite was true for all P-containing constituents except SOC-P. TDP and orthophosphate-P loads actually decreased slightly at UTLP, but increased considerably at PLBR. These results are qualitatively consistent with previous work by our team on highway bioswales in Maryland (showing high effectiveness in removing orthophosphate-P, but low or negative effectiveness in removing N—especially NO_3-N). Further, the results for all three suspended/particulate constituents showed lower rates of increase at UTLP than at PLBR (i.e., in the case of both PP and PN) or an actual decrease in load (in the case of TSS)—reflecting the effects of completing the conversion of the disturbed area of the UTLP watershed to suburbanized development (with GSI) on erosion and sediment concentrations.

The LOADEST model also proved useful in estimating loads and streamwater concentrations of *E. coli* in the two watersheds. Observed concentrations in baseflow and stormflow during the post development phase ranged from 2 – 44,000 (geometric mean = 300) CFU/100 mL at UTLP and 29 – 58,000 (geometric mean = 1,500) CFU/100 mL at PLBR. The modeling results for UTLP produced considerably fewer monthly exceedances of EPA's recommended *E. coli* criteria than the results for PLBR—although the exceedances typically occurred during the summer months when any recreational use would likely be higher. The results are directionally consistent with the idea that *E. coli* levels can be attenuated by GSI, but the lack of "pre-development" *E. coli* data precludes us from drawing that conclusion.

Overall, our water quality results represent a cautionary note that GSI is not a panacea; in fact, data from this study and from a related study of bioswales on Maryland highways (Eshleman et al. 2025) suggest that the term "bioretention" may be a misnomer. While there is strong evidence for <u>hydrologic</u> (i.e., physical) retention of some aquatic pollutants (e.g., NO_3-N, Cl) in the current study and for <u>chemical</u> retention of another important pollutant (PO_4-P) in the latter study, we have been unable to provide empirical evidence for biological retention of any of these (or other) water quality constituents. These findings are not unique, as many other experimental studies have demonstrated strong retention of PO_4-P through chemisorption onto soil clay particles and minimal (or negative) retention of NO_3-N in bioretention cells.

Introduction

Urban stormwater runoff is a world-wide hydrological problem with both water quantity and water quality impacts, particularly in the Chesapeake Bay watershed (Chanat and Yang 2018). It has only been about three decades since the earliest studies of urban stormwater runoff were published and efforts to mitigate stormwater impacts were first initiated primarily by local and state governments (Prince George's County 1999). Traditionally, stormwater management in the U.S. and other countries has been treated as a "routing" problem by civil engineers. The types of hardened "gray" infrastructure (e.g., concrete curbs and gutters, inlet boxes, storm sewers, etc.) designed and used to manage "rainfall excess" from impervious urban landscapes reflected a goal of conveying stormwater off of the land surface and into receiving water bodies at a rapid rate in order to minimize urban flooding (Roy et al. 2008). Stream ecologists in the latter part of the 20th century gradually began to understand that the rapid conveyance of stormwater into receiving streams and rivers was contributing to other problems downstream, however, as natural channels were effectively being forced to frequently convey discharges that might have occurred very rarely—if ever—prior to urbanization. The resultant stream geomorphological and ecological changes (scouring, gullying, sedimentation, habitat degradation, etc.) commonly associated with altered hydrology have come to be seen as symbols of traditional stormwater management gone awry (i.e., the "urban stream syndrome"; Walsh et al. 2005)—precipitating a search for a "cure", namely "greener" stormwater best management practices (BMPs) that might effectively mitigate these and other hydrological impacts of urbanization.

Modern urban stormwater management is an effort to incorporate structural and non-structural components (i.e., BMPs) onto the urban landscape that can effectively diminish the "*routing hyper-efficiency*" that is an inherent characteristic of impervious (and low pervious) surfaces and traditional stormwater management features; such practices are commonly lumped into the category of green stormwater infrastructure (GSI) that includes swales, retention ponds, detention basins, infiltration basins, permeable pavements, and various types of bioretention facilities (e.g., rain gardens, biofilters, bioswales, etc.; Fan et al. 2017). The distinguishing feature of all types of GSI is that *water storage* (i.e., transient detention or quasi-permanent retention of "rainfall excess" on or below the land surface through soil infiltration, permeation, and evaporation) is promoted. In the case of new development, the principal goal of GSI is often to maintain the hydrological behavior of the landscape in its original, pre-development condition. In the case of legacy development, GSI implementation usually takes the form of retrofits such as highway bioswales in Maryland (Eshleman et al. 2025). Secondary objectives in employing GSI include maintaining (or improving) water quality by reducing loads of stormwater pollutants—most commonly through the use of spatially-distributed bioretention facilities that promote infiltration across a watershed. Enhancing infiltration often

has the effect of promoting interactions between percolating water and soil media—thus providing opportunities for biological reactions (e.g., plant uptake, denitrification, etc.) and chemical reactions (e.g., sorption) that can provide either permanent or temporary sinks for pollutants of concern (Shetty et al. 2018).

It is reasonably well-accepted that the primary objectives of GSI as they pertain to stormwater management are essentially four-fold: (1) protection of receiving surface waters from nonpoint source pollution; (2) attenuation of stormwater discharge peaks (including increasing hydrologic lag times), (3) diminishment of stormwater runoff volumes; and (4) enhancement of the recharge/discharge behavior of shallow groundwater sustaining stream baseflow (Davis et al. 2009). While a reasonably extensive literature has rapidly evolved to quantify the effectiveness of individual urban stormwater BMP facilities in achieving these stormwater management objectives at the site scale (Dietz 2007, Barrett 2008, Liu et al. 2014, Kratky et al. 2017), there have been only a handful of carefully-designed experimental studies that have demonstrated the effectiveness of contemporary urban stormwater BMPs at the *watershed scale* (Rose and Peters 2001, Hood et al. 2007, Selbig and Bannerman 2008, Bedan and Clausen 2009, Schuster and Rhea 2013, Loperfido et al. 2014, Jarden et al. 2016, Walsh et al. 2022, Smith et al. 2023). The cited studies have addressed this problem at only seven different urban locations in the U.S. (Atlanta GA, Waterford CT, Cross Plains WI, Cincinnati OH, Washington DC metro area, Parma OH, Columbus OH) and none of these studies addressed all four stormwater management objectives.

A common design feature apparent in all seven studies is the comparison of the observed hydrologic responsiveness of one or more watersheds with extensive GSI vs. one or more watersheds developed using traditional stormwater management practices. Four of the cited studies (Bedan and Clausen 2009, Schuster and Rhea 2013, Jarden et al. 2016, Smith et al. 2023) employed the well-accepted “before-after, control-impact” (BACI) design in which the actual observed impacts following development/treatment are quantified relative to predicted impacts based on a pre-development calibration with a control system—thus allowing for explicit tests of *causality* as the method effectively corrects for year-to-year differences in precipitation and other hydroclimatic variables. The other four studies relied on designs that attempted to “control” for non-impact related response differences through careful watershed selection.

The BACI experimental design has been widely employed in long-term paired-catchment studies where the goal is usually to detect and ascribe post-treatment changes to a particular type of treatment (Webster et al. 2022, Wondzell et al. 2025). Most commonly, these paired-catchment studies have been used to address the effects of forest harvesting on runoff (e.g., Hornbeck et al. 1970, Bosch and Hewlett 1982, Harr et al. 1982), but studies have also

addressed effects on water quality (Likens et al. 1970), water temperature (Moore and MacDonald 2024), and sediment transport (Bormann et al. 1974). While the number of paired-catchment studies addressing the hydrologic effects of urbanization is comparatively low, results from these studies have revealed that incorporating GSI into development plans typically results in reduced peak discharges and flood volumes and increased lag times *relative to* traditional development/stormwater management practices. Only two of the seven studies (Bedan and Clausen 2009, Smith et al. 2023) were able to address the effectiveness of using GSI to achieve water quality goals (again, relative to traditional stormwater management), so another comprehensive study that considers both water quality and quantity at the watershed scale would provide a useful and timely addition to the literature.

Study Design, Research Objectives & Hypotheses

The overarching objective of this research study was to monitor stormflow hydrology in a pair of contiguous, gaged research watersheds in suburban Baltimore, Maryland in order to quantify the integrated effectiveness of green stormwater infrastructure (GSI) in treating runoff from impervious surfaces. In the study design, one of the selected watersheds was considered "developing" since the monitoring occurred during a period in which suburban development was active, while the sister watershed was considered "developed" since most of the suburban development and land use change had occurred many decades prior to the study. The developing watershed was thus considered to be the "experimental" or "treated" watershed, while the "developed" watershed was treated as a "control" or "reference" system for reducing extraneous variations (e.g., due to hydro-climatological conditions) as much as is reasonably possible (Wondzell et al. 2025). The study design was meant to capture the changes in stormwater responses during and after the period in which the GSI was implemented. It should be recognized that, since suburban development often occurs incrementally throughout a watershed, it is very possible that the roles (i.e., "treated" vs. "reference") of these two watersheds in a particular BACI design could have been reversed at another time in the past.

A set of testable hypotheses was clearly stated prior to implementing the research:

1. For each stormflow response variable of interest, a statistically-significant linear relationship can be found between the observations for the "treated" watershed and the observations for the "reference" watershed during a calibration period prior to the treatment (i.e., in this case prior to implementing the GSI). The stormflow response variables of interest include the following:
    - Event runoff (volume)
    - Event peak runoff
    - Event runoff coefficient

- Event direct runoff coefficient
- Event baseflow runoff coefficient
- Event mean concentrations (17 water quality constituents including total suspended solids, conductivity, major anions, total N, total P, and dissolved/particulate forms of N and P)
- Event loads (of the same 17 constituents)

2. Assuming that such statistically significant linear relationships can be found for the stormflow response variables of interest for the calibration period, predicted responses for the treated watershed during post-treatment periods should be statistically different from the observed responses—reflecting on-the-ground "treatment effects" of the GSI treatment.
3. Differences between predicted and observed mean stormflow responses scale linearly with the watershed area being treated.
4. Following treatment, statistically significant differences in stormflow response variables between the watersheds would be also evident in the data.
5. Bioretention can also be shown to reduce streamwater chloride levels attributed to the application and wash-off of road deicing salts, as well as *E. coli* and total coliform bacteria levels.

Study Sites

Two contiguous suburban Baltimore (Maryland, USA) watersheds located in north-central Howard County, Maryland were identified and deemed suitable for assessing the effectiveness of GSI treatment of stormwater runoff: 1) Plumtree Branch (PLBR, the reference watershed): a 2.1 km^2 watershed that was mostly developed in the 1960s and 1970s and features the use of traditional gray stormwater infrastructure; and 2) an unnamed tributary to the Little Patuxent River (UTLP, the treated watershed): a 0.80 km^2 watershed that was partially developed in the 1990s and 2000s when more stringent stormwater management regulations were being put into effect in Maryland (Figure 1). Importantly, new suburban residential development of a significant portion of the UTLP watershed was already underway at the time (February 2020) it was selected as the treated watershed for this project; prior to monitoring, a 0.09 km^2 tract of forested land in the southwestern corner of the watershed had been cleared. The tract had been graded and surrounded with double silt fencing to control erosion and sedimentation; sediment traps had also been installed throughout the cleared section at this point in time. These traps would later be converted into bioretention facilities as development was completed. Several townhomes had also been completed and several other buildings were

under construction; all of the roads in the development had been constructed, but only a section of one road had been paved by this time. Permanent stormwater infrastructure had yet to be installed. Residential development in the UTLP watershed would continue through summer 2023 when all of the planned stormwater infrastructure—including 22 bioretention cells and about 50 dry wells—would be fully operational. The progressive development and implementation of the GSI in the UTLP watershed is illustrated in Figure A-1.

Stormwater monitoring in the PLBR watershed commenced in November 2019, but did not begin until March 2020 in the UTLP watershed. Given the fact that development was well underway by the time that monitoring began, there is no true "pre-development" period for calibrating responses between the two watersheds. For this reason, data from the one-year period from April 2020 through March 2021—representing the "early phase" of development in which permanent stormwater facilities were not operational—was used for calibration. A "late phase" of development (2.5-year period from April 2021 through September 2023) was defined as the period during which the stormwater infrastructure gradually became operational. Stormwater monitoring during the early and late phases of development was supported by a separate grant from Chesapeake Bay Trust (CBT) Pooled Monitoring Program; results from that project were summarized in a separate report to the sponsor (Eshleman 2023). During the two-year "post phase" of development (October 2023 through September 2025) supported by the current CBT grant, all stormwater infrastructure was fully operational. As discussed below, identical stormwater monitoring occurred throughout the entire 5.5-year study period in both watersheds, so data collected in the prior development phases was combined with the recent data to provide an integrated analysis using the BACI design.

Based on analysis of annual high-resolution aerial photography for the two watersheds, total imperviousness (18.9%) was determined to be stable in the PLBR watershed throughout the study period (although new suburban development of a ~0.11 km^2 tract in the northwestern quadrant of the watershed began in late 2024). In the UTLP watershed, total imperviousness increased from 12.4% in 2020 to 16.1% in 2023 (an increase in impervious surface area of about 30%), while the disturbed area decreased by about 36% over this time period (Figure 2).

Field Hydrologic Methods

Stream discharge ($m^3 s^{-1}$) from both watersheds was measured at the watershed outlets using standard gaging methods recommended by U.S. Geological Survey (Rantz et al. 1982). A corrugated, galvanized steel stilling well with steel plate bottom and 5 cm dia. intake pipe was installed in the streambank at each site to facilitate continuous 5-min water level measurements using a digital recorder (Unidata model 6541-21/C) housed in an instrument shelter bolted onto the top of the well. Recorder readings were checked against a staff gage at least once per month. Manual wading streamflow measurements (mid-section method) were

made periodically using a top-setting rod and an electromagnetic current meter (Marsh-McBirney, Inc. “Flo-Mate” model 2000) to establish a rating curve for each station (and for adjusting the curve to reflect channel shifts due to scouring or sedimentation, if necessary; Figure 3). In addition to frequent baseflow measurements, wading measurements were made during flood events to capture the upper end of the rating curves for these flashy watersheds. A sonde (In Situ Aqua TROLL 500) was used to provide 5-min water level, temperature, turbidity, and conductivity data from each monitoring station. Re-calibration of the sonde occurred on a monthly basis.

Point rainfall (mm, 15-min data) was monitored at two fixed stations using unshielded tipping bucket gages (Isco model 674). Both rainfall stations were situated in the U.S. Rte. 40 median near (but outside) the watersheds. Rainfall data were recorded using an interface module (Isco model 2105) powered by a 12V car battery and solar panel charger and downloaded periodically. The station nearest to the watersheds (“Kappa”: 39°16'40.9"N 76°50'26.3"W) was operated throughout the entire study, while a second station (“Delta”: 39°17'41.8"N 76°54'01.0"W) was operated until July 30, 2024 (when the equipment was destroyed in a motor vehicle accident).

Baseflow “grab” samples were collected on a monthly basis at each watershed outlet using pre-cleaned, acid-leached, 1L polypropylene bottles. Stormflow samples were collected during selected rainfall (and snowmelt) events using an automatic sequential sampler (Sigma model 1350) programmed to collect 24 1L samples at a pre-selected frequency dependent upon the expected duration of stormflow runoff; most commonly, stormflow was sampled at a frequency of one sample per hour, one sample per 1.5 hours, or one sample per two hours, but snowmelt event samples were typically collected at a frequency of four or six samples per day. All water samples were placed on ice (4°C) as soon as possible and transported to the analytical laboratory for processing; samples were typically processed within 24 hours of collection, but some stormflow samples could only be processed within 48 hours of collection. In some cases, samples were collected unnecessarily (e.g., when forecasted rainfall never arrived), while in other cases “extra” baseflow samples were collected for the event prior to the arrival of rainfall. In each these situations, the extra samples were not processed and analyzed. In other cases, sampling had to be extended beyond the 24 samples (e.g., to capture the recession limb of the hydrograph); in these situations, the “extra” samples were considered to be part of the same event and were processed identically. Overall, 1,903 streamwater samples (157 baseflow samples and 1,746 storm event samples) were collected and analyzed during the 5.5-year project. Event rainfall samples were also obtained using a bulk funnel collector over a three-year period primarily in support of a sister project focused on nitrate isotopes.

Laboratory Methods

Water samples were analyzed using standard analytical methods within appropriate holding times. At the time of processing, an aliquot of each well-mixed water sample was poured off and frozen for later digestion and analysis of total N (TN) and total P (TP) using a Lachat flow injection analyzer (FIA, method 4500-P (J); APHA 2017). A second aliquot was used for measuring conductivity (method 300.1; USEPA 1993). A third aliquot was filtered (Whatman GF/F) for determination of total suspended solids (TSS; method 160.2; USEPA 1993). Aliquots of the filtrate of each sample were preserved for later determination of major anions (Cl^-, NO_3^-, and SO_4^{2-}) by ion chromatography (method 300.1; USEPA 1993), total dissolved N (TDN) and total dissolved P (TDP; method 4500-P (J); APHA 2017), and dissolved nutrients (i.e., NH_4-N, NO_2-N + NO_3-N, NO_3-N, and PO_4-P) using FIA methods (Fishman 1993; USEPA 1993). Dissolved organic N (DON) was computed as the difference between TDN and the sum of NH_4-N, NO_2-N, and NO_3-N; soluble organic and colloidal P (SOC-P) was computed as the difference between TDP and PO_4-P. Particulate N (PN) and particulate P (PP) were computed as the difference between TN and TDN and TP and TDP, respectively. Finally, *E. coli* and total coliform bacteria levels were determined on selected (n = 157) water samples using the Colilert® method (No. 9223 B; APHA 2017); all samples used for *E. coli*/total coliform analysis were incubated for 24h beginning within 24h of sample collection.

Data Analyses

Water balances

Point rainfall (15-min data, "Kappa" station) and 5-min runoff data for the two study watersheds were used to generate continuous records of daily, monthly and annual rainfall and runoff from which annualized water balances for the three development periods were computed; runoff ratios were computed from the annualized rainfall and runoff data. Annualized runoff was compared with data obtained for five subwatersheds within the Patuxent River basin gaged by U.S. Geological Survey for the same time periods; daily streamflow data were downloaded (https://waterdata.usgs.gov/state/Maryland/), integrated, and converted into common units (mm y^{-1}).

Event hydrologic analyses

Stormflow events in the hydrologic record were identified manually—typically on a monthly basis as rainfall and runoff data were downloaded from the field recorders. The objective of the workflow was to identify all major stormflow-producing events that occurred in either (or commonly both) of the two study watersheds. Typically, the events were identified first (as peaks) using the runoff data, then confirmed using the point rainfall data. Since both watersheds responded very quickly to intense rainfall pulses, it was very straightforward to determine the timing (i.e., beginning) of both event rainfall and event runoff for each event.

More than 200 rainfall-runoff events were characterized (Tables E-1 – E-3). Interestingly, two other "events" in 2023 at PLBR occurred without any rainfall; the first event in May was due to a confirmed water main break that released over 4,600 m^3 (>1.2 x 10^6 gal) of water into PLBR over a 27-h period. A second smaller unconfirmed "event" (~330 m^3 = 90,000 gal) in October was of similar duration, but was more likely due to an illicit discharge (e.g., from a neighborhood swimming pool).

Event areal rainfall. A more difficult task was quantifying event areal rainfall, since it quickly became apparent that spatially-variable rainfall was a more common feature in this area than was originally expected (or desired!). For this reason, NEXRAD WSR-88D Level III radar rainfall intensity data (dual polarization, DPR) from the nearest station (Sterling, Virginia, station LWX) for each day of each event were ordered and downloaded from archives on one of two different servers (i.e., NCEI: https://www.ncei.noaa.gov/nexradinv/); or THREDDS: https://thredds.ucar.edu/thredds/catalog/nexrad/level3/DPR/LWX/catalog.html) using the NOAA Weather and Climate Toolkit (WCT). Unadjusted event areal rainfall for the two watersheds was directly computed by numerical time-integration of the DPR time series. The actual method made use of the WCT "point subset tool" to estimate rainfall for the two point gage stations, as well as for 16 "pseudo-stations" located within the two watersheds. Each of these stations includes a polygon "weight" for converting the individual point rainfall amounts for each pseudo-station into an event areal rainfall depth for each watershed (sum of weights = 1). The next step was to compute a mean event field bias factor (*FBF*) from the actual point measurements and the NEXRAD-estimated rainfall at the two stations: $FBF_i = \Sigma R_{Gi}/\Sigma R_{Ei}$ where FBF_i is the field bias factor for event *i*, R_{Gi} are the gaged point rainfall depths for event *i*, and R_{Ei} are the NEXRAD-estimated depths for event *i*. The gage-adjusted event areal rainfall was computed by multiplying the (unadjusted) areal rainfall from the NEXRAD DPR time series by the appropriate *FBF*. Finally, the coefficient of variation (CV) of event areal rainfall was computed for each event in the database; only events with CV < 0.25 were used in paired (i.e., between-watersheds) analyses. Overall, 85% (n = 175) of 205 rainfall events met this criterion: 34 (of 40) events in the early phase; 63 (of 72) events in the late phase, and 78 (of 93) events in the post phase. Data from six snowmelt/rain-on-snow events were also excluded from paired analyses, since estimates of snowpacks were poor.

Event runoff. Event runoff (cm) was computed by time-integrating the 5-min stream discharge (m^3 s^{-1}) record for the duration of each event (and dividing by the respective watershed area).

Event runoff coefficient. The (dimensionless) event runoff coefficient was computing by dividing event runoff by event areal rainfall.

Peak event runoff. The peak event runoff (cm h^{-1}) was defined as the maximum mean hourly runoff value measured during a particular event (divided by the respective watershed area).

Direct runoff and baseflow runoff coefficients. Hydrograph separations were performed using two different methods: 1) the classical two-component, hydrochemical separation of storm hydrographs into pre-event (i.e., "old") and event (i.e., "new") water contributions (Sklash et al. 1976; Freeze and Cherry 1979); and 2) the recursive digital filter (RDF) approach of Eckhardt (2004) for separating hydrographs into direct runoff (DR) and baseflow (BF). For the hydrochemical separations, stream conductivity (i.e., 5-min specific conductance) and 5-min discharge data were used to compute instantaneous old and new water contributions for each storm event hydrograph; for simplicity, it was assumed that the conductivity of new water was 0 $\mu S\ cm^{-1}$ (although actual rainfall measurements suggested values in the range of 4 – 10 $\mu S\ cm^{-1}$). Given that the measured conductivity of pre-event water was typically around 600 $\mu S\ cm^{-1}$ at both stations, the separation results were virtually insensitive to this simplifying approximation (Figure B-1). Old and new water hydrographs were time-integrated to produce one- or multi-day estimates of old and new water runoff (depending on event duration). An on-line version of Eckhardt's (2004) RDF (https://sephydro.hydrotools.tech/pageMain.php) was used to separate the multi-year hydrographs (daily data) with α (groundwater recession constant) values estimated directly for each watershed; BFI_{max} parameter values were optimized using the results of the hydrochemical separations by equating new water from the hydrochemical separation with DR in the RDF separation. DR and BF coefficients (i.e., *DRC*, *BFC*) were computed by dividing each value by the total runoff for the particular date or event period. For the PLBR watershed, the 1st 3.5 years of discharge data were used to calibrate the RDF, while the latter two years of data were used for RDF validation. For the UTLP watershed, hydrograph separation data were subdivided into the three development phases to test for differences in BFI_{max} between time periods.

Event mean concentrations and loads. A discharge-weighted event mean concentration (*EMC*) for each of the measured constituents was computed for each of the selected events for which stormflow samples were collected and analyzed:

$$EMC = \sum_{i=1}^{n} C_i Q_i / \sum_{i=1}^{n} Q_i \quad (1)$$

where C_i is the concentration of a constituent measured on the *i*th sample analyzed during a particular event; Q_i is the instantaneous discharge measured at the time that the *i*th sample was collected; and *n* is the total number of samples analyzed for the event. The event load (*EL*) was computed as the product of the *EMC* and event runoff (*R*). Of the more than 200 events that were hydrologically characterized during the 5.5-y study, *EMCs* and *ELs* were computed for 51 events that had also been characterized for water quality at both sites (Tables E-4, E-5); of these events, seven were snowmelt/rain-on-snow events and six others did not meet the CV of rainfall criterion—leaving 38 rainfall-driven events for performing paired *EMC* and *EL* comparisons (early period: 8 events; late period: 14 events; post period: 16 events).

Annualized constituent loads. Aggregated constituent loads for the PLBR and UTLP watersheds for the three development periods were estimated using either LOADEST (Cohn et al. 1989; Runkel et al. 2004) or a simpler "C-Q" rating curve model (e.g., Crawford 1991). For LOADEST, estimates were based on the use of complete hourly input files (i.e., instantaneous concentrations and discharge) followed by aggregation of hourly loads to annualized values; constituent models with a positive efficiency (i.e., *NSE* > 0, Nash and Sutcliffe 1970) and bias percentages within the range of ±25% were deemed acceptable. For each constituent for which an acceptable LOADEST model could not be obtained for either watershed, linear regression of constituent concentrations and mean daily discharge values was used to produce a concentration time series from which loads could be readily simulated. The concentration file used in the regression was created from the raw concentration data files by combining monthly baseflow values with discharge-weighted mean concentration values for dates for which multiple stormflow samples had been analyzed; loading model *NSE* values were computed. More details on the load modeling component of the study can be found in Appendix C.

Statistical analyses

The sets of paired events for the three development phases were considered to represent samples of independent observations that could be used to test the hypotheses using parametric statistics. After testing data for normality (i.e., Kolgomorov-Smirnov tests), differences in (mean) response variables among the three time periods were evaluated using t-tests. Linear regression was used to develop predictive BACI models for the stormflow response variables using data from the early phase of development; statistically-significant regression models were then used to make predictions of stormflow responses for the UTLP watershed for both the late and post phases of development (i.e., using the PLBR stormflow data as the independent variable). The BACI model for event peak runoff was developed using log-transformed data. Paired t-tests were used to test for differences between the predicted and observed values (i.e., to quantify a "treatment effect"), as well as for comparing PLBR and UTLP responses within each of the three phases. Statistical significance was determined using a $P \leq 0.05$ criterion for every test. The same general BACI approach was also applied to the discharge-weighted *EMC* and *EL* datasets, as well as to the baseflow water quality data.

Results

Annualized runoff values for the PLBR watershed during the three study periods (from integration of hydrographs shown in Figure D-1) were similar to the range of runoff for five USGS-gaged Patuxent River subwatersheds. Data from the latter subwatersheds suggest a consistent pattern that might be explained by differences in precipitation, local hydrogeology, land use, or a combination of these factors. In both the early and late development periods, the annualized runoff from the PLBR watershed (445 mm y^{-1} and 325 mm y^{-1}, respectively) was

virtually identical to runoff from the Cattail Creek watershed, while PLBR runoff in the post development period (463 mm y^{-1}) was closer to runoff from the Little Patuxent River at Guilford, MD station (451 mm y^{-1}). Obviously, the late period of the project was, on average, much drier than either the early or post development periods. Over the entire 5.5-y study period, runoff and precipitation for PLBR were 2,185 (397 mm y^{-1}) and 5,600 mm (1,018 mm y^{-1}), respectively; the runoff ratio was 0.39. These values are 6.6% and 13% lower than estimated normal annual runoff (457 mm; MDE 2026) and precipitation (1,090 mm; Krug et al. 1990) for Howard County (MD), respectively. The computed runoff ratio (0.39) was slightly lower than the normal value (0.42) based on the long-term data, likely reflecting drier than normal conditions. Runoff from the UTLP watershed (based on integration of the data presented in Figure D-2) was consistently lower than that of any other watershed in the group, however; the 5.5-y runoff was 1,335 mm with an annual runoff ratio of 0.24 (Figure 4).

A BFI_{max} value of 0.675 produced excellent agreement between DR from the RDF separation and new water from the hydrochemical separations for PLBR (Figure 5). For the 3.5-year calibration period, a regression model had slope of 0.97 and R^2 of 0.96; for the 2-year validation period, the calibrated model had a slope of 0.99 and R^2 of 0.95 (not shown). Similarly, using BFI_{max} = 0.750 for UTLP, regression models for the early, late, and post-development phases had slopes of 0.95, 1.01, and 1.02, respectively; R^2 values were 0.98, 0.99, and 0.99, respectively (not shown), suggesting that a single calibrated RDF can produce acceptably robust results across the entire study period despite the watershed changes that occurred. The overall slope is 1.00 with an R^2 of 0.99 (Figure 6). The annualized BF index value (i.e., BF_A/R_A, computed from the long-term data presented in Figure D-3) for UTLP (0.433) was slightly (~7%) lower than the comparable value for PLBR (0.464, computed from data shown in Figure D-4) during the early development period. The value for UTLP was much (~34%) higher during the drier late development period and somewhat (~8%) higher during the post development phase (Figure 7)—presumably reflecting the completion of the GSI.

While some variations in hydrologic response metrics were apparent in the PLBR data across the three time periods, the only statistically significant differences in mean values were found for the event runoff coefficient which was lower in the early phase (0.22) compared to the other two phases (0.31, 0.32; Figure 8). This difference could be explained by: 1) a much lower frequency of events with maximum 1-h rainfall intensity less than 1 cm h^{-1}; 2) a lower frequency of events with event areal rainfall in the range of 1 – 2 cm; or 3) a lower frequency of events with runoff in the range of 0.5 to 1.0 cm during the early phase of the project; the hydroclimatologically-driven differences among the time periods for the PLBR watershed underscore the importance of developing and employing BACI models (Figure 9).

Regression models (UTLP vs. PLBR) for all six primary stormflow event variables (i.e., event areal rainfall, event runoff, event runoff coef., peak event runoff, event *DRC*, and event *BFC*) developed using data from the early development phase (n = 34) were statistically significant. Regression slopes ranged between 0.75 and 1.29; R^2 values ranged from 0.57 to 0.95. The utility of excluding those events with high event areal rainfall CV from the regression modeling is graphically illustrated (i.e., as "outlier" points; Figure 10). For the early phase of development, only mean values of event runoff, peak event runoff, and event runoff coefficient for UTLP were statistically different from PLBR based on paired-t tests; UTLP means were 27%, 32%, and 44% lower than the PLBR means, respectively. For the late and post phases of development, all variable means except event areal rainfall were statistically significant. Using the BACI regression models, predicted mean values for all stormflow variables except event rainfall were statistically different from the observed means for both the late and post development periods. For the post development period, mean observed event runoff from UTLP (0.44 cm) was 29% lower than the predicted mean value (0.62 cm) using the regression model; similarly, the mean observed event runoff coefficient for UTLP (0.15) was 33% lower than the predicted mean value (0.22). The (back-transformed) mean observed peak runoff value (0.019 cm h^{-1}) was 30% lower than the predicted mean value (0.027 cm h^{-1}), while the mean observed event *DRC* for UTLP was 26% lower. The only variable that exhibited a statistically significant increase relative to the predicted mean value was *BFC* (52%, Table 1).

At both stations, streamwater chemical concentrations were usually highly dynamic during the course of the sampled events; for most constituents, the largest changes relative to antecedent baseflow conditions occurred near the peak of the storm hydrograph. Intense rainfall producing the highest peak discharges was often accompanied by the most extreme (high or low) concentrations, depending on the constituent; baseflow recessions were accompanied by gradual returns of water quality to antecedent values. Moreover, the event concentration data revealed dynamic patterns that persisted among the various events. A few constituents (e.g., Cl, SO_4, SC, and NO_3-N) typically exhibited negative chemodynamic behavior (i.e., dilution), while the others (including all P-containing constituents, all N-containing constituents except NO_3-N; and all particulate constituents) mostly showed positive behavior (i.e., concentration). The results for stormflow event "AE" (in response to about 2 cm of rainfall that occurred in early March of 2023) are fairly typical of the storms that were sampled during the study (Figures 12, 13). Although both SC and Cl displayed the typical dilution behavior during event "AE", both constituents were observed to increase during snowmelt events due to the application and wash-off of road deicing salts.

Although baseflow chemistry for all of the constituents was relatively stable throughout the entire project, statistically significant linear relationships (i.e., BACI models) between PLBR and UTLP concentrations measured during the early phase of development were identified for 10 of

the 17 constituents. When applied to the other periods, the BACI model for one constituent (TP) produced a significant difference between mean observed and predicted concentrations for UTLP for the late phase, while models for four other constituents (IC-NO_3-N, TN, TDN, and FIA-NO_3-N) produced significant differences for the post development phase. In each of the five cases, the observed mean concentration was higher than the mean predicted concentration, however. Since NO_3-N was the dominant component of both TDN and TN throughout the study, all of the post period results can be explained by slightly (i.e., ~15%) higher than predicted mean baseflow NO_3-N concentrations (Table 2).

Stormflow *EMCs* were considerably more variable between the two watersheds; mean *EMCs* for eight of the constituents were significantly different during the early phase. Significant BACI models were found for five constituents (i.e., SC, Cl, IC-NO_3-N, SO_4, and DON), but application of the models produced significant differences between observed and predicted means for UTLP for only two constituents (DON in the late phase and SO4 in the post phase; Table 3). Predictive *EL* regression models were found for 12 of the 17 constituents. Four of the models (SC, Cl, IC-NO_3-N, and FIA-NO_3-N) produced significant differences for the late phase, but only one model (SO_4) produced a significant difference for the post development phase (Table 4). With the exception of DON, all of the constituents for which significant treatment effects on either EMC or event load or both were found exhibited negative chemodynamic behavior.

One of the major limitations of the BACI design was the fact that significant BACI *EMC* and *EL* models could not be found for every key water quality constituent (e.g., TSS). As a way of getting around this problem, variations in annualized loads between the time periods and between the watersheds were used to assess overall water quality changes owing to the development sequence at UTLP. These loads effectively combine the baseflow and stormflow loads that were addressed separately. Due to the much lower runoff from both watersheds during the late phase of development (Figure 4), it is not surprising that annualized loads for every constituent were lower compared to both the early and post phases. Given the focus here on the role of land use change and GSI, the more interesting comparison is between the post and early phases; annualized runoff was also more comparable during these two periods than during the late phase.

One way of evaluating changes in loads at UTLP is to compare observed load ratios (post phase: early phase) and use the ratio for PLBR as the “expected” change in the absence of development. Interestingly, the PLBR post:early load ratio was higher for 10 of the 17 constituents modeled (all with ratios > 1.0) including all of the P constituents except SOC-P. The UTLP watershed post:early load ratio was higher for six of the constituents and all are N-containing constituents—a result that is directionally consistent with the baseflow results (Table 2). Perhaps not unexpected was the behavior of TSS among the phases of development

at UTLP. The PLBR load ratio "predicted" a 25% increase in TSS in the post development period, but the data actually show a 19% reduction as the temporary erosion and sediment controls (i.e., sediment traps, super silt fencing) were replaced with bioretention cells and the pervious land surfaces were ultimately revegetated; the estimated reduction in the annualized TSS load at UTLP is also directionally consistent with observed reductions in PP and PN relative to PLBR (Table 5).

Chloride *EMCs* for snowmelt/rain-on-snow events were significantly higher than *EMCs* for rainstorm events at both sites (by about a factor of five)—demonstrating clear, immediate water quality responses to road-salting in the watersheds; several other constituents (PO_4-P, TDP, and DON) showed the opposite response (results not shown). Yet no Cl treatment effect for the post development period was identified using the BACI regression approach (Tables 2 - 4). Therefore, to address the road deicing salt problem, we used: 1) LOADEST-generated annualized (water year basis) loads of Cl, 2) annual BF runoff from the hydrograph separations, and 3) mean BF Cl concentrations in each stream to estimate annual SF loads for each year of the study. Mathematically, the annual SF load was obtained as the difference between the total annual Cl load (from LOADEST) and the annual BF load (product of BF concentration and BF runoff). For water year 2020 (beginning April 1 after any snowmelt had ended for the water year), the stormflow load was essentially zero—so the results were able to be used to provide a check on the overall calculation. Results for PLBR showed that estimated annual SF Cl loads varied from -8 to 95 kg/ha, while BF Cl loads ranged from 102 to 259 kg/ha. Results for UTLP produced ranges from 7 to 67 kg/ha and 117 to 189 kg/ha for the BF Cl loads, respectively. For both watersheds, the lower value for the SF Cl load corresponded to the 2020 water year, while the highest BF and total Cl loads occurred in water year 2024 with the greatest amount of winter precipitation. With the exception of water year 2021, BF Cl loads (expressed as a percentage of the estimated total annual Cl load) were consistently higher at UTLP than at PLBR. The BF load dominated the total Cl load in both watersheds—averaging 77% and 69% for water years 2022-2025 at UTLP and PLBR, respectively (Figure 15 a, b). The final step in the computation involved expressing these loads per unit total impervious surface area (ISA), effectively normalizing the results to the relative area of potentially salt-treated surfaces within the watersheds. PLBR and UTLP SF Cl loads per unit ISA in 2020 and 2021 varied by less than 100 kg/ha, but a positive difference (PLBR – UTLP) became apparent in 2022 and persisted through water year 2025 (range of difference = 120 – 290 kg/ha; Figure 15c).

Baseflow *E. coli* concentrations ranged from 2 – 649 CFU/100 mL and from 29 – 2420 CFU/100 mL at PLBR and UTLP, respectively; highest concentrations were typically observed in the warmer periods of the year, and lowest concentrations during the coldest months. Stormflow *E. coli* concentrations ranged from 9 – 43,500 CFU/100 mL at UTLP and from 172 – 57,900 CFU/100 mL at PLBR (Figure 16). Since no *E. coli* samples were analyzed prior to the post phase

of development at UTLP, the BACI approach was not a viable option. The LOADEST model, however, produced satisfactory estimates of *E. coli* concentrations based on high R^2 values and slopes near unity (Figure 17); load statistics (R^2, *NSE*, and percent bias) were also deemed satisfactory: UTLP: 0.89, 0.48, and 76%, respectively; PLBR: 0.94. 0.72, and 51%, respectively. It should be noted that the LOADEST software generated the dreaded "skull and crossbones" warnings due to the fact that the percent bias was higher than the maximum acceptable value (±25%). Storm-by-storm comparisons of observed and modeled concentrations also showed reasonably good agreement and the positive percent bias is curiously not obvious in the individual graphs of each storm event (Figure 18). Finally, computed monthly geometric mean and statistical threshold values based on the modeled hourly results provided similar numbers of monthly exceedances for each site over the two-year period: 23 or 22 of the 24 months for PLBR (Figure 19) and 14 or 12 of the 24 months for UTLP (Figure 20), respectively.

Discussion

The results from the BACI study provide strong support for the interpretation that the "conversion" of a large parcel of disturbed land within a watershed to a stable suburbanized land use with modern GSI can produce consistent hydrologic "treatment effects" that are detectable and quantifiable using traditional stream gaging methods complemented with radar rainfall estimation. In the case of the UTLP watershed, the conversion of about 12.5% of the watershed from a disturbed (early development) state to a fully developed (post development) state produced a consistent percentage (~30%) reduction in some key hydrologic metrics—notably event runoff, event peak runoff, event runoff coefficient, and event *DRC* (Table 1). These results raise questions about the mechanistic role of the GSI in the reductions (and in the increase in mean event *BFC*), as well as whether the percentage reductions might be predicted independently.

Regarding the role of the GSI, it is very straightforward to show that the consistency in the percentage reductions in event runoff, peak runoff, and runoff coefficient are consistent with hydrologic "retention" that the two types of GSI (i.e., dry wells, bioretention cells) ostensibly provided. This can be easily demonstrated by considering that the storm hydrograph can be represented as an isosceles triangle with height (h) representing the peak discharge per unit watershed area (i.e., Q_p/A) and the base (b) representing time (t). Assuming that the storm hydrograph starts at the origin (i.e., $h = Q_p/A = 0$ and $b = t = 0$) and ends at the point $h = 0$ and $b = 1$, the runoff (R) can be computed by integration of the triangle (i.e., $R = ½bh = ½(1)(h) = ½h$; Figure 13). The BACI results for event peak runoff suggest that if h for the predicted post development storm hydrograph for UTLP is equal to 1.0, then h for the observed post development hydrograph would be equal to 0.7 (i.e., reflecting the computed percentage reduction of 30%). Using this example, the predicted and observed values of R would be 0.50 and 0.35, respectively (also a 30% reduction). Finally, assuming the same event rainfall (P), the

event runoff coefficient (*R*/*P*) would expectedly show the same 30% reduction. Therefore, the situation where the percentage reductions in both event runoff and peak runoff are equivalent is a special case that is explained solely by hydrologic retention. A greater percentage reduction in peak runoff is, of course, possible (while keeping *R* constant), but only if the peak of the hydrograph (triangle) is diminished and the (triangle) base is extended. In this case, a change in the shape of the triangular hydrograph would represent a redistribution of runoff owing to the temporary storage of water ("detention") and subsequent release from the system (Chow et al. 1988). The BACI results do not suggest that this type of redistribution by GSI was an important mechanism in the study.

The same conceptualization can also be used to examine the treatment effects on event DR and BF. Given that the predicted and observed mean *DRC* values were 0.67 and 0.50, respectively (Table 1), it is easily shown that the predicted and observed DR hydrographs would have h = 0.67 and 0.35, respectively. Integrating, the predicted and observed event DR runoff would be 0.335 and 0.175, respectively, demonstrating another key treatment effect of GSI—a 48% reduction in DR runoff (volume). Similarly, with predicted and observed mean *BFC* values of 0.33 and 0.50, event BF runoff (volume) can be easily shown to have increased slightly (~6%) due to the GSI. Given the uncertainties in the BACI models, the computed 6% increase in event BF runoff volume may not be statistically significant. However, even if event BF runoff volume remained constant throughout the development sequence, this would mean that 100% of the estimated hydrologic retention was of "new water" conveyed as overland runoff from impervious surfaces (or possibly from soils with relatively low infiltration capacity) and captured by the GSI (Figure 14). While not a BACI result, the increasing aggregated baseflow contribution (i.e., BF_A/R_A) at UTLP from the early through the post development period provides further support for this conceptual model of the hydrologic retention process (Figure 7).

The ~30% reductions in mean event runoff, peak runoff, runoff coefficient, and *DRC* by retention are of the same magnitude as the ~36% reduction in disturbed (D_S) plus impervious (I_S) surface area over the life of the project (Appendix A)—suggesting that the GSI has mostly eliminated overland runoff from the newly developed portion of the UTLP watershed directly conveying into the stream. The small difference in the two percentages could be interpreted in one of two ways: 1) since the mean values of the metrics are based on storm events with a wide range of runoff characteristics, the most obvious possibility is that the GSI totally *eliminated* overland runoff for all storms less than the design rainfall depth (often designated "P_E"), but only *reduced* overland runoff for storms greater than the P_E; or 2) while there was a 36% reduction in $D_S + I_S$, a portion of the disturbed area did not uniformly contribute overland runoff during the early phase of development (i.e., less intense/smaller storms might have been more completely infiltrated by the disturbed soils). Either way, the results are strongly supportive of the idea that the hydrologic effects of GSI scale directly with the portion of the

watershed treated. One reason for this roughly 1:1 scaling is no doubt related to the design of the bioretention cells and dry wells that comprise the GSI at UTLP. Unlike older GSI in Maryland that was designed to capture 2.54 cm (i.e., 1.0") rainfall depths, much of the GSI in this study was designed to capture 6.6 cm (i.e., 2.6") rainfall depths. In Ellicott City, Maryland, the return period of 60-min rainfall of 2.54 cm is about one year, while the return period of 60-min rainfall of 6.6 cm is about 25 years (Bonnin et al. 2006). Another desirable feature of the newer bioretention cells in the UTLP watershed is the location of the outfalls near the edge of a protected forested floodplain, thus effectively buffering the stream from the outflow runoff and providing an opportunity for re-infiltration and evapotranspiration.

What are the ramifications of this conceptualization for understanding the treatment effects of the GSI on stormwater quality? While there were quite a few water quality variables for which significant BACI models could be found for baseflow concentration, *EMC*, and *EL*, very few of these showed any statistically significant treatment effects. There are several possible explanations for this result, but the conceptualization of stormflow treatment as primarily a hydrologic "retention" process should provide some insight into which of these explanations is most plausible. NO_3-N (measured using IC: IC-NO_3-N) is a dominant form of TN in both streams that consistently showed negative chemodynamic behavior (i.e., baseflow concentrations were higher than stormflow EMCs; Figures 11, 12). Nitrate-N has shown to exhibit the same behavior in other urban watersheds (e.g., Duncan et al. 2017). Statistically significant BACI models were found for IC-NO_3-N baseflow concentrations, *EMCs*, and *ELs*. If we consider the *EMC* and *EL* of IC-NO_3-N as being controlled by the same mixing process that was used to estimate *DRC* and *BFC* by hydrograph separation, the selective retention of "new water" (with a lower concentration) by the GSI should be expected to: 1) increase the mean *EMC*; 2) decrease the mean *EL*; and 3) have no direct effect on the mean baseflow concentration of NO_3-N during the post phase, all else being equal.

Treating the *EL* of NO_3-N as a mixing problem where the event load is the sum of the loads of direct runoff ("new water") and baseflow ("old water"), it is possible to compute mean *EMC* and *EL* values and compare these against predicted and observed values for UTLP. To estimate the mean *EMC*, we used:

$$EMC = (C_n)(DRC) + (C_o)(BFC) \quad (1)$$

where all of the variables are means for a particular development period. If it is assumed that C_o can be equated with the observed mean baseflow concentration, C_n can be computed directly by rearranging the equation and substituting observed values from Tables 1 – 3. The computations produced estimated mean C_n values of 0.39, 0.50, and 0.60 mg N/L for the early, late, and post development periods, respectively. These values are all very close to the estimated concentration of NO_3-N + NH_4-N (0.4 mg N/L) in rainfall in eastern Maryland (Du et

al. 2014), lending further support to the hydrologic mixing explanation. Lastly, given the relatively small differences between the estimates, the results suggest that the primary treatment effects involving NO_3-N are not explained by reductions in C_n (as might be achieved, for example, through plant uptake or denitrification in the GSI or through in-stream processes). Rather, the results seem to confirm hydrological control with the mean DR contribution (i.e., $R*DRC*C_n$) of NO_3-N being reduced by the GSI, even as the mean old water contribution (i.e., $R*BFC*C_o$) increased. Comparing results from the early and post phases, the mean DR contribution of NO_3-N—driven by a decrease in mean *DRC*—decreased by 29% (from 0.016 to 0.011 kg ha^{-1}), while the mean baseflow contribution—driven by increases in both *BFC* and C_o—increased by 18% (from 0.023 to 0.027 kg ha^{-1}).

What caused the apparent increase in C_o? One possible explanation is that localized recharge of subsurface water through interactions with the GSI are contributing to (slightly) elevated groundwater NO_3-N concentrations. In a related long-term study of two nearby highway bioswales equipped with comparable bioretention cells, fairly high *EMCs* of NO_3-N were measured in the underdrainage: mean = 1.02 mg/L (range = 0.05 – 5.04) based on n = 54 events sampled at one swale; mean = 2.56 mg/L (range = 0.05 – 8.52 mg/L) based on n = 28 events sampled at the other swale (Eshleman et al. 2025). In that study, the excessive NO_3-N in the underdrainage was attributed primarily to mineralization/nitrification of N present in the biosoil used to construct the cells; a smaller portion was attributed to atmospheric N sources. Other experimental studies have addressed the difficulties of "bioretaining" an inherently mobile form of N such as NO_3-N (Bedan and Clausen 2009, Stagge et al. 2012, Shetty et al. 2018, Smith et al. 2023) unless the cells are modified so as to create anaerobic conditions that encourage denitrification (Hsieh et al. 2007). The same phenomenon could be occurring in the UTLP watershed—although the results showed that the "extra" NO_3-N appears to be accompanying the BF rather than the DR component of the runoff. The fact that this phenomenon showed up only in the post development period might also suggest an additional significant NO_3-N source in the watershed. One obvious possibility is NO_3-N released from the bioretentions into shallow groundwater or discharged into the riparian zone. Our own experimental research on highway bioswales confirmed that bioretention cells can act as major sources of NO_3-N—especially when the design includes a highly efficient underdrain system (Eshleman et al. 2025). A second possible source could be attributed to the use of N-containing lawn fertilizers during the post period, coupled with local contamination of the subsurface through leaching (either independent of the GSI or in combination with it). The annual loading results also support the possibility of a new source of N contributing to the NO_3-N loads at UTLP following development; only six of the 17 constituents showed higher post:early load ratios for UTLP than for PLBR and all six are N-containing (Table 5). Law et al. (2004) estimated mean fertilizer N application rates of about 100 kg N ha^{-1} y^{-1} in urban watersheds in the Baltimore metro area, so it would not take a very large percentage of the

plausible fertilizer N application rate to significantly raise the ambient streamwater NO_3-N loads in UTLP (Table 5)—even if the land area receiving the fertilizer input is a relatively small portion of the developed watershed.

Our research also failed to detect any significant *EL* or *EMC* treatment effects for any P-containing constituents, despite the noted hydrological retention of overland runoff. This result has to be qualified by noting again that we failed to develop significant BACI models for several important constituents such as TP and PP (Tables 3, 4). However, comparisons of annual loads of all P-containing constituents (except SOC-P) showed the opposite effect as reported for the N-containing constituents, namely somewhat higher post:early ratios for P at PLBR compared to UTLP (Table 5). In the CBT-sponsored project examining the effectiveness of highway swales in Maryland, Eshleman et al. (2025) reported mean *EMC*s for TP (0.59 mg/L) and TDP (0.49 mg/L) for grassed swales that are substantially higher than the values reported for the same constituents in UTLP (0.15, 0.05 mg/L, respectively; Table 3). Mean underdrainage *EMC*s for TP (0.29 mg/L) and TDP (0.22 mg/L) for the P-retentive bioswales in the highway study were also higher than those for UTLP stormwater. Using Eq. 1, we computed mean C_n values for TP, as well as mean DR and BF loads for the three development periods at UTLP. It turns out that in this case, the mean BF loads of TP are negligible compared to the mean DR loads (i.e., 3% vs. 97%, respectively) and computed mean C_n values steadily increased over time: 0.24 mg/L in the early phase, 0.37 mg/L in the late phase, and 0.41 mg/L in the post phase. These values are all of the same magnitude as the highway bioswale underdrainage TP values noted earlier. Interestingly, if we substitute the mean underdrainage value for C_n and recompute the mean TP *EL* for the post period, the result is 0.0067 kg ha^{-1}—28% less than the initial estimate of 0.0093 kg ha^{-1}. The similarity of this result to the 30% value for hydrologic retention leads us to speculate about an additional P source associated with the new development. Is it possible that the new GSI in the watershed initially reduced TP as expected, but an additional source (lawn fertilizer P?) essentially cancelled out that reduction?

Chloride-containing road deicing chemicals (“salts”) are clearly having a major impact on Cl concentrations (and SC) in both of these suburban Baltimore streams and elsewhere as others (Kaushal et al. 2018, Kaushal et al. 2022) have demonstrated. The most extreme impacts on streamwater concentrations were observed during winter and spring snowmelt/rain-on-snow events as Cl is dissolved and rapidly transported in overland flow from salted surfaces to the receiving streams; the SF Cl load from the two watersheds was higher in years with greater winter precipitation that presumably necessitated higher applications of road salt on roads and other surfaces. The Cl load in BF actually dominated the total annual load in both watersheds, however—suggesting that a legacy of groundwater Cl contamination by road salt is the major driver of the Cl load on an annual basis (Figure 15).

Chloride was actually one of only four chemical variables (the others SC, IC-NO_3-N, and FIA NO_3-N) for which we found a significant treatment effect on *ELs* for the late period, but no significant effect for the post period; those results reveals that the mean reduction in Cl load during the late period was approximately 30%--in line with the ~30% reductions in mean event runoff and *DRC* in UTLP for the post phase (Table 1). Closer examination of Cl load results for the post period reveals that while a significant ($P \leq 0.05$) reduction was not detected, the computed reduction during the latter period was 21% with a P value was 0.10 (Table 4). In other words, as in the case of both NO_3-N and SC, a significant treatment effect for Cl load "disappeared" between the late and post phases of the study. Our explanation of this phenomenon is similar to the one we used for NO_3-N: a "new" watershed source of Cl. In this case the likely source is quite obvious: application of Cl-containing salts to "new" impervious surfaces in the UTLP watershed during winter snow and ice events.

What do these and our other results indicate about the efficacy of the GSI for Cl retention? The inability to detect a treatment effect of the bioretention cells on Cl loads (or *EMCs*) in the UTLP watershed for the post phase is consistent with hydrological theory accepting Cl is a conservative ion and other recent findings showing that modern stormwater infrastructure (e.g., bioretentions, ponds, etc.) lacks the capacity to retain Cl ions over the long term (Snodgrass et al. 2017, Burgis et al. 2020). Integrative studies—including one conducted in Maryland—have confirmed that detention by stormwater infrastructure owes to temporary storage along groundwater flowpaths through interactions with the GSI (e.g., Kaushal et al. 2018). The finding of an increasing percentage of the total Cl load associated with BF in UTLP is also consistent with the groundwater contamination/transport pathway. Two caveats to this explanation need to be noted, however: 1) none of the event comparisons included data for the snowmelt/rain-on-snow events for which *ELs* of Cl were much higher than the rainfall events (i.e., those events were excluded from our BACI analysis due to their relatively small number in the database); and 2) unlike the results for NO_3-N, we did not find a post phase treatment effect for baseflow Cl concentration.

Moreover, the significant treatment effects of the GSI on Cl and NO_3-N disappeared during the late phase of development which we interpreted as a response to new sources of pollution in the watershed: most likely the use of N-containing lawn fertilizers and the application of Cl-containing salts to roads, driveways, and sidewalks within the recently-developed portion of the watershed. Overall, our water quality results represent a cautionary note that GSI is not a panacea; in fact, data from this study and from a related study of bioswales on Maryland highways (Eshleman et al. 2025) suggest that the term "bioretention" may be a misnomer. While there is strong evidence for hydrologic (i.e., physical) retention of some aquatic pollutants (e.g., NO_3-N, Cl) in the current study and for chemical retention of another important pollutant (PO_4-P) in the latter study, we have been unable to provide solid empirical evidence

for biological retention of these or any other water quality constituents. These findings are not unique, as many other experimental studies have demonstrated strong retention of PO_4-P through chemisorption onto soil clay particles and minimal (or negative) retention of NO_3-N in bioretention cells.

As documented in many other studies (e.g., Stumpf et al. 2010, Rowny and Stewart 2012, Wang et al. 2018), data for both suburban streams showed very high levels of *E. coli*, particularly during stormflow (i.e., so-called "wet weather") conditions. The ranges (and geometric means) of *E. coli* concentrations in UTLP and PLBR stormflow were very similar to those reported by Rowny and Stewart (2012) for an urbanizing watershed in the Research Triangle area of the North Carolina Piedmont—particularly those with relatively high (15 – 34%) levels of ISA. While we found only one published study (Dwivedi et al. 2013) that used LOADEST to estimate *E. coli* loads, stream discharge has been shown to be a strong predictor of microbial concentrations (and thus loads) in virtually every published study we reviewed. Notwithstanding the relatively low density of *E. coli* sampling, this provides us with a high degree of confidence that the patterns presented in Figure 19 are reasonable representations of variations in *E. coli* concentrations throughout the study. The inclusion of intra-annual periodic terms in the LOADEST model is also important, given evidence of strong seasonality in loads and concentrations in some regions; for example, in a study of *E. coli* loads in the Nashville, TN area, Stallard et al. (2016) showed that the highest concentrations were typically observed in the winter and spring. Our two-year *E. coli* study showed the opposite pattern in both streams, with lowest concentrations in the winter and spring months, but it is possible that the drought conditions and low runoff in those months in water year 2025 were the primary driver of the pattern (Figure 19). Results from the current study can certainly be used to identify correlates or predictor variables (e.g., discharge) of high *E. coli* loads, but identification of actual sources of microbial contamination (e.g., domestic sewage, animal feces, etc.) in our watersheds through examination of genetic marker genes (Ahmed et al. 2019, Lancaster et al. 2024) was beyond the scope of the current research. Regardless of the specific model or mechanism of *E. coli* loading applicable to the study watersheds, it would be tempting to attribute the differences in *E. coli* concentrations and exceedances between the two watersheds to the recent implementation of GSI in the developing portion of the UTLP watershed. The lack of any "pre-treatment" data precludes us from drawing that conclusion, however.

Conclusions

A BACI design, combined with stormwater data from an intensive, 5.5-year monitoring program in two small watersheds in north-central Howard County, MD, allowed us to detect and quantify statistically significant changes in many event-based hydrologic metrics (e.g., event runoff, peak event runoff, event direct runoff) during a recent period of suburban development in the "developing" UTLP watershed. Despite the lack of data from a true "pre-development"

period and the fact that a relatively small portion (~13%) of the watershed was disturbed, the treatment effects were internally consistent and could be explained by hydrologic theory through use of a conceptual model. In particular, the highly effective retention of stormflow produced from "new" impervious watershed surfaces by distributed GSI (i.e., bioretentions, dry wells) in the watershed was demonstrated. Overall, these mean event-based metrics were reduced by ~30%, while the combined disturbed plus impervious areas of the watershed decreased by about 36% from the early phase to the post phase of development. The impressive reduction in overland runoff from impervious surfaces was largely explained by the fact that: 1) the bioretention cells were designed and built to infiltrate storms of much greater magnitude than those for which GSI in Maryland has historically been required to address; and 2) the bioretention outfalls were located at the edge of a protected forested floodplain, effectively buffering the stream from the effects of the outflows and providing an opportunity for re-infiltration and evapotranspiration.

Concurrent with these event runoff (and peak runoff) reductions, we found significant reductions in mean event loads Cl and NO_3-N for the late phase of development that were roughly proportional to the overall runoff reductions. No significant treatment effects were observed for the post development phase for any of the five P-containing constituents that were measured during the study—underlining the importance of stream discharge and erosion (both sheet and channel) as likely dominant sources of these constituents. Moreover, the significant treatment effects of the GSI on Cl and NO_3-N disappeared during the late phase of development which we interpreted as a response to new sources of pollution in the watershed (i.e., N from the bioretentions or from the use of N-containing lawn fertilizers and Cl from the application of Cl-containing salts to roads, driveways, and sidewalks within the recently-developed portion of the watershed during winter snow and ice events). Overall, our water quality results provide a cautionary note that GSI is not a panacea; in fact, data from this study and from a related study of bioswales on Maryland highways suggest that the term "bioretention" may be a misnomer. While there is strong evidence for hydrologic (i.e., physical) retention of some aquatic pollutants (e.g., NO_3-N, Cl) in the current study and for chemical retention of another important pollutant (PO_4-P) in the latter study, we have been unable to provide empirical evidence for biological retention of any of these (or other) water quality constituents. These findings are not unique, as many other experimental studies have demonstrated strong retention of PO_4-P through chemisorption onto soil clay particles and minimal (or negative) retention of NO_3-N in bioretention cells.

Acknowledgments

The research and monitoring described in this report were funded by grants from CBT to University of Maryland Center for Environmental Science (UMCES) through three separate awards (no. 16920, 20588, and 22063). The project team also recognizes the institutional

financial support for each of these projects provided by UMCES Appalachian Laboratory. We sincerely thank Mark Richmond from Howard County Government (HoCoG) Stormwater Management Division for assistance with site selection and issuance of permits to install and operate stormwater monitoring stations on two streams in Howard County parkland. Caroline Rexford (HoCoG) provided us with estimates of watershed imperviousness using data layers generated by analysis of annual aerial photography. Katie Kline, Ev Demott, and Gage Jacobs assisted with analysis of water samples in the laboratory. Neal Eshleman assisted with installation of stilling wells at the beginning of the project and gets credit for wading Plumtree Branch to make a discharge measurement near the peak of a major flash flood in 2020. Elizabeth Eshleman voluntarily served as the principal investigator's faithful field assistant beginning with the onset of the COVID-19 pandemic and she continued in that unofficial role through the end of the project.

References

Ahmed, W., K. Hamilton, S. Toze, S. Cook, and D. Page. 2019. A review of microbial contaminants in stormwater runoff and outfalls: potential health risks and mitigation strategies. *Sci. Tot. Environ.* ***692***:1304-1321; https://doi.org/10.1016/j.scitotenv.2019.07.055.

APHA. 2017. *Standard Methods for the Examination of Water and Wastewater*, 23rd Edition. American Public Health Association, Washington, DC.

Barrett, M.E. 2008. Comparison of BMP Performance Using the International BMP Database. *J. Irrig. Drain. Eng.* ***134***:556-561.

Bedan, E.S., and J.C. Clausen. 2009. Stormwater runoff quality and quantity from traditional and low impact development watersheds. *J. Amer. Water Resour. Assoc.* ***45***:998-1008.

Bieroza, M.Z., A.L. Heathwaite, M. Bechmann, K. Kyllmar, and P. Jordan. 2018. The concentration-discharge slope as a tool for water quality management. *Sci. Tot. Environ.* ***630***:738-749.

Bonnin, G.M., D. Martin, B. Lin, T. Parzybok, M. Yekta, and D. Riley. 2006. NOAA Atlas 14, *Precipitation-frequency atlas of the United States, Volume 2, Version 3.0*; U.S. Department of Commerce, NOAA, NWS, Silver Spring, MD; https://hdsc.nws.noaa.gov/pfds/pfds_map_cont.html?bkmrk=md

Bormann, F.H., G.E. Likens, T.G. Siccama, R.S. Pierce, and J.S. Eaton. 1974. The export of nutrients and recovery of stable conditions following deforestation at Hubbard Brook. *Ecol. Monogr.* ***44***:255-277.

Bosch, J.M., and J.D. Hewlett. 1982. A review of catchment experiments to determine the effect of vegetation changes on water yield and evapotranspiration. *J. Hydrol.* ***55***:3-23.

Burgis, C.R., G.M. Hayes, D.A. Henderson, W. Zhang, and J.A. Smith. 2020. Green stormwater infrastructure redirects deicing salt from surface water to groundwater. *Sci. Tot. Environ.* ***729***:138736; https://doi.org/10.1016/j.scitotenv.2020.138736.

Chanat, J.G., and G. Yang. 2018. Exploring drivers of regional water-quality change using differential spatially referenced regression—a pilot study in the Chesapeake Bay watershed. *Water Resour. Res.* ***54***:8120-8145.

Chow, V.T., D.R. Maidment, and L.W. Mays. 1988. *Applied Hydrology.* McGraw-Hill Book Company, New York, NY.

Cohn, T.A., L. L. DeLong, E.J. Gilroy, R.M. Hirsch, and D.K. Wells. 1989. Estimating constituent loads, *Water Resour. Res.* ***25***:937– 942.

Crawford, C.G. 1991. Estimation of suspended-sediment rating curves and mean suspended-sediment loads. *J. Hydrol.* ***129***:331-348.

Davis, A.P., W.F. Hunt, R.G. Traver, and M. Clar. 2009. Bioretention technology: overview of current practice and future needs. *J. Environ. Eng.* ***135***:109-117; https://doi.org/10.1061/(ASCE)0733-9372(2009)135.

Dietz, M.E. 2007. Low impact development practices: a review of current research and recommendations for future directions. *Water Air Soil. Pollut.* ***186***:351-363.

Du, E. W. de Vries, J.N. Galloway, X. Hu, and J. Fang. 2014. Changes in wet nitrogen deposition in the United States between 1985 and 2012. *Environ. Res. Lett.* ***9***:095004; doi:10.1088/1748-9326/9/9/095004.

Duncan, J.M., C. Welty, J.T. Kemper, P.M. Groffman, and L.E. Band. 2017. Dynamics of nitrate concentration-discharge patterns in an urban watershed. *Water Resour. Res.* ***53***:7349-7365; doi:10.1002/2017WRR020500.

Dwivedi, D., B.P. Mohanty, and B.J. Lesikar. 2013. Estimating *Escherichia coli* loads in streams based on various physical, chemical, and biological factors. *Water Resour. Res.* ***49***:2896-2906; doi:10.1002/wrcr20265.

Eckhardt, K. 2004. How to construct recursive digital filters for baseflow separation. *Hydrol. Proc.* ***19***:507-515; https://doi.org/10.1002/hyp.5675.

Eshleman, K.N. 2023. *Assessing the effectiveness of environmentally-sensitive design (ESD) for achieving stormwater management objectives in the Upper Little Patuxent River Watershed, Howard County, MD.* Final report to Chesapeake Bay Trust Pooled Monitoring Program.

Eshleman, K.N., B. Mentzer, J. Garlitz, and T. Frissell. 2025. *Comparative field-scale assessment of the stormwater treatment effectiveness of bioswales on Maryland highways.* Final report to Chesapeake Bay Trust Pooled Monitoring Program. University of Maryland Center for Environmental Science, Appalachian Laboratory, Frostburg, MD.

Fan, R., S.T.Y. Tong, and J.G. Lee. 2017. Determining the optimal BMP arrangement under current and future climate regimes: case study. *J. Water Resour. Plan. Manage.* ***143***.

Freeze, R.A., and J.A. Cherry. 1979. *Groundwater.* Prentice-Hall, Inc., Englewood Cliffs, NJ, 604 pp.

Fishman, M.J. 1993. Methods of analysis by the U.S. Geological Survey National Water Quality Laboratory—determination of inorganic and organic constituents in water and fluvial sediments. *U.S. Geological Survey Open-File Report 93-125.*

Harr, D.R., A. Levno, and R. Merscreau. 1982. Streamflow changes after logging 130-year-old Douglas fir in two small watersheds. *Water Resour. Res.* ***22***:1095-1100.

Hood, M.J., J.C. Clausen, and G.S. Warner. 2007. Comparison of stormwater lag times for low impact and traditional residential development. *J. Amer. Water Resour. Assoc.* ***43***:1036-1046.

Hornbeck, J.W., R.S. Pierce, and C.A. Federer. 1970. Streamflow changes after forest clearing in New England. *Water Resour. Res.* ***6***:1124-1132.

Hsieh, C. A.P. Davis, and B.A. Needelman. 2007. Nitrogen removal from urban stormwater runoff through layered bioretention columns. *Water Environ. Res.* ***79***:2404-2411.

Jarden, K.M., A.J. Jefferson, and J.M. Grieser. 2016. Assessing the effects of catchment-scale urban green infrastructure retrofits on hydrograph characteristics. *Hydrol. Proc.* ***30***:1536-1550.

Kaushal, S.S., G.E. Likens, M.L. Pace, R.M. Utz, S. Haq, J. Gorman, and M. Grese. 2018. Freshwater salinization syndrome on a continental scale. *Proc. Nat. Acad. Sci.* ***115***:E574–E583.

Kaushal, S.S., J.E. Reimer, P.M. Mayer, R.R. Shatkay, C.M. Maas, W.D. Nguyen, W.L. Boger, A.M. Yaculak, TR. Doody, M.J. Pennino, N.W. Bailey, J.G. Galella, A. Weingrad, D.C. Collison, K.L. Wood, S. Haq. T.A. Newcomer Johnson, S. Duan, and K.T. Belt. 2022. Freshwater salinization syndrome alters retention and release of 'chemical cocktails' along flowpaths: from stormwater management to urban streams. *Freshwater Sci.* ***41***:420–441; doi:10.1086/721469.

Knapp, J.L.A., J. von Freyburg, B. Studer, L. Kiewiet, and J.W. Kirchner. 2020. Concentration-discharge relationships vary among hydrological events, reflecting differences in event characteristics. *Hydrol. Earth Syst. Sci.* ***24***:2561-2576; https://doi.org/10.5194/hess-24-2561-2020.

Kratky, H., Z. Li, Y. Chen, C. Wang, X. Li, and T. Yu. 2017. A critical literature review of bioretention research for stormwater management in cold climate and future research recommendations. *Front. Environ. Sci. Eng.* ***11***:1-15.

Krug, W.R., W.A. Gebert, D.J. Graczyk, D.L. Stevens, B.P. Rochelle, and M.R. Church. 1990. Map of mean annual runoff for the Northeastern, Southeastern, and Mid-Atlantic United States, water years 1951-80; *Water-Resources Investigations Report 88-4094*; U.S. Geological Survey, Madison, WI; https://www.usgs.gov/publications/map-mean-annual-runoff-northeastern-southeastern-and-mid-atlantic-united-states-water.

Lancaster, E., R. Winston, J. Martin, and J. Lee. 2024. Urban stormwater green infrastructure: evaluating the public health service role of bioretention using microbial source tracking and bacterial community analyses. *Water Res.* ***259***:121818; https://doi.org/10.1016/j.watres.2024.121818

Law, N.L., L.E. Band, and J.M. Grove. 2004. Nitrogen input from residential lawn care practices in suburban watersheds in Baltimore County, MD. *J. Environ. Plan. Manage.* ***47***: 737-755.

Likens, G.E., F.H. Bormann, N.M. Johnson, D.W. Fisher, and R.S. Pierce. 1970. Effects of forest cutting and herbicide treatment on nutrient budgets in the Hubbard Brook watershed-ecosystem. *Ecol. Monogr.* ***40***:23-47.

Liu, J., D.J. Sample, C. Bell, and Y. Guan. 2014. Review and research needs of bioretention used for treatment of urban stormwater. *Water* ***6***:1069-1099.

Loperfido, J.V., G.B. Noe, S.T. Jarnagin, and D.M. Hogan. 2014. Effects of distributed and centralized stormwater best management practices and land cover on urban stream hydrology at the catchment scale. *J. Hydrol.* ***519***:2584-2595.

MDE. 2026. *Normal Monthly Precipitation Totals (in Inches) for Maryland Counties*. Maryland Department of the Environment; https://mde.maryland.gov/programs/water/waterconservation/pages/normalprecip_new.aspx.

Moore, R.D., and R.J. MacDonald. 2024. Quantifying the influence of forestry and forest disturbance on stream temperature: methodologies and challenges. *Hydrol. Proc.* ***38***; https://doi.org/10.1002/hyp.15223.

Nash, J.E., and J.V. Sutcliffe. 1970. River flow forecasting through conceptual models, Part I — A discussion of principles. *J. Hydrol.* ***10***:282–290.

Prince George's County. 1999. *Low-Impact Development Design Strategies: An Integrated Design Approac*h. Prince George's County, Maryland, Department of Environmental Resource Programs and Planning Division, Largo, MD.

Rantz, S.E. *et al.* 1982. Measurement and computation of streamflow: Vol. 1, Measurement of stage and discharge. *Geological Survey Water-Supply Paper 2175*, Washington, DC.

Rose, S., and N.E. Peters. 2001. Effects of urbanization on streamflow in the Atlanta area (Georgia, USA): a comparative hydrological approach. *Hydrol. Proc.* ***15***:1441-1457.

Rowny, J.G., and J.R. Stewart. 2012. Characterization of nonpoint source microbial contamination in an urbanizing watershed serving as a municipal water supply. *Water Res.* ***46***:6143-6153; http://dx.doi.org/10.1016/j.watres.2012.09.009.

Roy, A.H., S.J. Wenger, T.D. Fletcher, C.J. Walsh, A.R. Ladson, W.D. Shuster, H.W. Thurston, and R.R. Brown. 2008. Impediments and solutions to sustainable, watershed-scale urban stormwater management: lessons from Australia and the United States. *Environ. Manage.* ***42***:344-359.

Runkel, R.L., C.G. Crawford, and T. Cohn. 2004. Load estimator (LOADEST): a FORTRAN program for estimating constituent loads in streams and rivers: *U.S. Geological Survey Techniques and Methods 4-A5*, 75 p.; https://doi.org/10.3133/tm4A5.

Schuster, W., and L. Rhea. 2013. Catchment-scale hydrologic implications of parcel-level stormwater management (Ohio USA). *J. Hydrol.* ***485***:177-187.

Selbig, W.R., and R.T. Bannerman. 2008. A comparison of runoff quantity and quality from two small basins undergoing implementation of conventional- and low-impact-development (LID)

strategies: Cross Plains, Wisconsin, water years 1999-2005. *U.S. Geological Survey Scientific Investigations Report 2008-5008.*

Shetty, N., R. Hu, J. Hoch, B. Mailloux, M. Palmer, D.N. Menge, K. McGuire, W. McGillis, and P. Culligan. 2018. Quantifying urban bioswale nitrogen cycling in the soil, gas, and plant phases. *Water* ***10***(11):1627.

Sklash, M.G., R.N. Farvolden, and P. Fritz. 1976. A conceptual model of watershed response to rainfall, developed through the use of oxygen-18 as a natural tracer. *Can. J. Earth Sci.* ***13***:271-283.

Smith, J.S., R.J. Winston, D.M. Wituszynski, R.A. Tirpak, K.M. Boening-Ulman, and J.F. Martin. 2023. Effects of watershed-scale green infrastructure retrofits on urban stormwater quality: a paired watershed study to quantify nutrient and sediment removal. *Ecol. Eng.* ***186***:106835; doi:10.1016/j.ecoleng.2022.106835.

Stagge, J.H., A.P. Davis, E. Jamil, and H. Kim. 2012. Performance of grass swales for improving water quality from highway runoff. *Water Res.* ***46***:6731-6742; doi:10.1016/j.watres.2012.02.037.

Stallard, M.A., R.R. Otter, S. Winesett, M. Barbero, M. Bruce, A. Layton, and F.C. Bailey. 2016. A watershed analysis of seasonal concentration- and loading-based results for *Escherichia coli* in inland waters. *Bull. Environ. Contam. Toxicol.* ***97***:838-842.

Stumpf, C.H., M.F. Piehler, S. Thompson, and R.T. Noble. 2010. Loading of fecal indicator bacteria in North Carolina tidal creek headwaters: hydrographic patterns and terrestrial runoff relationships. *Water Res.* ***44***:4704-4715.

USEPA. 1993. Methods for the Determination of Inorganic Substances in Environmental Samples. *EPA/600/R-93/100*, U.S. Environmental Protection Agency, National Exposure Research Laboratory (NERL) Microbiological and Chemical Exposure Assessment Research Division (MCEARD), Cincinnati, OH.

Walsh, C.J., A.H. Roy, J.W. Feminella, P.D. Cottingham, P.M. Groffman, and R.P. Morgan II. 2005. The urban stream syndrome: current knowledge and the search for a cure. *J. N. Amer. Benthol. Soc.* ***24***:706-723.

Walsh, C.J., M. Imberger, M.J. Burns, D.G. Bos, and T.D. Fletcher. 2022. Dispersed urban-stormwater control improved stream water quality in catchment-scale experiment. *Water Resour. Res.* ***58***; https://doi.org/10.1029/2022WR032041.

Wang, C., R.L. Schneider, J-Y Parlange, H.E. Dahlke, and M.T. Walter. 2018. Explaining and modeling the concentration and loading of *Escherichia coli* in a stream—a case study. *Sci. Tot. Environ.* ***635***:1426-1435.

Webster, K.L., J.A. Leach, P.W. Hazlett, J.M. Buttle, E.J.S. Emilson, and I.F. Creed. 2022. Long-term stream chemistry response to harvesting in a northern hardwood watershed

experiencing environmental change. *Forest Ecol. Manage.* ***519***; https://doi.org/10.1016/j.foreco.2022.120345.

Wondzell, S., S. Johnson, G. Grant, D. Henshaw, and A. Ward. 2025. Rethinking paired-catchment studies: should we be replicating our controls? *Water Resour. Res.* ***61***; https://doi.org/10.1029/2024WR038981.

Tables

Table 1. Observed stormflow values (means) for PLBR and UTLP for early, late, and post phases of suburban development, plus predicted mean values for UTLP (and % differences) using the BACI models. Mean values and differences shown in bold italics are statistically significant based on a paired t-test.

Stormflow variable, units	Early phase		Late phase		Post phase			
	PLBR (obs.)	UTLP (obs.)	PLBR (obs.)	UTLP (obs.)	PLBR (obs.)	UTLP (obs.)	UTLP (pred.)	% difference
Event areal rainfall, cm	2.51	2.40	2.39	2.34	2.21	2.16	2.10	3
Event runoff, cm	***0.71***	***0.52***	***0.80***	***0.32***	***0.83***	***0.44***	***0.62***	***-29***
Event runoff coefficient, -	***0.22***	***0.15***	***0.31***	***0.12***	***0.32***	***0.15***	***0.22***	***-33***
Event peak runoff*, cm h^{-1}	***0.048***	***0.027***	***0.045***	***0.016***	***0.048***	***0.019***	***0.027***	***-30***
Event direct runoff coefficient, -	0.60	0.60	***0.65***	***0.52***	***0.66***	***0.50***	***0.67***	***-26***
Event baseflow coefficient, -	0.40	0.40	***0.35***	***0.48***	***0.34***	***0.50***	***0.33***	***52***

*Values determined from back-transformation of means of log-transformed data

Table 2. Observed mean baseflow concentrations (mg L^{-1}, unless noted) at PLBR and UTLP for early phase of development, plus observed and predicted mean values for UTLP baseflow for the late and post phases of development (the latter based on a BACI model: R^2 value shown). Mean values shown in bold italics are statistically significant based on a paired t-test. N/S: not significant.

Constituent	Early phase			Late phase		Post phase	
	PLBR (obs.)	UTLP (obs.)	R^2	UTLP (obs.)	UTLP (pred.)	UTLP (obs.)	UTLP (pred.)
SC, $\mu S\ cm^{-1}$	546	560	N/S	555	-	548	-
TSS	2.3	2.0	0.42	2.2	2.1	1.6	2.5
Cl	***100***	***113***	N/S	112	-	102	-
IC-NO_3-N	1.02	1.11	0.49	1.17	1.16	***1.24***	***1.08***
SO_4	16.4	16.8	0.33	16.7	17.2	17.6	17.1
TP	***0.031***	***0.011***	0.31	***0.014***	***0.012***	0.015	0.013
TN	1.26	1.29	0.54	1.33	1.31	***1.44***	***1.28***
TDP	***0.017***	***0.008***	0.42	0.010	0.010	0.010	0.010
TDN	1.25	1.27	0.53	1.31	1.29	***1.42***	***1.27***
PP	*	*	*	-	-	-	-
PN	*	*	*	-	-	-	-
PO_4-P	***0.017***	***0.008***	N/S	0.008	-	0.007	-
NH_4-N	***0.023***	***0.007***	0.66	0.010	0.011	0.010	0.009
NO_2-N	0.004	0.003	N/S	0.003	-	0.002	-
FIA-NO_3-N	1.09	1.19	0.54	1.20	1.19	***1.33***	***1.15***
DON	***0.15***	***0.09***	0.78	0.12	0.10	0.09	0.10
SOC-P	*	*	*	-	-	-	-

*insufficient uncensored data to evaluate

Table 3. Observed mean stormflow EMCs (mg L^{-1}, unless noted) at PLBR and UTLP for early phase of development, plus observed and predicted mean EMCs for UTLP for the late and post phases of development (the latter based on a BACI model: R^2 value shown). Mean values shown in bold italics are statistically significant based on a paired t-test. N/S: not significant.

Constituent	Early phase (n = 8)			Late phase (n = 14)		Post phase (n = 16)	
	PLBR (obs.)	UTLP (obs.)	R^2	UTLP (obs.)	UTLP (pred.)	UTLP (obs.)	UTLP (pred.)
SC, µS cm^{-1}	***240***	***310***	0.62	280	290	360	390
TSS	75	187	N/S	132	-	146	-
Cl	***36***	***52***	0.76	46	48	63	70
IC-NO_3-N	***0.38***	***0.68***	0.49	0.82	0.72	0.92	0.78
SO_4	***6.1***	***9.2***	0.53	8.7	11	***11***	***15***
TP	0.27	0.15	N/S	0.20	-	0.21	-
TN	1.2	1.6	N/S	1.8	-	1.8	-
TDP	***0.075***	***0.047***	N/S	0.083	-	0.051	-
TDN	***0.86***	***1.2***	N/S	1.5	-	1.4	-
PP	0.19	0.11	N/S	0.12	-	0.16	-
PN	0.36	0.39	N/S	0.36	-	0.45	-
PO_4-P	***0.062***	***0.035***	N/S	0.065	-	0.038	-
NH_4-N	0.029	0.016	N/S	0.035	-	0.022	-
NO_2-N	0.009	0.007	N/S	0.009	-	0.007	-
FIA-NO_3-N	***0.39***	***0.72***	N/S	0.80	-	0.99	-
DON	0.44	0.43	0.62	***0.63***	***0.47***	0.38	0.34
SOC-P	0.015	0.013	N/S	0.018	-	0.013	-

Table 4. Observed mean event stormflow loads (kg ha^{-1}, unless noted) at PLBR and UTLP for early phase of development, plus observed and predicted mean loads for UTLP for the late and post phases of development (the latter based on a BACI model: R^2 value shown). Mean values shown in bold italics are statistically significant based on a paired t-test. N/S: not significant.

Constituent	Early phase (n = 8)			Late phase (n = 14)		Post phase (n = 16)	
	PLBR (obs.)	UTLP (obs.)	R^2	UTLP (obs.)	UTLP (pred.)	UTLP (obs.)	UTLP (pred.)
SC, S ha^{-1}	***25***	***16***	0.82	***15***	***21***	10	13
TSS	9.0	16	N/S	11	-	14	-
Cl	***3.8***	***2.6***	0.87	***2.2***	***3.2***	1.6	2.1
IC-NO_3-N	0.042	0.038	0.90	***0.048***	***0.063***	0.035	0.034
SO_4	***0.64***	***0.45***	0.55	0.45	0.86	***0.31***	***0.61***
TP	***0.028***	***0.013***	N/S	0.016	-	0.016	-
TN	***0.14***	***0.10***	0.86	0.12	0.15	0.10	0.08
TDP	***0.0094***	***0.0036***	0.53	0.0069	0.0052	0.0034	0.0030
TDN	***0.095***	***0.066***	0.85	0.094	0.12	0.061	0.054
PP	0.018	0.0091	N/S	0.010	-	0.013	-
PN	0.040	0.032	0.73	0.029	0.036	0.036	0.031
PO_4-P	***0.0078***	***0.0029***	0.56	0.0053	0.0040	0.0026	0.0022
NH_4-N	***0.0023***	***0.0011***	N/S	0.0021	-	0.0014	-
NO_2-N	***0.0008***	***0.0005***	N/S	0.0006	-	0.0005	-
FIA-NO_3-N	0.043	0.040	0.89	***0.047***	***0.062***	0.037	0.037
DON	***0.050***	***0.027***	0.69	0.044	0.044	0.023	0.019
SOC-P	***0.0018***	***0.0009***	0.50	0.0016	0.0014	0.0008	0.0008

Table 5. Estimated annualized loads (kg ha^{-1} y^{-1}, unless indicated) for PLBR and UTLP watersheds for the three development phases. Ratios of post phase loads to early phase loads are also shown (values of the ratio in shaded grey cells are the higher of the two watersheds).

Constituent	Early phase		Late phase		Post phase		Ratio (Post:Early)	
	PLBR	UTLP	PLBR	UTLP	PLBR	UTLP	PLBR	UTLP
SC, S ha^{-1} y^{-1}	1500	1000	1180	799	1660	996	1.10	0.99
TSS	169	914	110	438	211	738	1.25	0.81
Cl	278	204	207	161	285	186	1.03	0.91
IC-NO_3-N	2.55	2.15	2.00	1.73	2.36	2.28	0.92	1.06
SO_4	41.1	25.0	39.0	22.6	50.6	26.8	1.23	1.07
TP	0.63	0.73	0.43	0.25	0.74	0.75	1.16	1.03
TN	5.21	4.60	4.08	3.00	5.30	4.93	1.02	1.07
TDP	0.23	0.18	0.16	0.07	0.26	0.18	1.12	0.98
TDN	4.32	4.20	3.42	2.95	4.26	4.91	0.99	1.17
PP	0.39	0.50	0.27	0.17	0.45	0.51	1.17	1.02
PN	0.81	1.73	0.55	0.59	0.94	1.80	1.16	1.04
PO_4-P	0.15	0.09	0.11	0.05	0.17	0.11	1.12	0.97
NH_4-N	0.13	0.06	0.09	0.03	0.12	0.06	0.92	0.94
NO_2-N	0.03	0.02	0.03	0.01	0.04	0.02	1.22	1.00
FIA-NO_3-N	2.62	2.21	2.01	1.81	2.45	2.35	0.94	1.06
DON	1.92	0.97	1.49	0.69	2.18	1.23	1.13	1.27
SOC-P	0.07	0.03	0.06	0.02	0.10	0.04	1.41	1.41

Figures

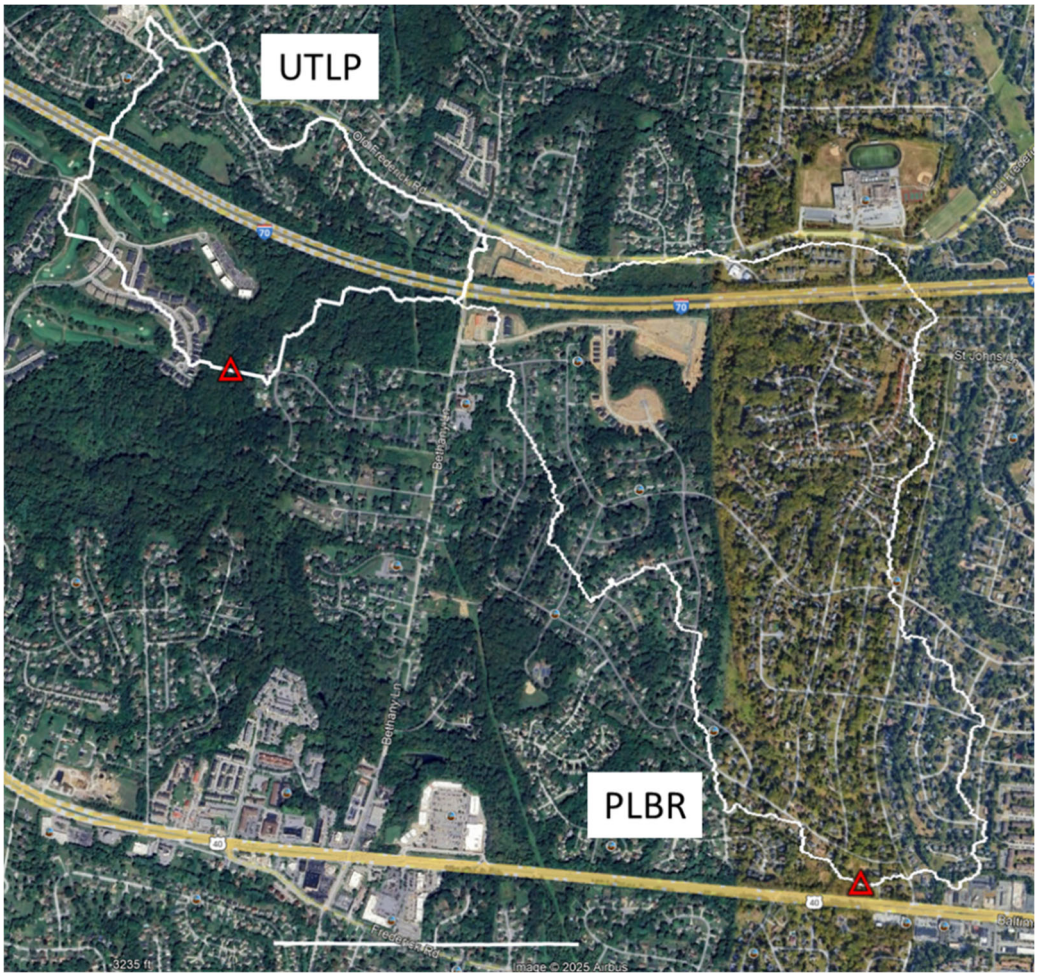

Figure 1. Map of PLBR and UTLP watersheds in north-central Howard County, MD. Google imagery is from October 2025 after recent development of UTLP watershed had been completed. Red triangles show location of stormwater monitoring stations. Rainfall stations not shown.

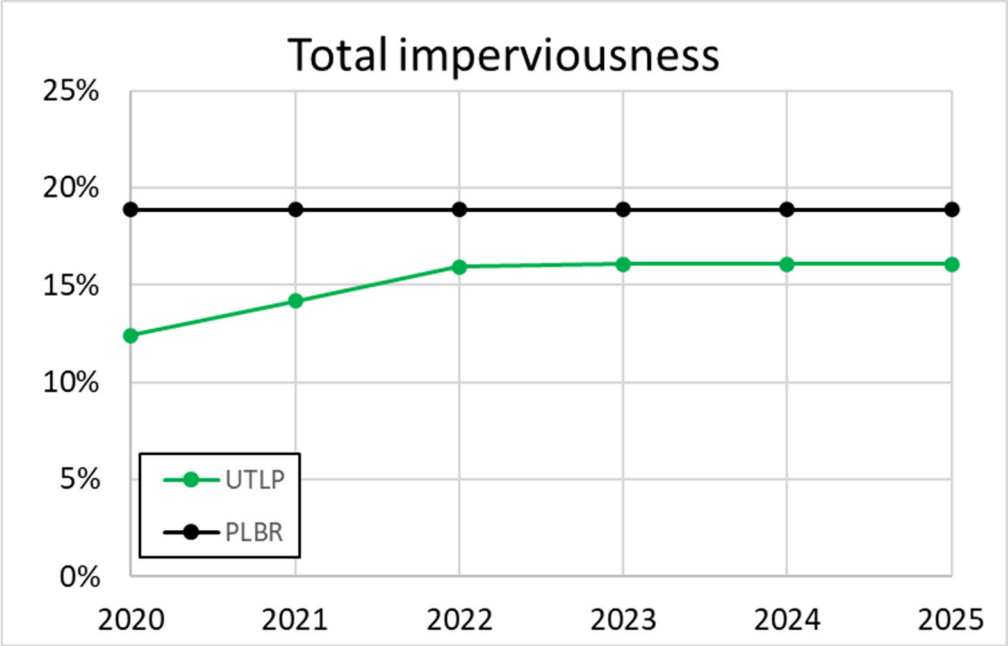

Figure 2. Changes in watershed imperviousness in the two watersheds during the study based on interpretation of aerial photography.

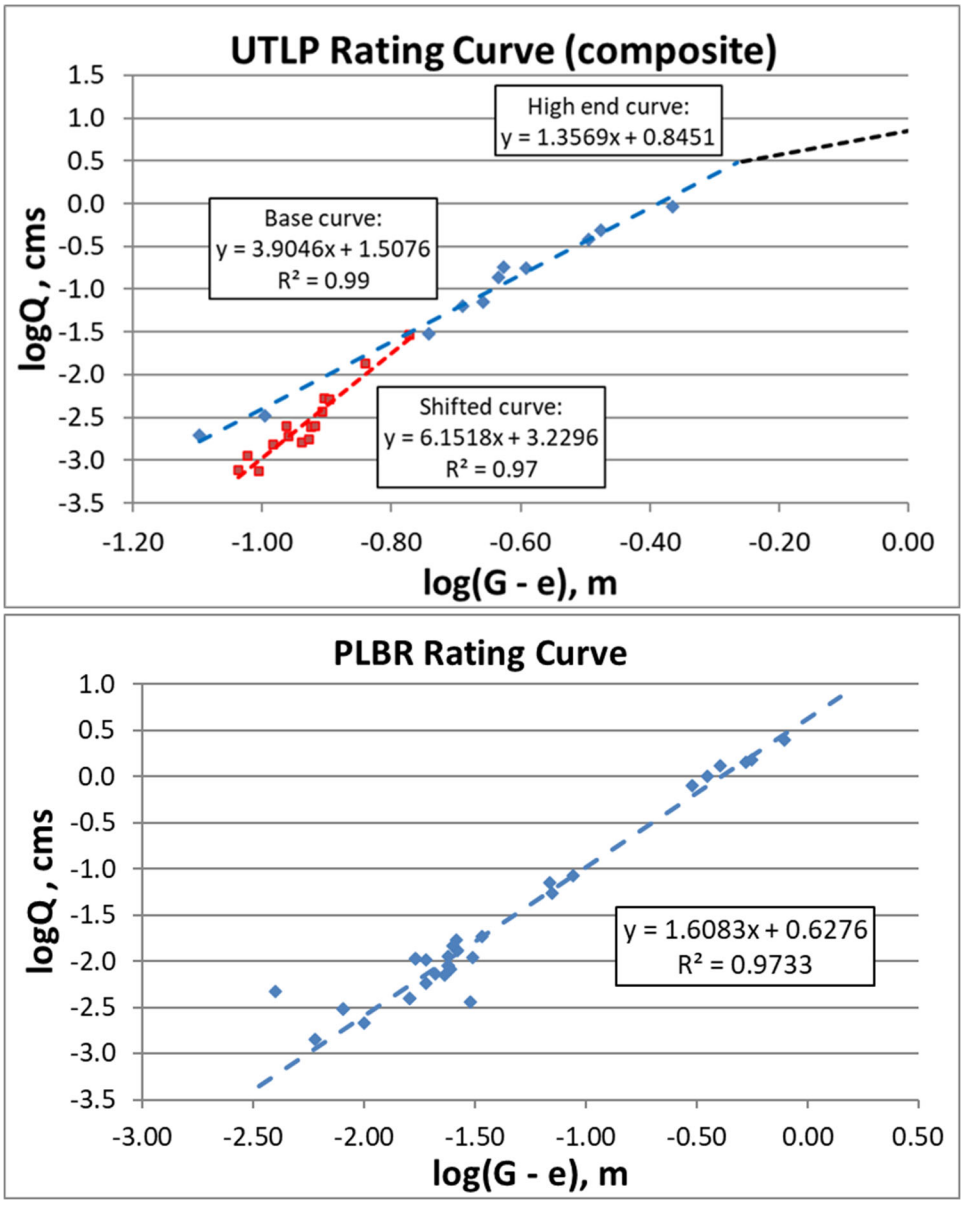

Figure 3. Rating curves (and rating equations: Q = discharge in $m^3 s^{-1}$ = cms; G = gage height in m; e = offset in m) for UTLP and PLBR based on manual wading-type discharge measurements made during the study. See text for description of shifted curve for UTLP.

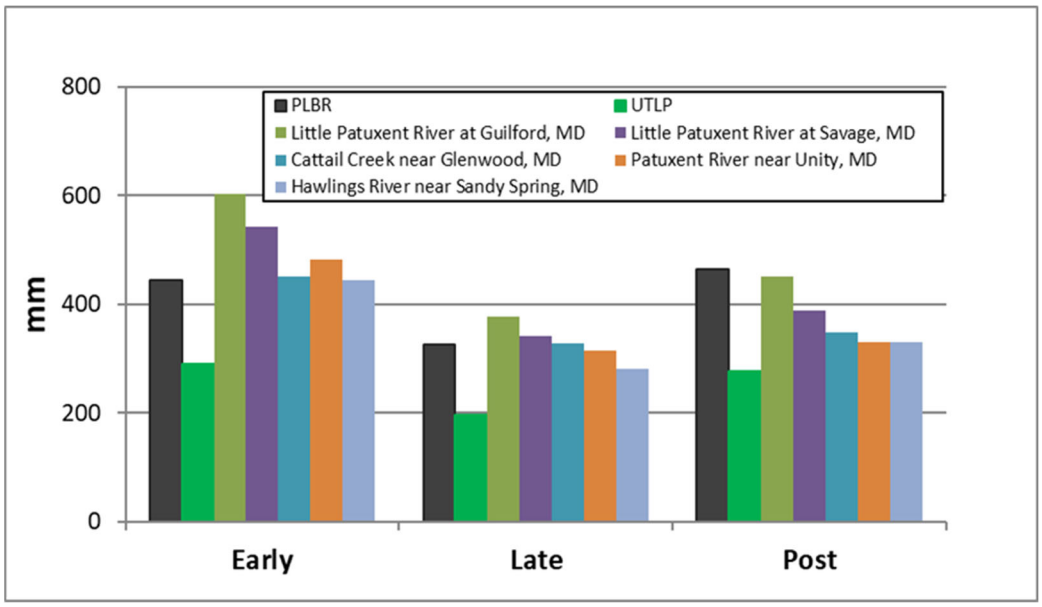

Figure 4. Computed annualized runoff for the three development phases (i.e., early = 4/20 – 3/21; late = 4/21 – 9/23; post = 10/23 – 9/25) for the two study watersheds (PLBR, UTLP). Comparable data for five Patuxent River subwatersheds gaged by U.S.G.S. are shown for comparison (data downloaded from https://waterdata.usgs.gov/state/Maryland/).

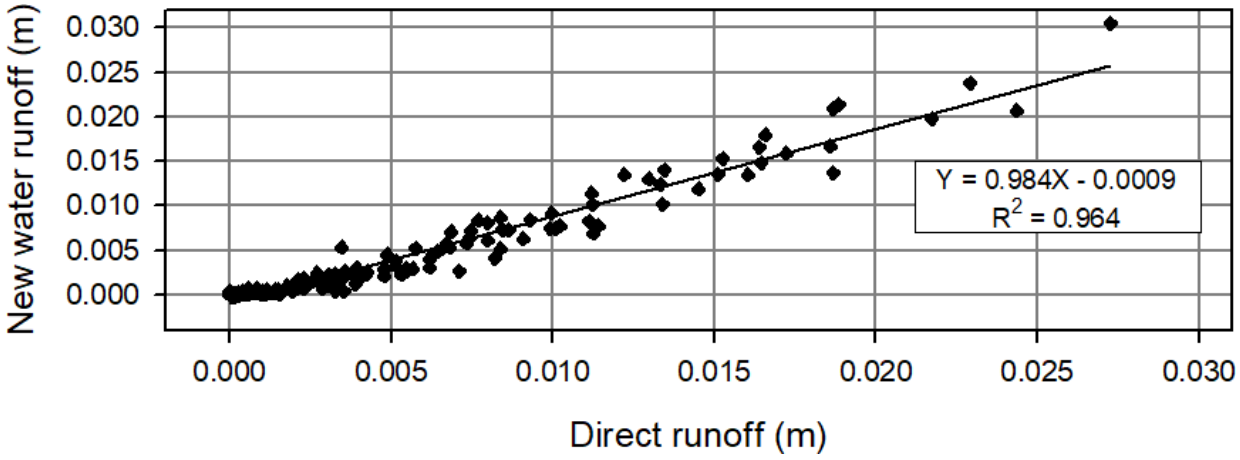

Figure 5. Relationship between event new water runoff at PLBR based on a conductivity mass balance (CMB) and event direct runoff obtained from a recursive digital filter (RDF; Eckhardt 2004) separation method; regression line was obtained using BFI_{max} of 0.675.

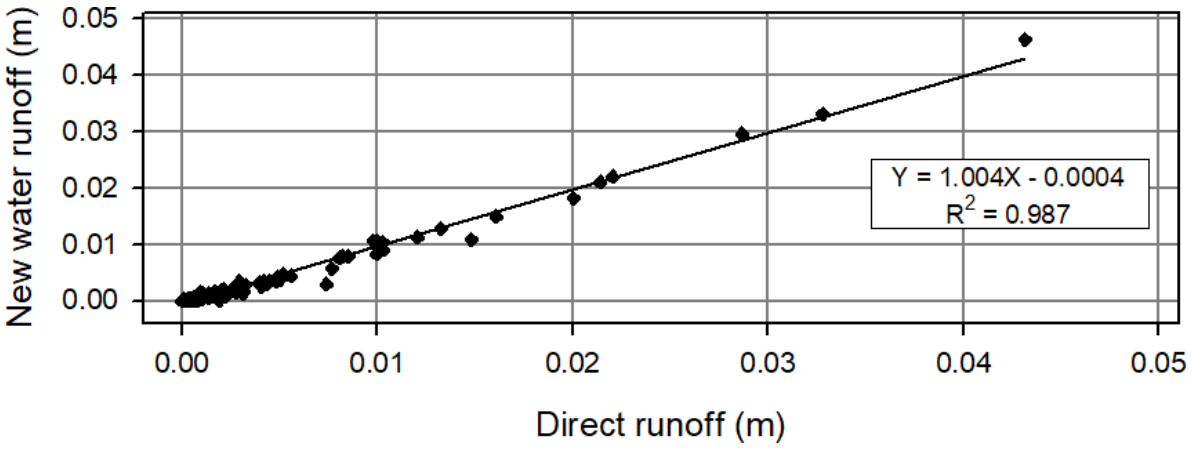

Figure 6. Relationship between event new water runoff at UTLP based on a conductivity mass balance (CMB) and event direct runoff obtained from a recursive digital filter (RDF; Eckhardt 2004) separation method; regression lines were obtained for each development phase obtained using BFI_{max} of 0.75.

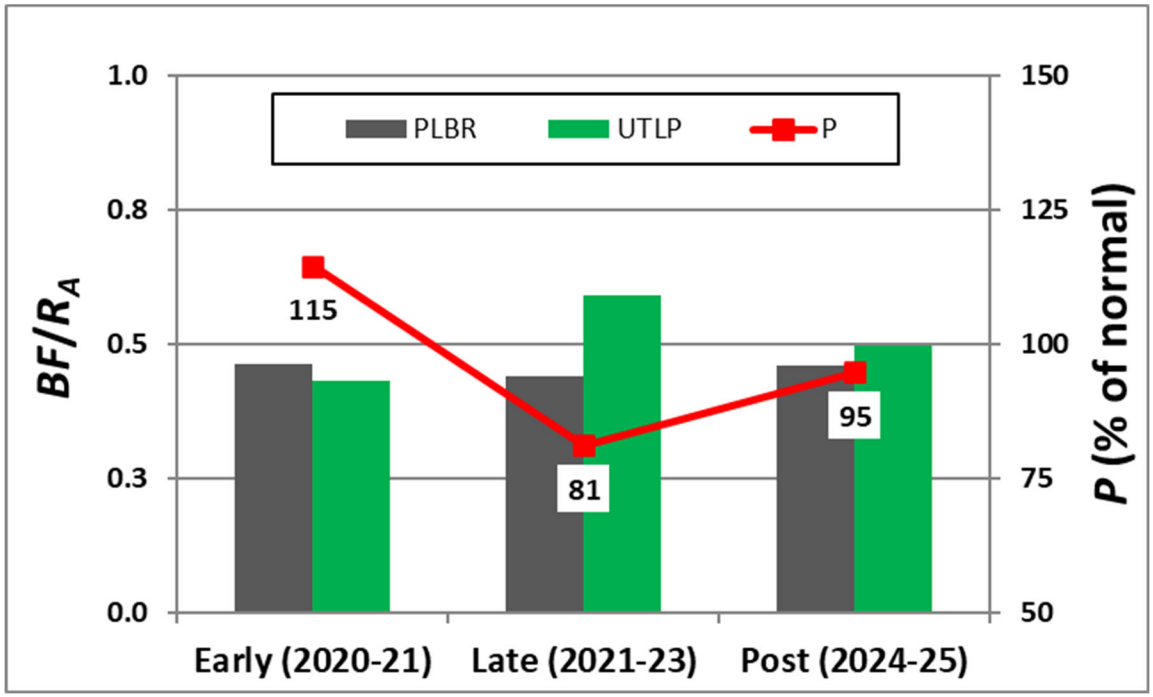

Figure 7. Annualized values of the baseflow index (i.e., BF_A/R_A) for the PLBR and UTLP watersheds during the three phases of development; annualized precipitation values (expressed as a percentage of normal) also shown.

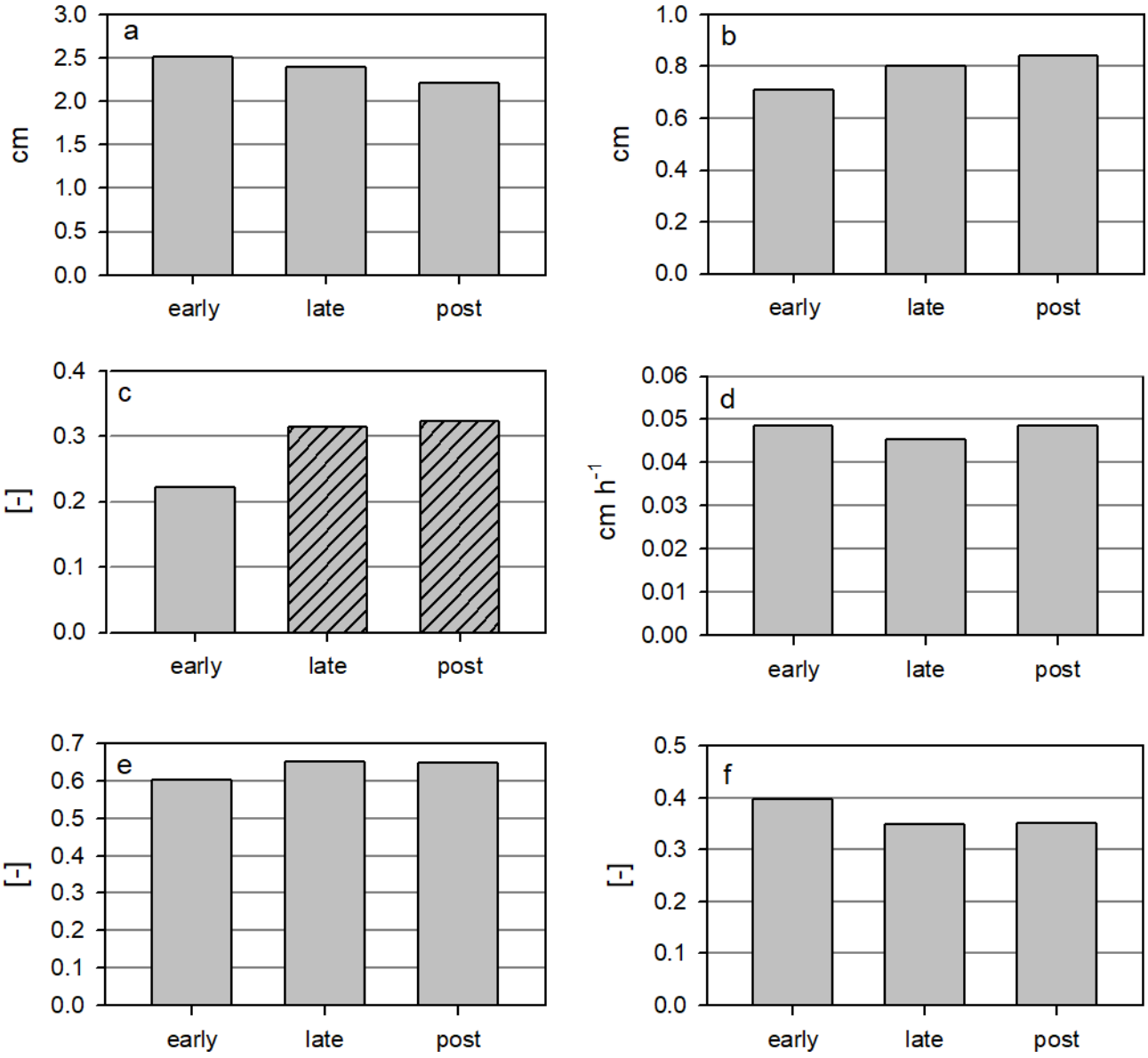

Figure 8. Comparisons of mean values of six hydrologic event metrics (a: areal rainfall; b: runoff (volume); c: runoff ratio; d: peak runoff; e: direct runoff coefficient; and f: baseflow coefficient) for PLBR based on event data measured during the three phases of development (early, late, and post). Means values shown with different patterns are statistically different based on a t-test ($P \leq 0.05$).

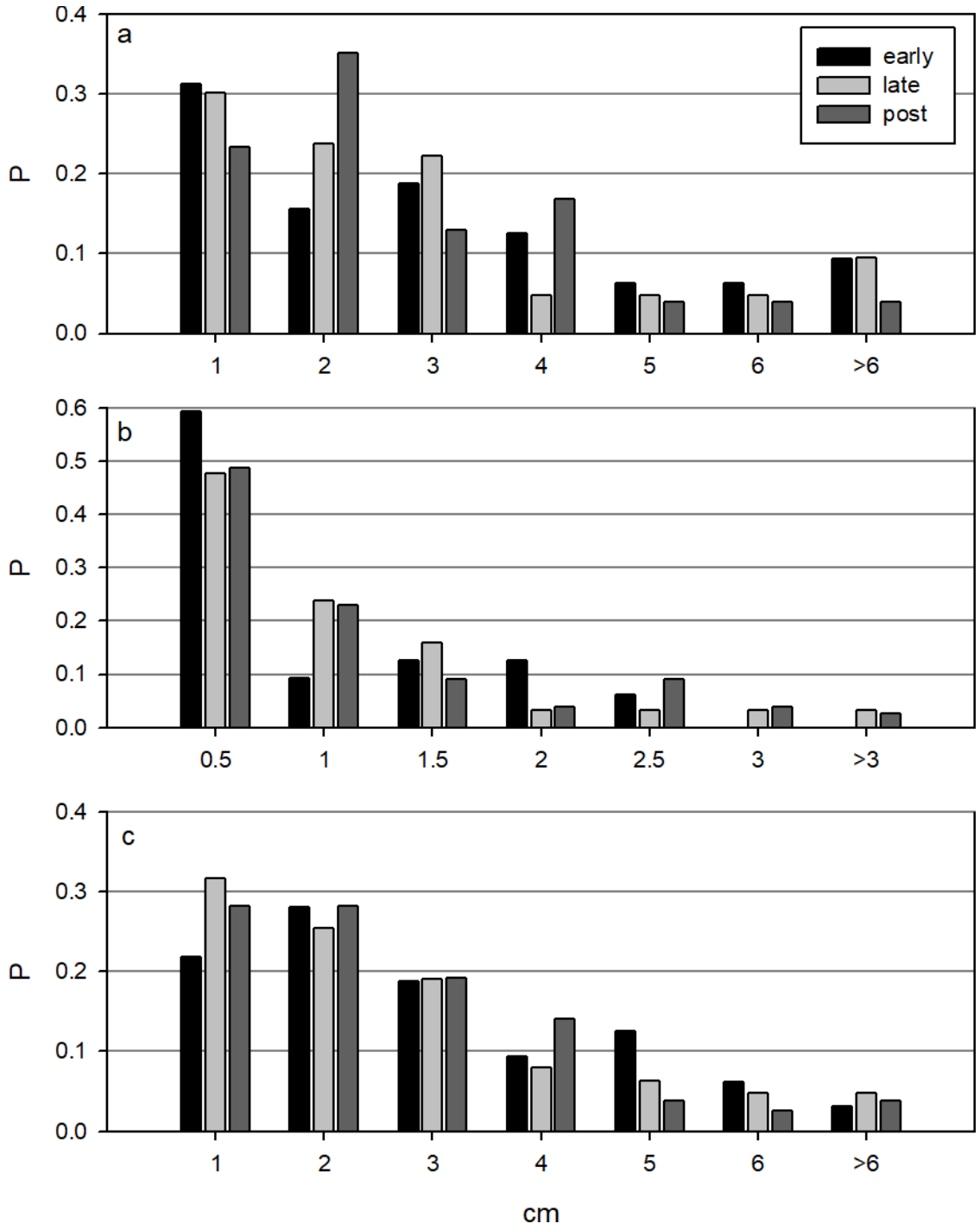

Figure 9. Frequency distributions of a) event areal rainfall, b) event maximum 1-hour rainfall, and c) event runoff for PLBR for the three phases of development (early, late, post).

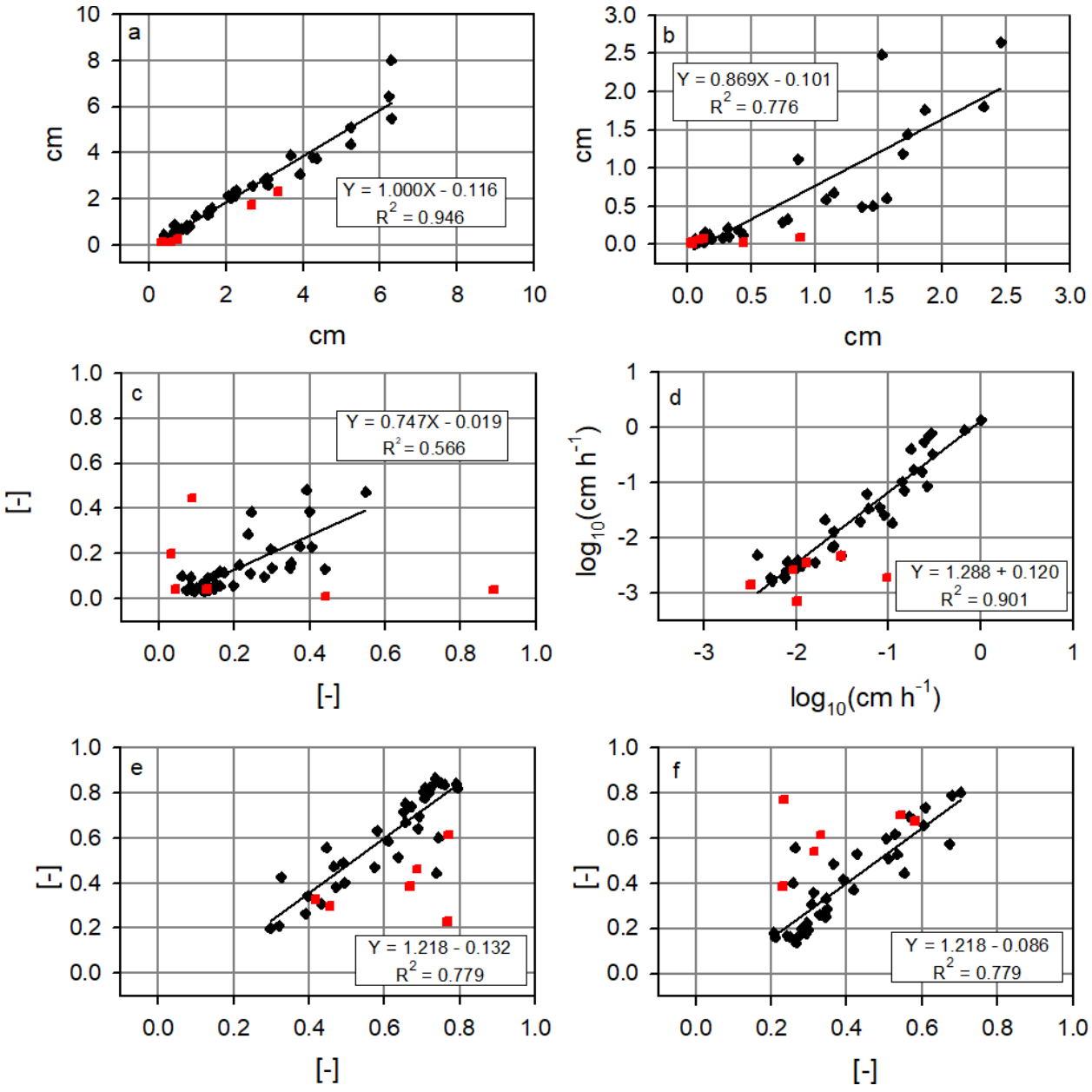

Figure 10. BACI regression models (UTLP, y-zxis vs. PLBR, x-axis) for six hydrologic metrics based on event data (black diamonds) analyzed for the early phase of development: a) areal rainfall; b) areal runoff (volume); c) runoff ratio; d) peak runoff (log transformed units to eliminate heteroscedasticity); e) direct runoff coefficient; and f) baseflow coefficient. Statistically significant regression lines and BACI model equations also shown. Storms graphed as red squares did not pass the rainfall C.V. criterion and are considered "outliers" for this analysis.

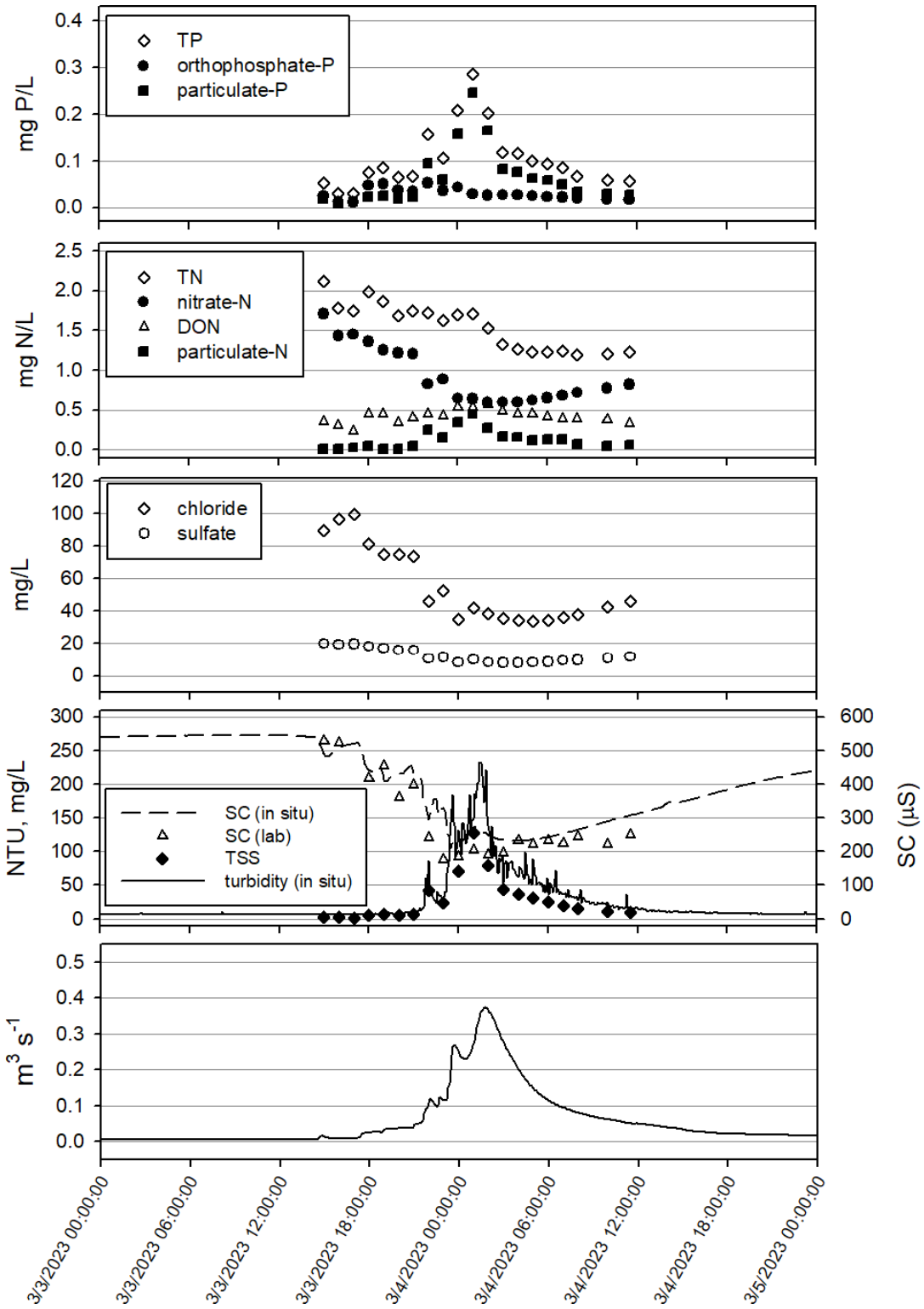

Figure 11. Stream discharge and measured concentrations in PLBR samples analyzed from storm event "AE" (3/23 – 24/2023).

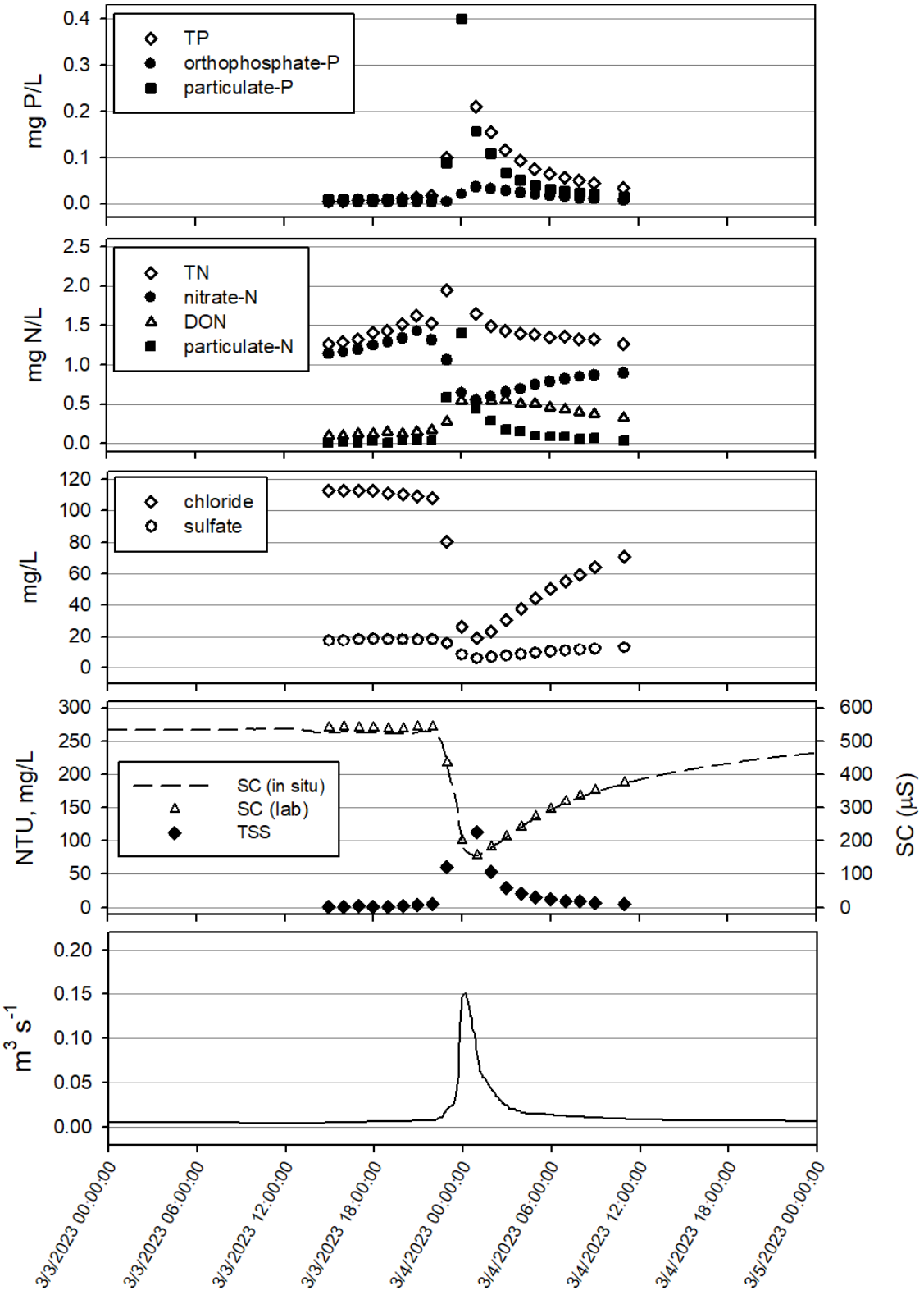

Figure 12. Stream discharge and measured concentrations in UTLP samples analyzed from storm event "AE" (3/23 – 24/2023); no field turbidity data available for this event due to instrument failure.

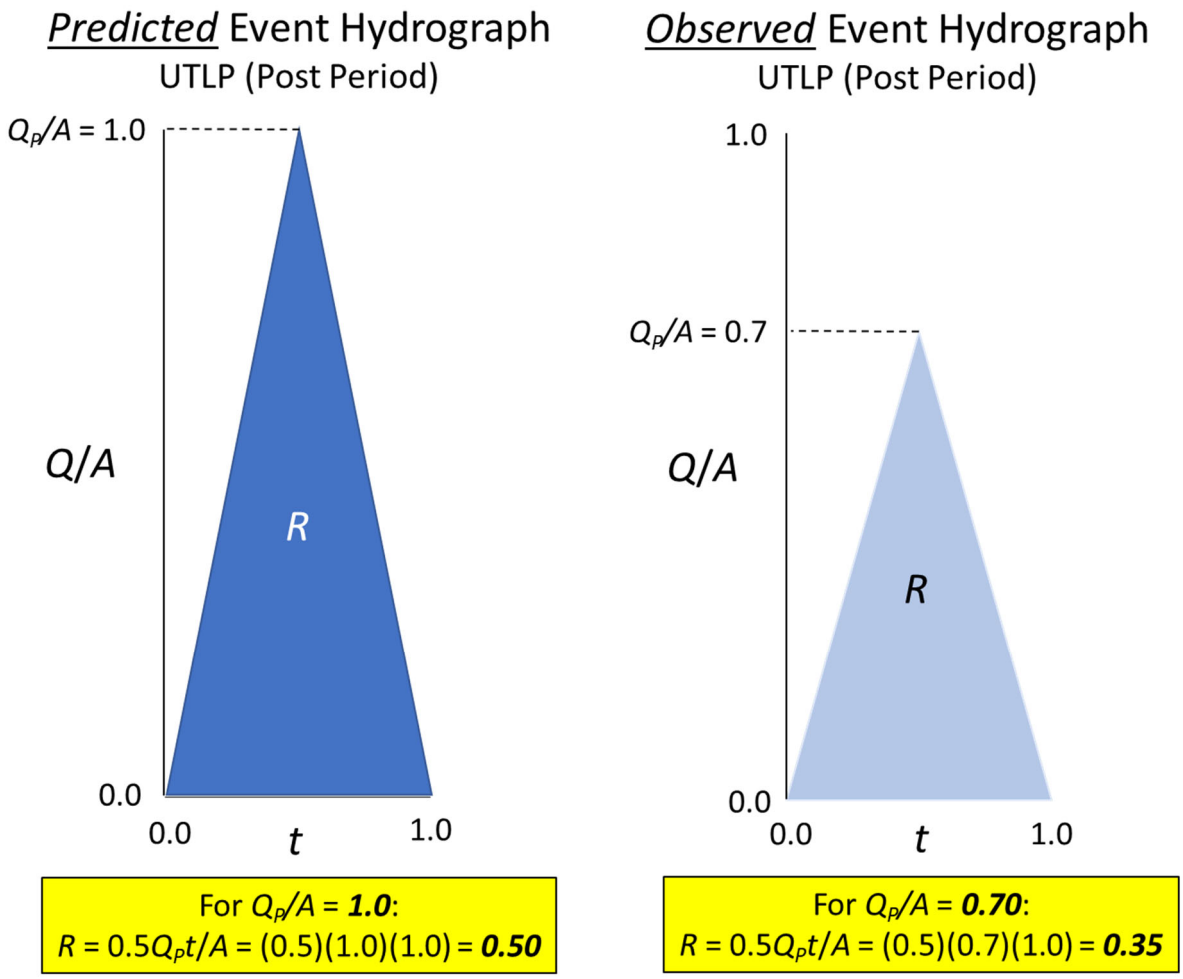

Figure 13. Conceptual model of the effects of stormwater retention on event runoff (R) and event peak discharge (Q_p) per unit watershed area (A).

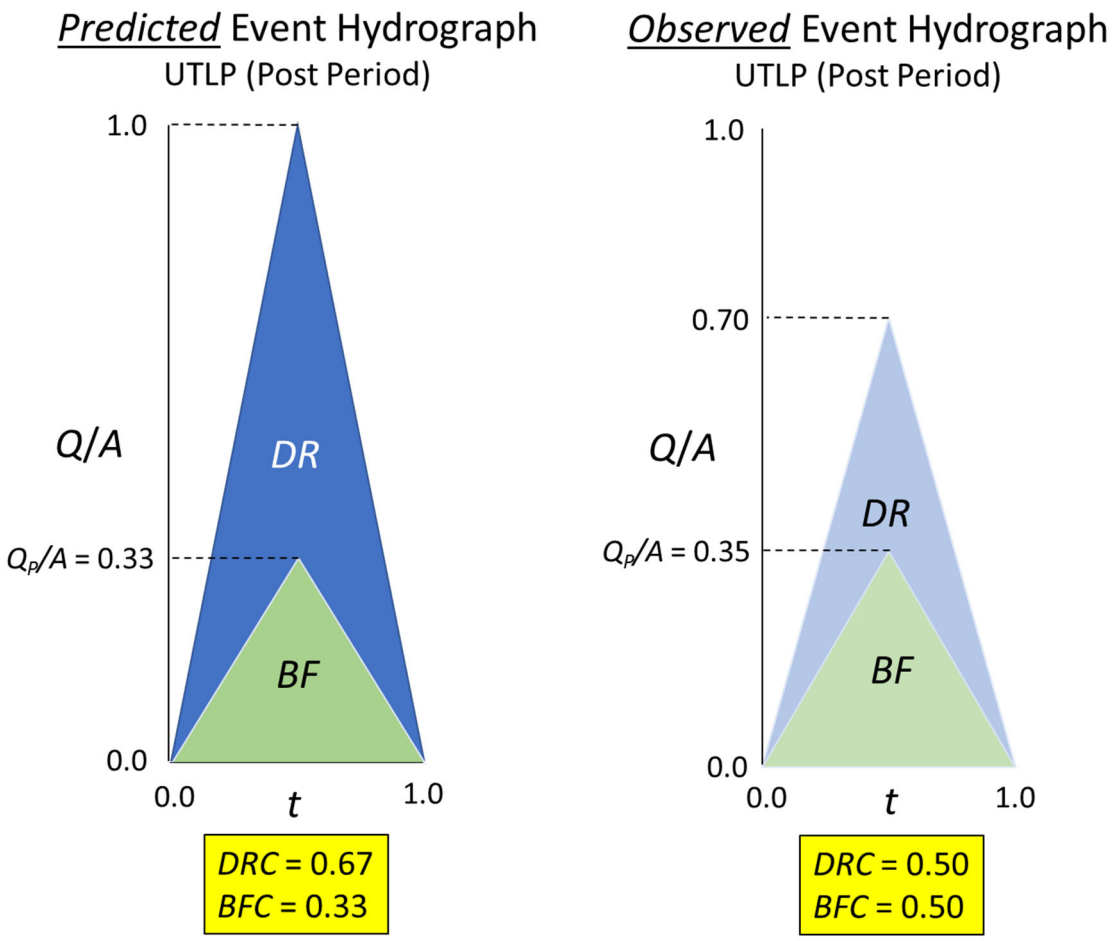

Figure 14. Conceptual model of the effects of stormwater retention on event peak discharges per unit area (Q_p/A) and volumes of baseflow (BF) and direct runoff (DR) given corresponding changes in the direct runoff coefficient (*DRC*) and baseflow coefficient (*BFC*).

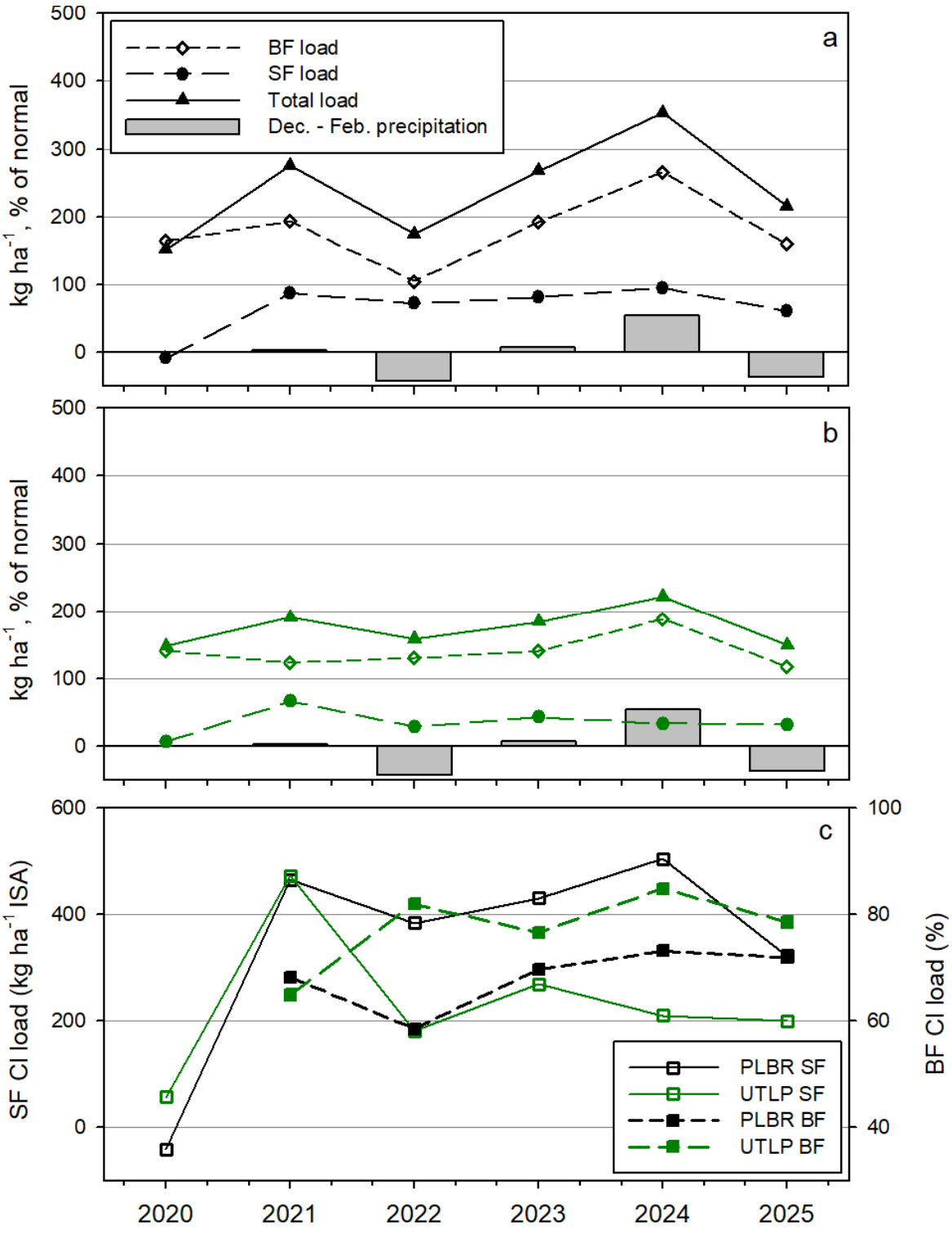

Figure 15. Estimated annual (water year basis) BF, SF, and total loads of Cl from a) PLBR and b) UTLP watersheds (Dec. – Feb. precipitation also shown); and c) annual SF Cl loads per unit impervious surface area (ISA) and BF Cl loads (%) from the two watersheds. Water year 2020 is a partial year (April – September).

a)

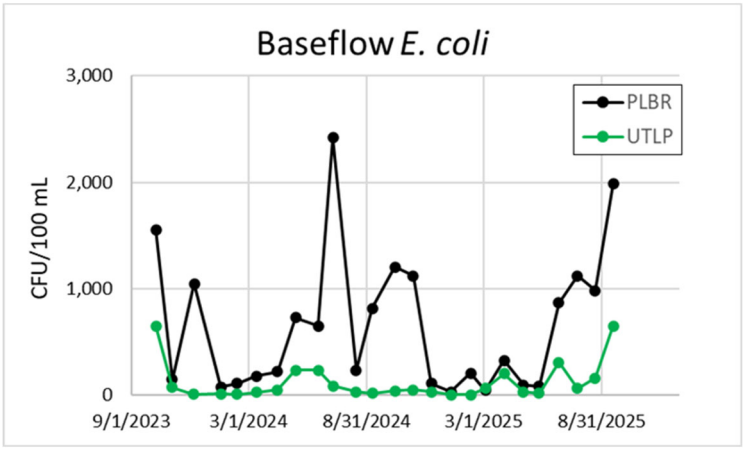

b)

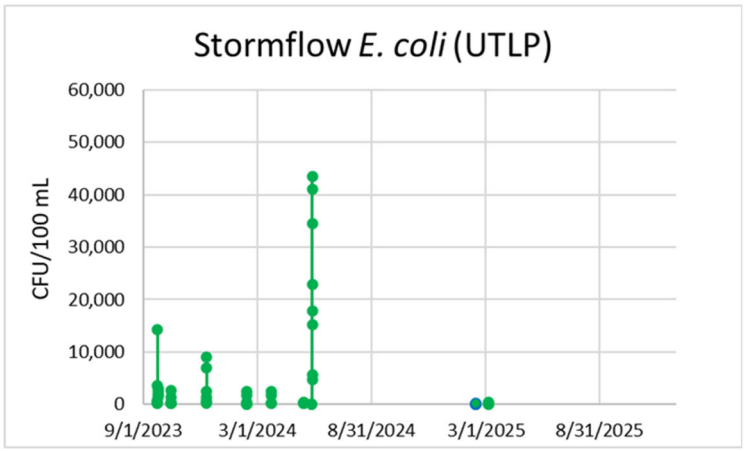

c)

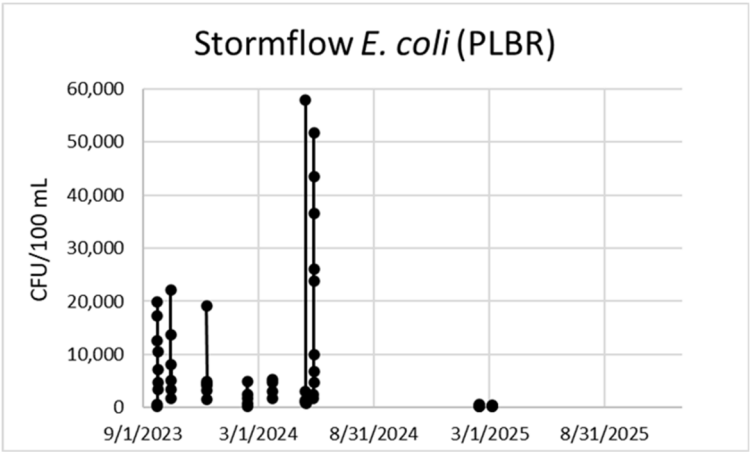

Figure 16. *E. coli* concentrations in a) baseflow samples at the two stations; b) stormflow samples at UTLP; and c) stormflow samples at PLBR.

a)

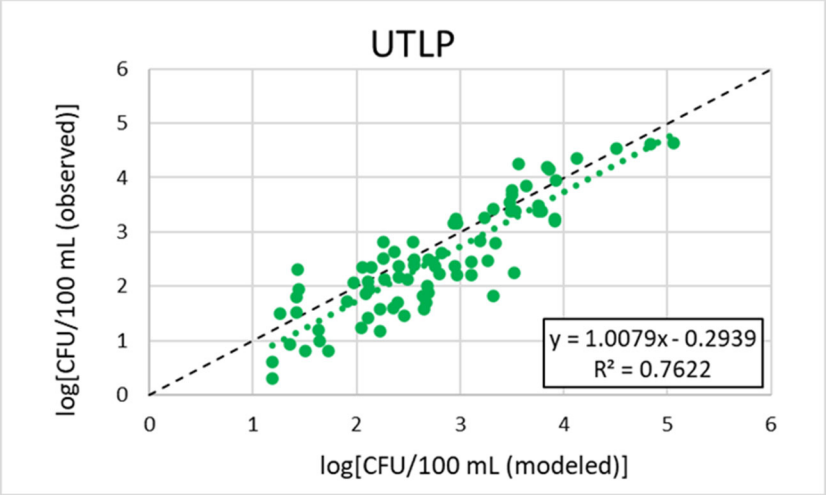

b)

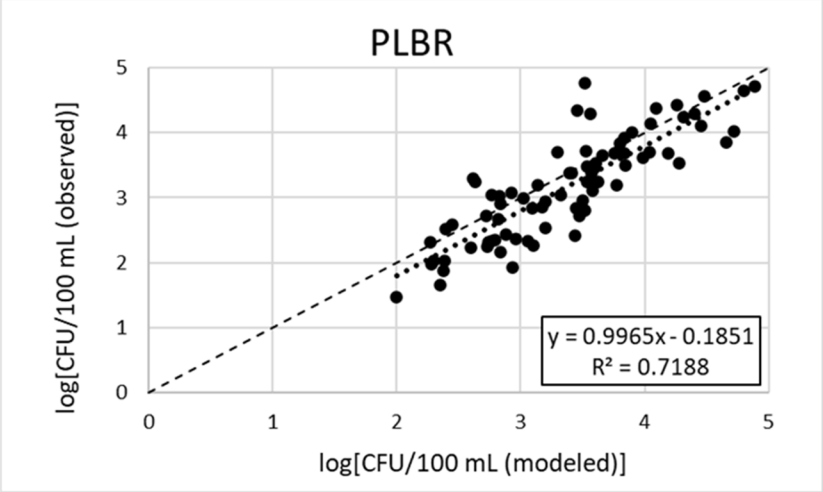

Figure 17. Observed vs. LOADEST-modeled *E. coli* concentrations (log_{10} units) in samples collected at a) UTLP and b) PLBR during the study.

a)

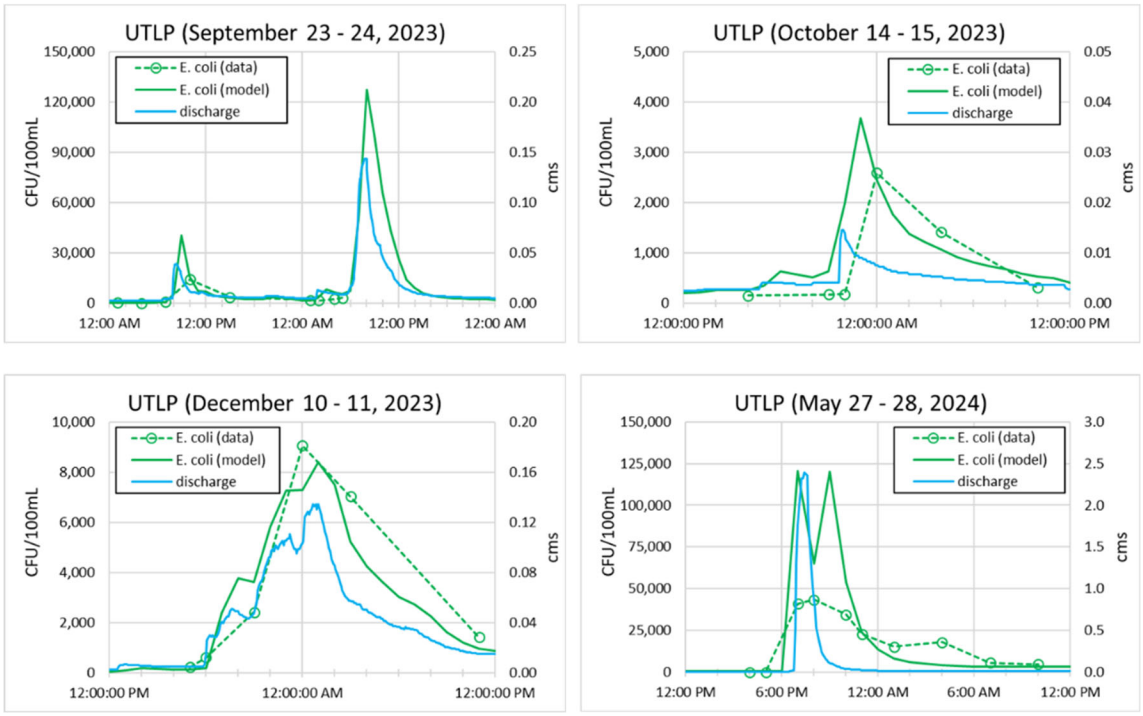

b)

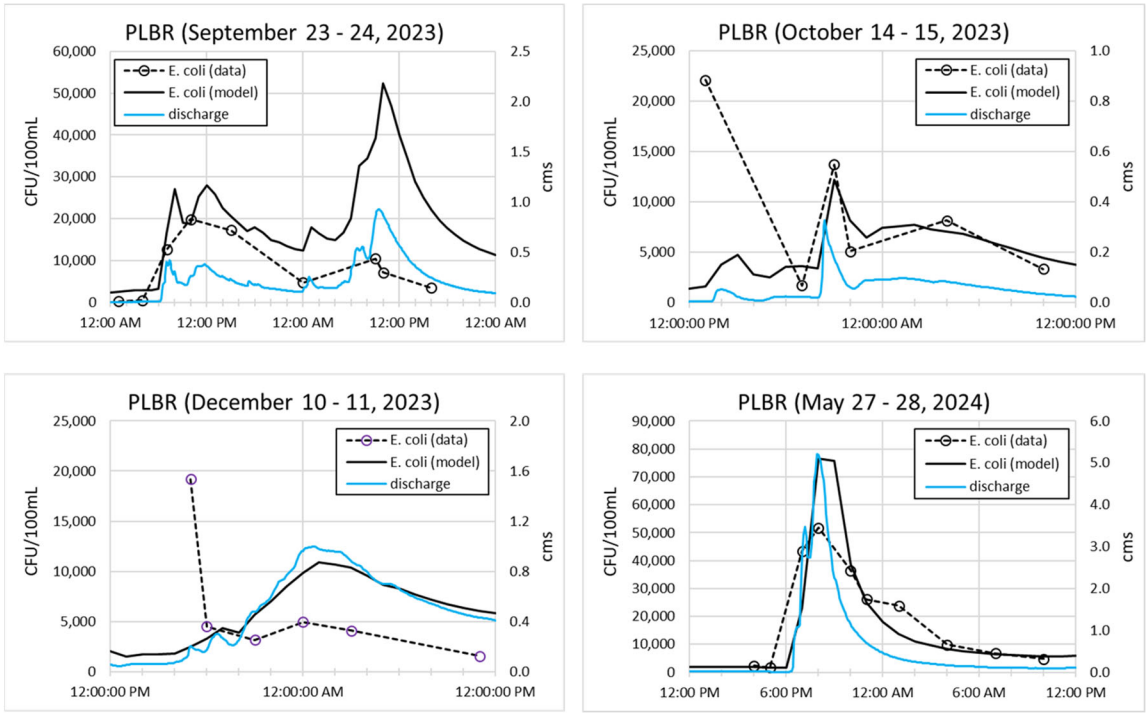

Figure 18. Comparison of observed and modeled stormflow *E. coli* concentrations for four storms sampled at a) UTLP; and b) PLBR. Stream discharge also shown.

a)

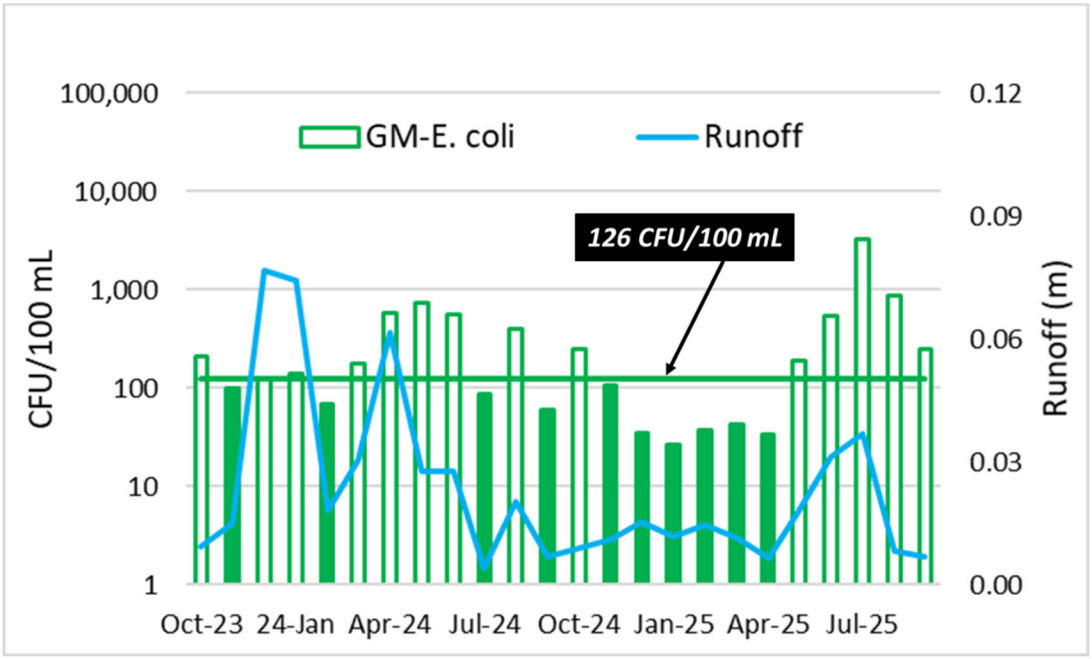

b)

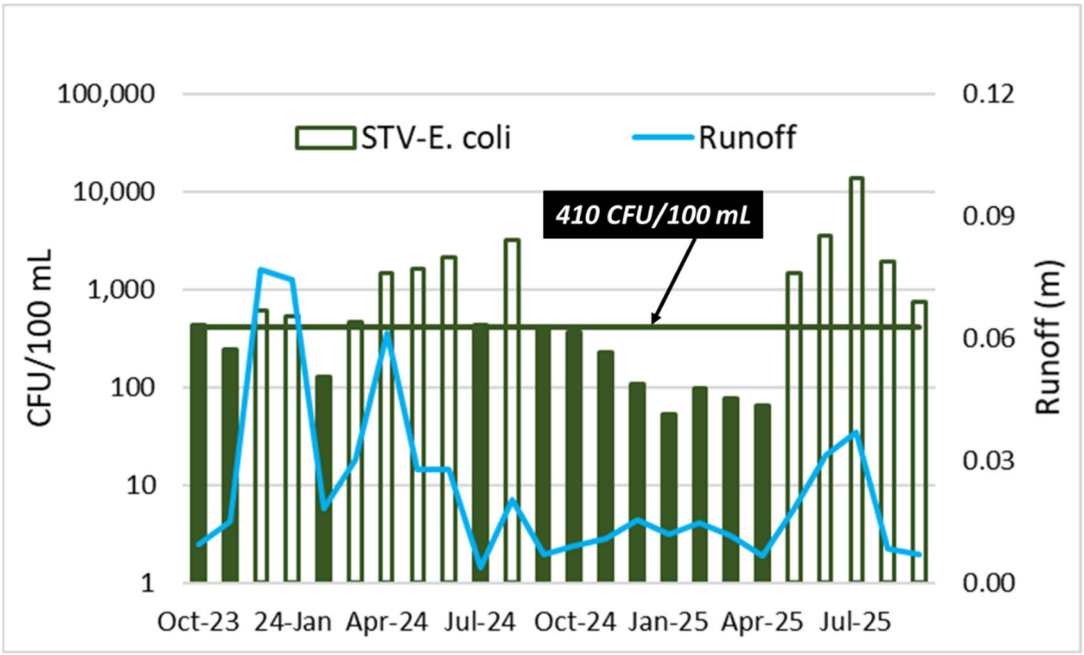

Figure 19. Monthly *E. coli* exceedances (open bars) using the a) geometric mean and b) standard threshold value comparisons for UTLP during the two-year study. Monthly runoff also shown.

a)

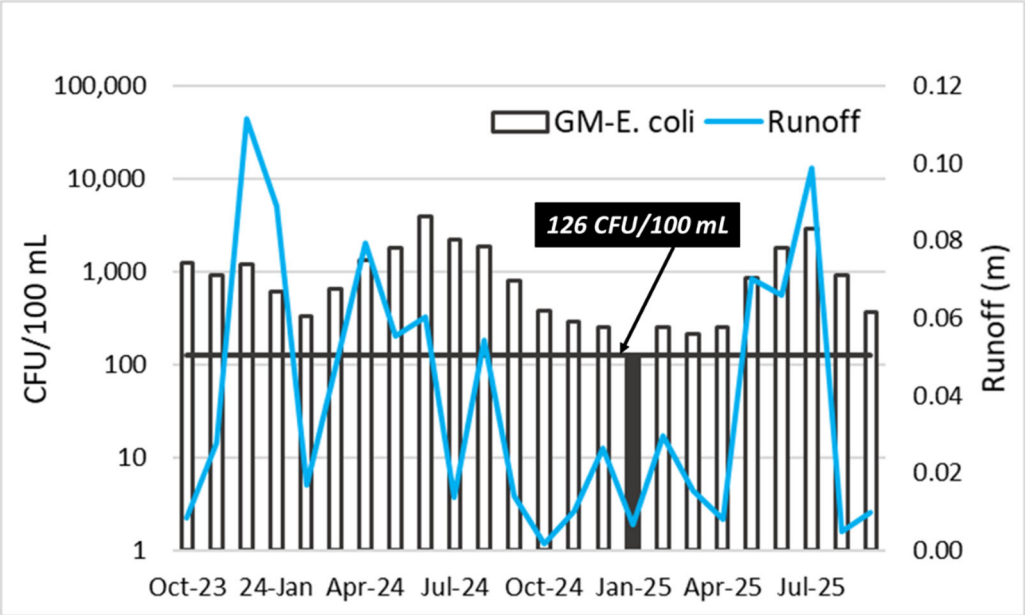

b)

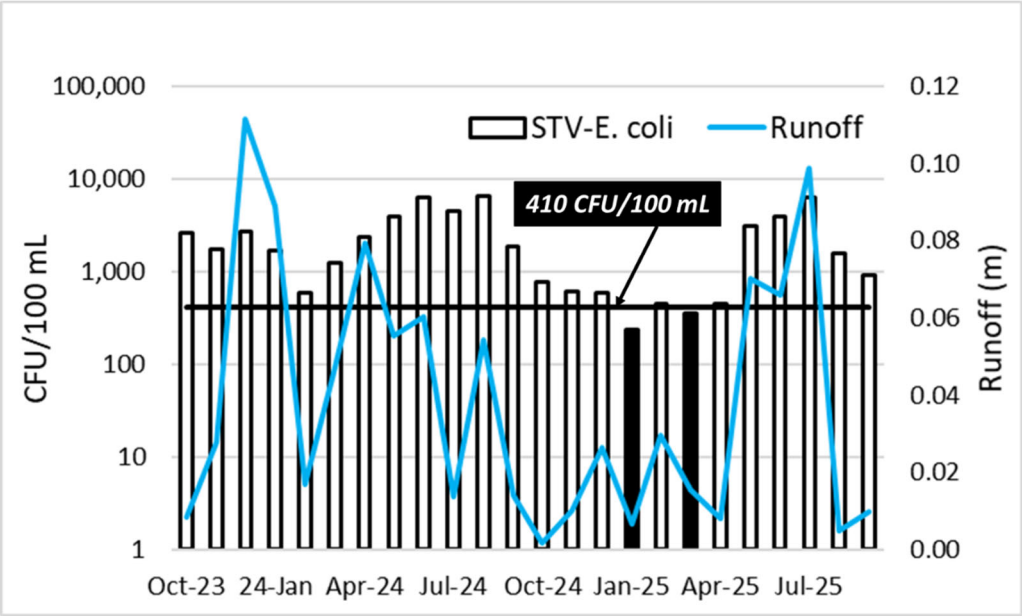

Figure 20. Monthly *E. coli* exceedances (open bars) using the a) geometric mean and b) standard threshold value comparisons for PLBR during the two-year study. Monthly runoff also shown.

Appendix A. Land use changes (UTLP)

a)

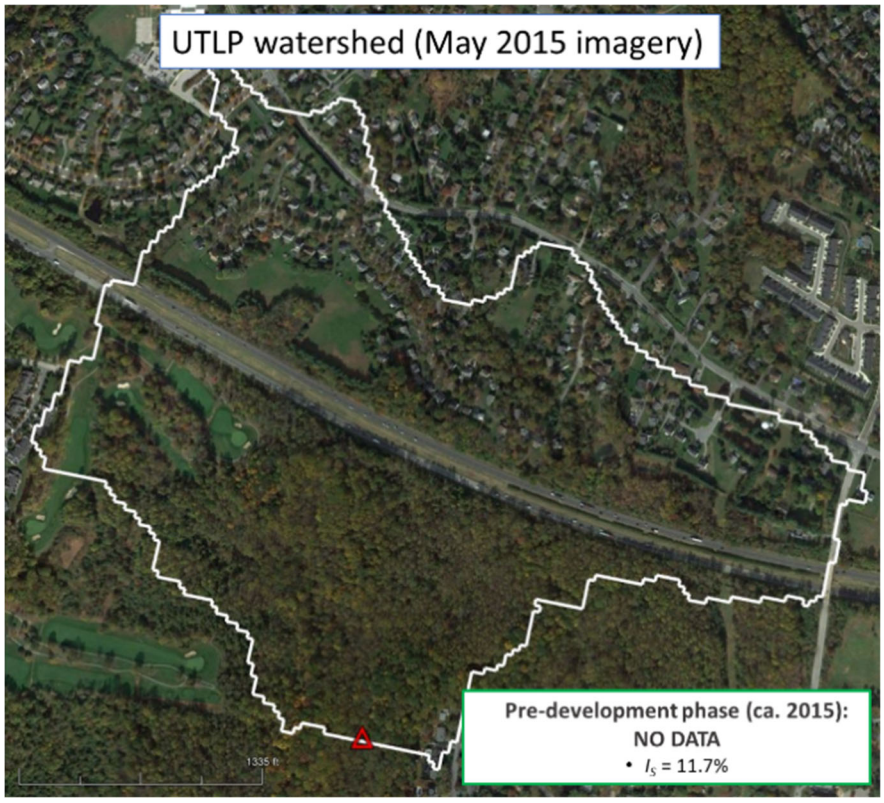

b)

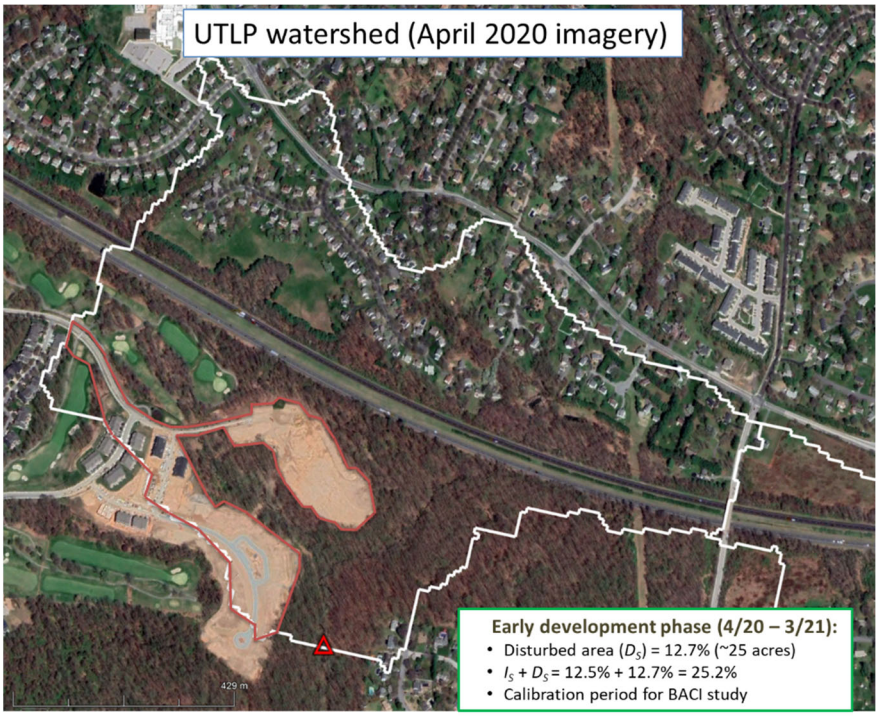

c)

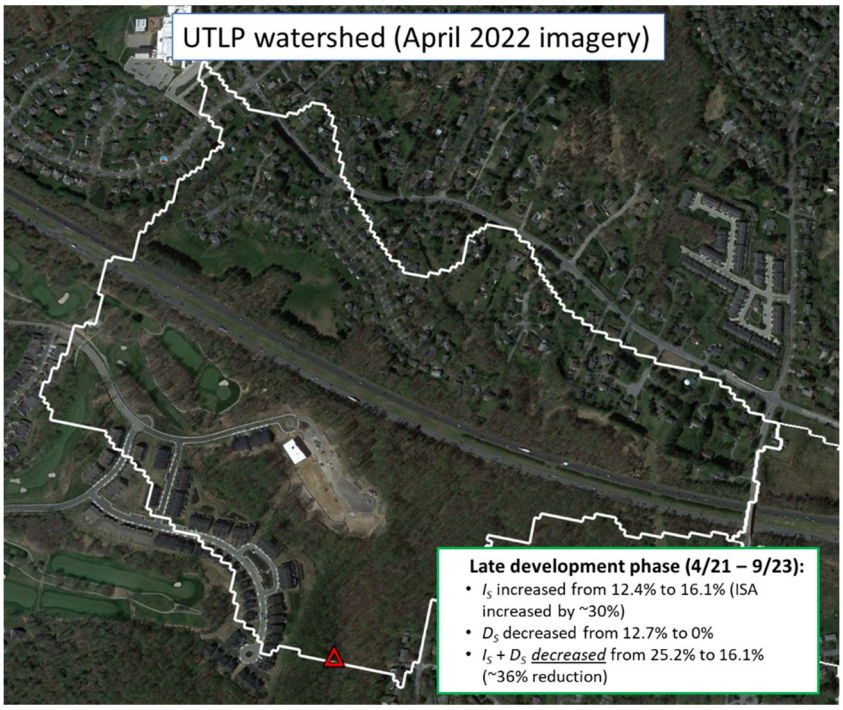

d)

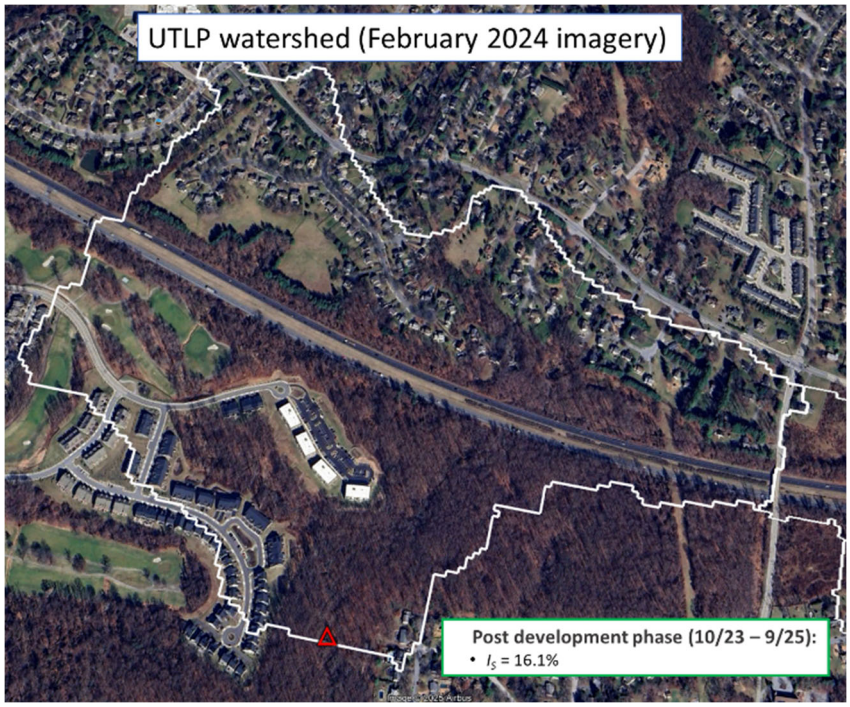

Figure A-1. Land use changes in the UTLP watershed (2015 – 2025) visualized using Google Earth imagery from a) May 2015; b) April 2020; c) April 2022; and d) February 2024. Red triangle shows location of stormwater monitoring system. Red boundary line in April 2020 image demarcates the limit of disturbance of most recent phase of development.

Appendix B. Example chemical hydrograph separation using specific conductance.

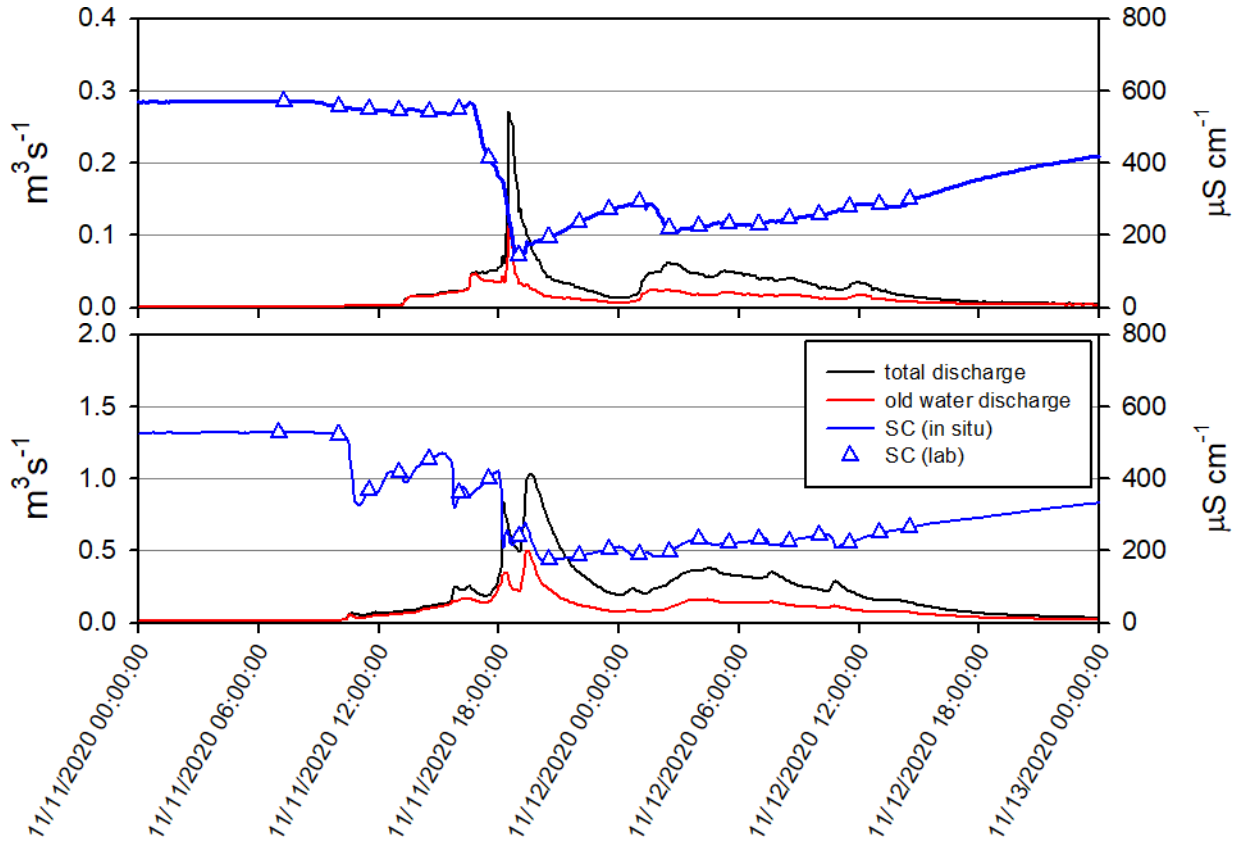

Figure B-1. Example chemical hydrograph separation for event "K" (11/11 – 11/12/20) for UTLP (top panel) and PLBR (lower panel) using the conductivity mass balance (CMB) method. New water discharge (not shown) is the difference between total discharge and old water discharge.

Appendix C. Load modeling methods and results.

Two models were used to estimate loads for the 17 different water quality constituents measured in the UTLP and PLBR watersheds. The first model that was used was LOADEST—an empirical loading model developed by USGS (Runkel et al. 2004; Cohn et al. 1989) that considers load variations as a function of discharge and time; the model has the capacity to address both long-term temporal and seasonal variations. LOADEST can be used with hourly or daily concentration (and discharge) data, so our first attempt made use of the higher resolution hourly data to estimate loads for the two watersheds. In general, the results using LOADEST and the hourly data file for PLBR were fairly successful with models explaining large percentages of the variation in the data with acceptable bias and producing high NSE values for most constituents; three constituents were exceptions to that rule, however: all suspended or particulate constituents (TSS, PP, and PN). These constituents generated outputs that did not meet the standard bias percentage criterion (±25%) in LOADEST or the accepted goodness-of-fit criterion (i.e., *NSE* > 0). The LOADEST modeling results for UTLP using hourly data were even less impressive: only ten constituents were modeled satisfactorily, with seven (TSS, PP, PN, OP, TP, TDP, NH_4-N) considered unsatisfactory. It was concluded that the hourly LOADEST model may not be a satisfactory loading model for small, flashy watersheds like UTLP as others have suggested, so an effort was made to find a satisfactory "plan B" model.

We first attempted an alternate LOADEST modeling approach that involved the use of a hybrid daily calibration dataset that might reduce some of the effects of the "flashiness" on the developed models. For all days in the record with baseflow samples only, the mean daily concentration was equated to the measured concentration for each constituent. For each day for which we had one or more analyzed stormflow samples, we computed a daily discharge-weighted mean concentration for each constituent. Lastly, we merged the concentration datafile with the mean daily discharge data file to create the final calibration file. The estimation files were based on the entire record of mean daily discharge developed for each watershed. This approach was a slight improvement on the initial LOADEST effort, but it still failed to produce satisfactory load estimates for the same constituents as in the previous version. Therefore, the decision was made to use those results that were considered satisfactory, but use yet another approach for those constituents that were not modeled satisfactorily with LOADEST.

For those constituents, we used a very simple "C-Q" model (e.g., Bieroza et al. 2018, Knapp et al. 2020) in which the daily (discharge-weighted mean) concentration (NOT the load!) is modeled as a function of the mean daily discharge; a power law form of the model is assumed (i.e., the actual model is of the form $logC = a logQ + b$). Daily loads (*CQ*) were computed using both the observed *C* data and the predicted *C* results for the same dates; this allowed for an equivalent calculation of the load *NSE* using the same formula as in LOADEST. Censored

observations were not used in the C-Q modeling approach and we found that we had to treat one datapoint (for 10/29/21) in each constituent file as an outlier to achieve satisfactory results for UTLP. We also considered the possibility that the C-Q relationships may have changed over time at UTLP, so we explored the use of three different models (one for each of the three development periods). For only one constituent (TSS) was the *NSE* higher than using just one C-Q model, so we used that model in our final analysis. Finally, we estimated daily loads of each constituent for the entire project period using one or the other modeling approach and then time-integrated the loading results for the three development periods. We did not "mix and match" models, however. Each constituent was modeled in the same way in both watersheds (Table C-1).

We also successfully used LOADEST and the hourly data to estimate *E. coli* loads (and concentrations) in the two watersheds for the post-development period. This approach recognizes the demonstrated importance of hydrometeorological drivers (i.e., antecedent conditions, stream discharge, rainfall, etc.) of microbial transport processes in small watersheds (Stumpf et al. 2010, Rowny and Stewart 2012, Stallard et al. 2016, Wang et al. 2018), as well as prior evidence of the utility of this particular model in simulating *E. coli* levels and loads (Dwivedi et al. 2013).

Table C-1. Load models with goodness-of-fit indices (R^2, *NSE*) and annualized results (all units of kg ha^{-1} y^{-1} unless indicated) for the three development periods.

Constituent	Model No.*	PLBR						UTLP					
		R^2	NSE	n	Early load	Late load	Post load	R^2	NSE	n	Early load	Late load	Post load
SC (mS ha^{-1})	1	0.96	0.65	182	1503	1179	1655	0.93	0.82	176	1002	799	996
TSS	2	0.58	0.54	182	169	110	211	0.48	0.46	174	914	438	778
Cl	1	0.93	0.39	181	278	207	255	0.86	0.56	175	204	161	186
IC-NO_3-N	1	0.95	0.74	181	2.55	2.00	2.36	0.93	0.84	175	2.15	1.73	2.28
SO_4	1	0.96	0.51	181	41.1	39.0	50.6	0.97	0.89	175	25.0	22.6	26.8
TP	2	0.77	0.74	182	0.63	0.43	0.74	0.70	0.69	175	0.73	0.25	0.75
TN	1	0.99	0.86	181	5.21	4.08	5.30	0.98	0.82	175	4.60	3.00	4.93
TDP	2	0.68	0.43	182	0.23	0.16	0.26	0.90	0.84	176	0.18	0.07	0.18
TDN	1	0.99	0.91	181	4.32	3.42	4.26	0.97	0.94	175	4.20	2.95	4.91
PP	2	0.58	0.55	154	0.39	0.27	0.45	0.53	0.52	98	0.50	0.17	0.51
PN	2	0.68	0.63	142	0.81	0.55	0.94	1.00	0.22	139	1.73	0.59	1.80
PO_4-P	2	0.82	0.66	182	0.15	0.11	0.17	0.87	0.86	176	0.09	0.05	0.11
NH_4-N	2	0.54	0.52	179	0.13	0.09	0.12	0.64	0.61	172	0.06	0.03	0.06
NO_2-N	1	0.94	0.66	182	0.03	0.03	0.04	0.92	0.19	175	0.02	0.01	0.02
FIA-NO_3-N	1	0.96	0.73	182	2.62	2.01	2.45	0.93	0.84	175	2.21	1.81	2.35
DON	1	0.97	0.06	181	1.92	1.49	2.18	0.89	0.52	169	0.97	0.69	1.23
SOC-P	1	0.96	0.39	141	0.07	0.06	0.10	0.92	0.86	88	0.03	0.02	0.04
E. coli (MCFU ha^{-1})	1	0.94	0.72	79	N/A	N/A	5.6×10^5	0.88	0.48	78	N/A	N/A	9.6×10^5

*Model 1 = hybrid daily LOADEST; model 2 = hybrid daily C-Q model (see text for modeling details)

Appendix D. Hydrographs, hyetographs, and hydrograph separation results.

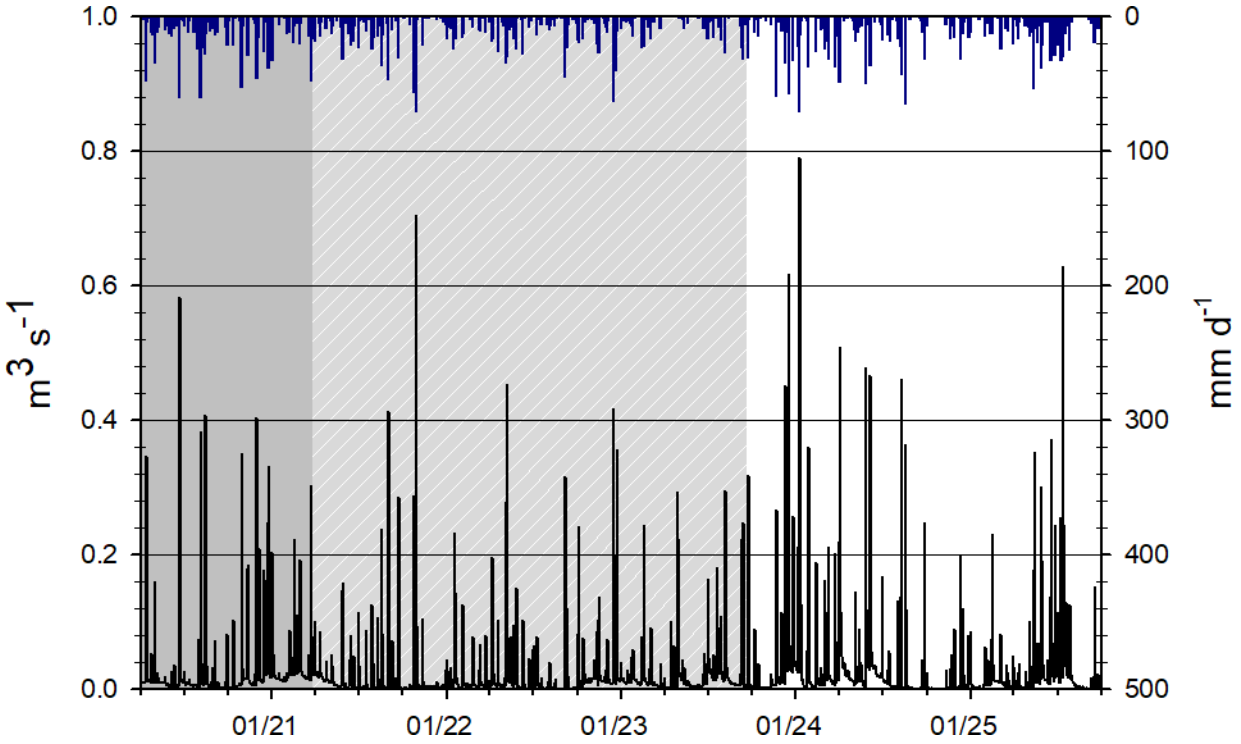

Figure D-1. Long-term streamflow (mean daily discharge) hydrograph and hyetograph (daily precipitation) for the PLBR watershed (4/1/20 – 9/30/25). Dark grey shading indicates early development period (4/1/20 – 3/31/21); light grey shading indicates late development period (4/1/21 – 9/30/23); and white area indicates post development period (10/1/23 – 9/30/25).

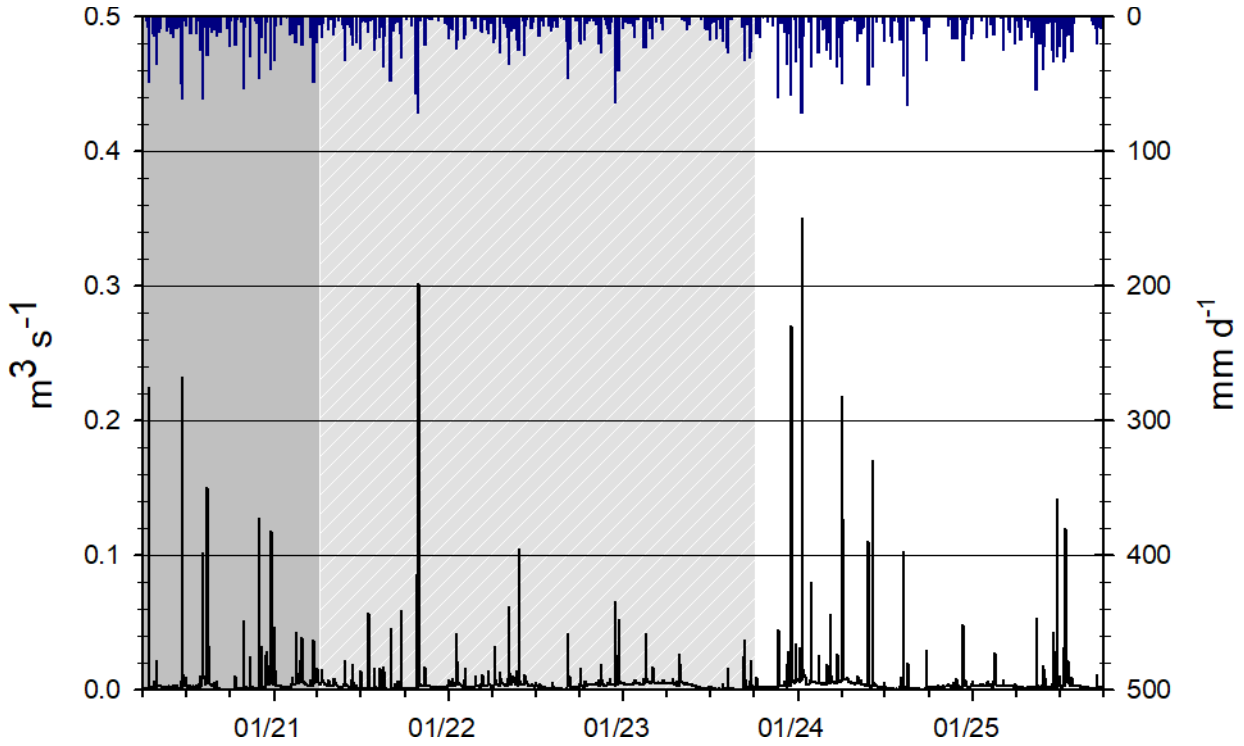

Figure D-2. Long-term streamflow (mean daily discharge) hydrograph and hyetograph (daily precipitation) for the UTLP watershed (4/1/20 – 9/30/25). Dark grey shading indicates early development period (4/1/20 – 3/31/21); light grey shading indicates late development period (4/1/21 – 9/30/23); and white area indicates post development period (10/1/23 – 9/30/25).

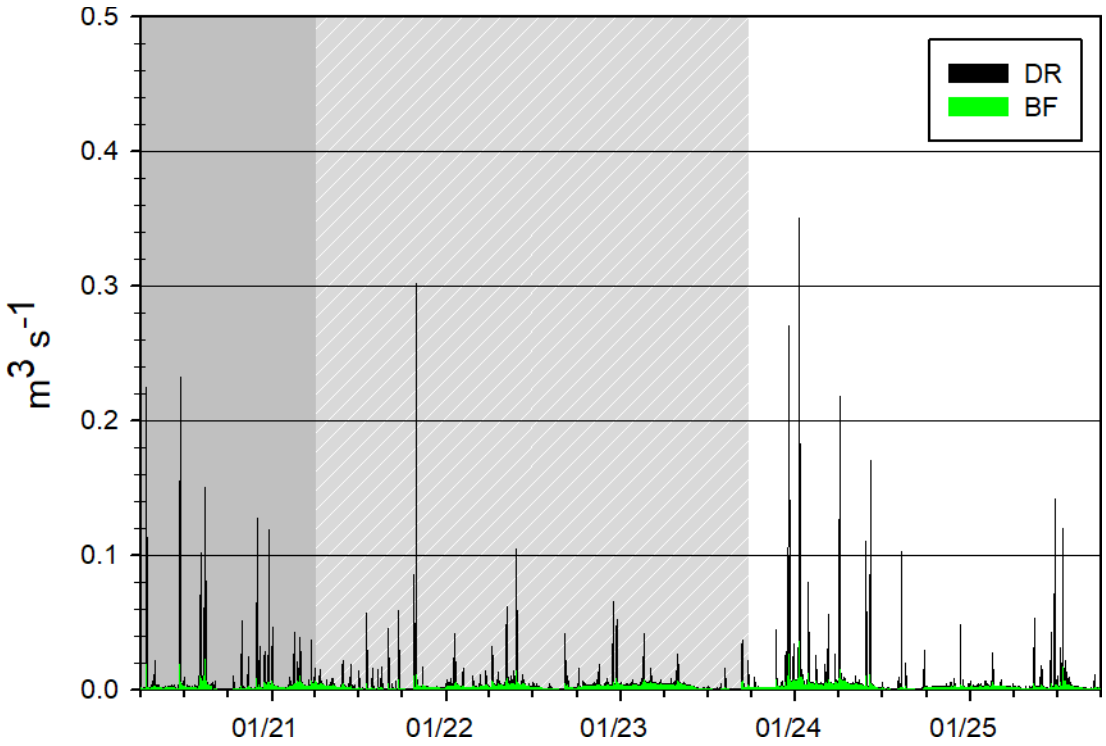

Figure D-3. Long-term direct runoff (DR) and baseflow (BF) hydrographs (mean daily values) based on the calibrated RDF separation for the UTLP watershed (4/1/20 – 9/30/25). Dark grey shading indicates early development period (4/1/20 – 3/31/21); light grey shading indicates late development period (4/1/21 – 9/30/23); and white area indicates post development period (10/1/23 – 9/30/25).

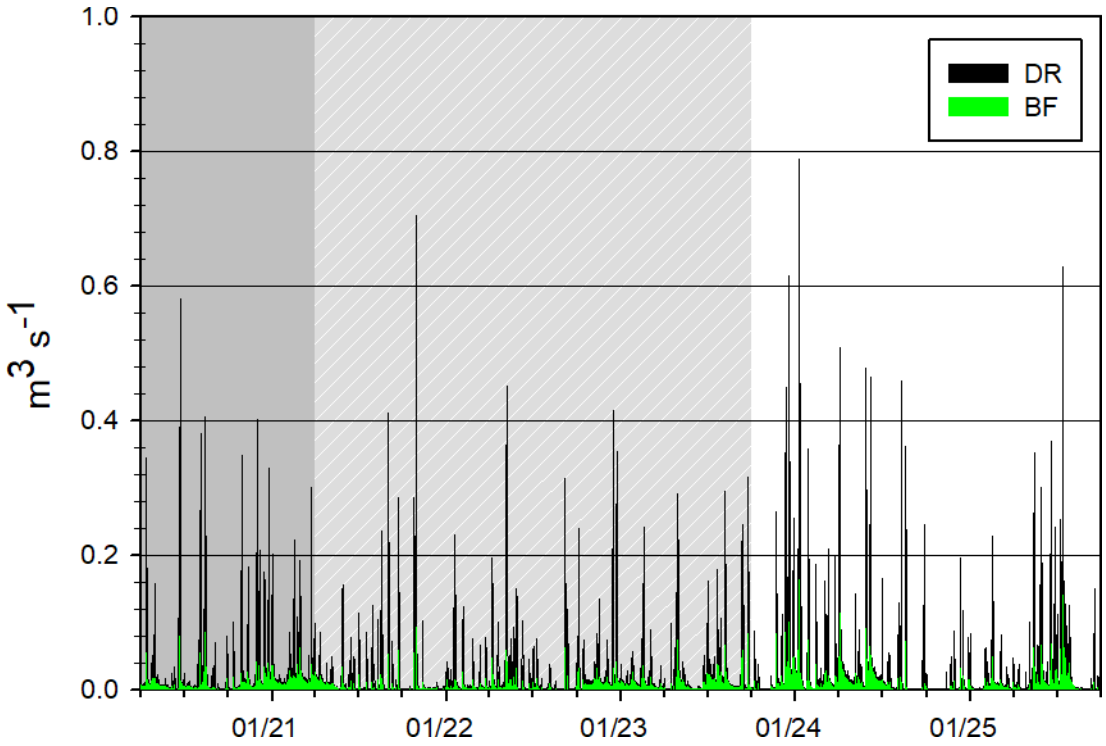

Figure D-4. Long-term direct runoff (DR) and baseflow (BF) hydrographs (mean daily values) based on the calibrated RDF separation for the PLBR watershed (4/1/20 – 9/30/25). Dark grey shading indicates early development period (4/1/20 – 3/31/21); light grey shading indicates late development period (4/1/21 – 9/30/23); and white area indicates post development period (10/1/23 – 9/30/25).

Appendix E. Data tables for stormflow events.

Table E-2. Event rainfall data. "Pilot study", "early" development, "late" development, and "post" development events shaded in light orange, brown, blue, and green, respectively.

Storm date(s)	Storm ID[1]	1-h rainfall (cm, Kappa sta.)	24-h rainfall (cm, Kappa sta.)	Areal rainfall (cm)	
				PLBR	UTLP
12/9-11/19	"A"	0.53	2.01	N/A	N/A
1/25-26/20	"B"	0.89	3.48	3.96	3.73
2/06-08/20	"C"	0.33	2.31	2.77	3.28
3/13/20	N/A	0.41	0.64	0.64	0.56
3/14-15/20	N/A	0.18	0.79	0.84	0.69
3/18-19/20	N/A	0.41	1.70	1.52	1.30
3/23/20	N/A	0.20	0.69	0.76	0.63
3/25/20	N/A	0.25	0.53	0.65	0.87
3/28/20	N/A	0.74	1.83	2.24	2.13
4/12-14/20	N/A	1.02	5.46	6.22	6.45
4/23-24/20	N/A	0.36	2.11	2.13	2.03
4/26-27/20	N/A	0.53	1.35	1.22	1.27
4/30-5/1/20	"D"	0.71	3.48	3.08	2.61
5/03-04/20	N/A	0.56	0.89	0.78	0.60
5/06-07/20	N/A	0.30	1.07	1.06	0.84
5/08-09/20	N/A	0.41	0.79	0.69	0.63
5/22/20	N/A	0.43	1.02	0.98	0.83
5/23/20	N/A	0.30	0.41	0.38	0.43
5/28/20	N/A	0.38	0.71	0.33	0.15
6/4-5/20	N/A	0.86	2.84	2.67	1.75
6/10-11/20	N/A	0.71	3.48	1.52	1.45
6/20-21/20	N/A	4.62	4.90	3.35	2.31
6/22-23/20	N/A	5.97	6.07	6.30	5.49
6/30-7/01/20	N/A	0.66	1.02	1.63	1.60
7/10-11/20	N/A	1.22	1.22	0.58	0.15
7/22-23/20	N/A	0.74	1.14	0.99	0.71
7/30-31/20	"E"	2.31	3.12	N/A	N/A
8/3-4/20	"F"	1.55	8.00	N/A	N/A
8/12-13/20	N/A	1.14	2.84	3.68	3.89
8/14-15/20	N/A	2.36	2.82	6.27	8.00
8/28-29/20	N/A	0.46	1.80	2.06	2.13
9/03-04/20	N/A	1.22	1.35	0.74	0.76
9/10/20	N/A	0.86	1.04	0.75	0.27
9/29-30/20	"G"	1.65	2.39	N/A	N/A
10/11-12/20	"H"	0.61	2.54	3.00	2.84
10/29-30/20	"J"	1.19	5.66	5.23	4.37
11/11-12/20	"K"	0.94	4.88	5.23	5.11
11/30-12/1/20	N/A	1.73	4.57	4.34	3.73

12/24-25/20	"L"	0.89	4.57	4.24	3.81
1/1-2/21	N/A	0.84	3.28	3.07	2.90
2/15-16/21	"N"	0.41	2.54	2.69	2.57
3/24-25/21	N/A	1.63	4.78	3.91	3.07
3/31-4/1/21	"Q"	0.66	2.39	2.26	2.39
5/28-29/21	"R"	2.26	4.29	4.65	4.27
7/17-18/21	"S"	0.64	1.07	1.50	2.82
8/17-19/21	"T"	0.79	4.37	5.54	5.26
8/20/21	N/A	0.46	1.40	1.30	1.14
9/1/21	"U"	0.71	4.75	4.24	3.68
9/23/21	"V"	1.80	3.05	2.87	2.92
10/25-26/21	N/A	1.91	5.72	6.10	6.60
10/29-30/21	"W"	1.83	7.14	6.83	6.76
1/16-17/22	N/A	1.07	2.44	2.49	2.49
2/2-4/22	"X"	0.25	1.96	2.82	2.44
4/5-6/22	"Y"	0.64	3.15	2.97	2.79
4/18-19/22	N/A	0.81	2.69	2.46	2.34
5/6-8/22	"Z"	0.94	5.36	6.88	6.25
5/22-23/22	N/A	0.71	1.65	1.57	1.85
5/27-28/22	N/A	1.88	2.51	2.84	3.07
6/08-09/22	N/A	2.13	2.79	3.43	3.43
6/22-23/22	N/A	0.20	1.32	1.27	1.42
7/08-09/22	"AA"	0.28	1.40	1.27	1.09
7/18-19/22	N/A	0.41	0.64	0.64	0.36
7/31/-8/1/22	N/A	0.20	0.46	0.81	0.86
8/04-05/22	N/A	0.56	1.04	1.12	0.99
8/05-06/22	N/A	0.61	0.74	0.81	1.04
8/14-15/22	N/A	0.30	0.69	0.76	0.66
8/17-18/22	N/A	1.32	1.35	0.53	0.33
9/5-7/2022	N/A	2.24	6.27	6.27	6.12
9/11-12/22	N/A	0.97	2.36	2.06	2.31
9/30-10/1/22	N/A	0.69	2.11	2.18	1.98
10/02-04/22	N/A	0.66	2.59	4.65	4.34
10/04-05/22	N/A	0.18	0.38	0.43	0.33
10/13-14/22	N/A	0.51	1.70	1.73	2.31
10/17-18/22	N/A	0.30	0.41	0.38	0.46
11/11-12/22	"AB"	0.86	2.34	2.36	2.24
11/15/16/22	"AC"	0.69	2.72	2.67	2.69
11/27/22	N/A	0.36	0.53	0.51	0.51
11/30-12/01/22	N/A	0.28	0.84	0.79	0.74
12/03-04/22	N/A	0.56	1.17	1.12	1.19
12/15-16/22	"AD"	0.66	6.91	7.04	6.48
12/22-23/22	N/A	0.76	5.05	5.05	4.57
12/31/22-1/01/23	N/A	0.25	0.86	0.86	0.79
1/05-06/23	N/A	0.20	0.36	0.20	0.13
1/12-14-23	N/A	0.18	0.66	0.86	0.69
1/19-20/23	N/A	0.28	0.51	0.56	0.58
1/22-24/23	N/A	0.15	1.12	1.04	0.91
1/25-26/23	N/A	0.48	1.50	1.32	1.32
2/12-14/23	N/A	0.58	2.39	2.46	2.29

2/16-18/23	N/A	0.89	3.68	3.68	3.81
2/27-28/23	N/A	0.36	0.91	0.84	0.84
3/3-4/23	"AE"	0.48	1.65	1.80	2.11
3/10-11/23	N/A	0.18	0.41	0.43	0.30
3/23-26/23	N/A	0.46	1.30	1.83	1.70
4/01-02/23	N/A	0.18	0.58	0.74	0.91
4/15-16/23	N/A	1.32	1.80	1.83	1.85
4/22-23/23	"AF"	1.30	1.68	2.54	1.70
4/28-5/1/23	"AG"	1.09	4.78	6.81	6.43
5/13-14/23	N/A	0.36	0.91	0.91	0.89
5/20-21/23	N/A	0.43	0.53	0.53	0.53
6/21-24/23	N/A	0.33	0.97	2.24	2.24
6/27-28/23	"AH"	0.79	0.86	0.51	0.18
6/30-7/1/23	N/A	0.91	0.97	0.92	0.95
7/1/23	N/A	1.60	1.68	1.37	1.03
7/14-15/23	N/A	1.52	1.55	0.97	0.57
7/21-22/23	N/A	1.93	2.26	1.80	1.43
7/24-25/23	N/A	0.51	0.79	0.63	0.54
7/28-29/23	N/A	1.73	1.78	2.34	2.67
8/6-7/2023	N/A	0.74	1.60	1.86	1.92
8/7-8/2023	N/A	2.39	2.64	2.85	3.17
8/10-11/23	N/A	0.05	0.05	0.88	0.93
9/08-09/23	N/A	0.66	0.89	1.33	0.74
9/10-12/23	N/A	1.19	2.31	2.28	3.71
9/12-13/23	N/A	2.11	3.20	3.04	3.12
9/17-18/23	N/A	0.23	0.61	0.60	0.60
9/22-25/23	"AJ"	1.07	3.84	5.47	5.18
10/7/23	N/A	1.02	1.19	0.79	1.24
10/14-15/23	"AK"	0.76	1.50	1.48	1.36
11/10-11/23	N/A	0.20	0.61	0.68	0.69
11/21-22/23	"AL"	1.19	5.99	5.54	5.50
11/26-27/23	N/A	0.28	0.48	0.43	0.42
12/1-2/23	N/A	0.13	0.43	0.46	0.42
12/3-4/23	N/A	0.38	1.14	1.35	1.38
12/10-12/23	"AM"	0.48	4.09	4.71	4.33
12/17-18/23	N/A	1.50	7.47	7.78	7.70
12/27-28/23	N/A	0.69	3.30	3.29	2.85
1/6-7/24	N/A	0.61	2.21	2.27	2.36
1/9-10/24	N/A	1.42	7.11	6.68	6.21
1/12-13/24	N/A	0.76	1.70	1.64	1.77
1/24-27/24	"AN"	N/A	N/A	0.37	0.34
1/28-29/24	"AN"	0.79	3.84	3.51	3.39
2/12-14/24	"AO"	0.76	3.25	3.20	3.06
2/18-19/24	N/A	N/A	N/A	0.19	0.17
2/22-23/24	N/A	N/A	N/A	1.00	1.03
2/28-29/24	N/A	0.48	0.86	1.04	0.85
3/2-3/24	N/A	0.56	2.51	2.44	2.30
3/5/24	N/A	0.64	1.83	1.67	1.59
3/9-10/24	"AP"	0.94	3.18	3.25	3.47
3/23-24/24	"AQ"	0.69	3.73	3.57	2.88

3/27-28/24	N/A	0.46	1.57	1.47	1.12
4/1/24	N/A	1.35	2.90	2.51	2.29
4/2/24	N/A	2.13	4.88	4.32	4.59
4/3-4/2024	N/A	1.52	3.25	3.36	2.57
5/4-5/24	N/A	0.48	2.49	2.66	2.11
5/9-10/24	N/A	0.30	0.61	0.39	0.47
5/11-12/24	N/A	0.91	1.27	1.29	1.16
5/14-15/24	"AR"	0.20	0.61	0.91	0.81
5/27-28/24	"AS"	4.72	4.95	5.56	4.55
6/5-6/24	N/A	3.02	3.68	4.62	5.41
6/29-30/24	N/A	1.73	2.36	2.25	1.76
7/12-13/24	N/A	0.91	1.35	1.72	2.23
7/16-17/24	N/A	1.78	2.03	1.31	0.89
7/22-23/24	"AT"	0.20	0.25	0.39	0.28
7/29-30/24	N/A	0.13	0.15	0.70	0.75
7/30-31/24	"AU"	0.25	0.30	0.15	0.01
8/2-3/24	N/A	1.45	1.68	1.25	1.19
8/3-4/24	"AV"	0.89	1.27	1.51	1.88
8/6-7/24	N/A	0.18	0.41	0.51	0.91
8/7-10/24	N/A	2.72	5.00	7.54	8.16
8/16-17/24	N/A	0.13	0.13	0.21	0.27
8/17-18/24	N/A	0.84	0.86	0.65	0.20
8/18-19/24	N/A	2.97	6.58	5.59	3.45
9/17-18/24	N/A	0.18	0.36	0.41	0.35
9/21-22/24	N/A	0.99	1.22	1.08	1.04
9/25/24	N/A	0.18	0.56	0.56	0.36
9/26-27/24	N/A	1.85	3.35	3.34	3.98
9/27-29/24	N/A	0.30	0.56	0.96	0.83
9/30/24	N/A	0.25	0.53	0.49	0.38
10/1-2/24	N/A	0.23	0.69	0.91	1.02
11/10-11/24	"AW"	0.48	1.19	1.08	1.09
11/20-21/24	N/A	1.47	1.85	1.79	1.38
11/22-23/24	N/A	0.13	0.71	0.68	0.68
11/26/24	N/A	0.43	0.48	0.61	0.66
11/27-28/24	N/A	0.56	1.55	1.59	1.49
12/10-12/24	"AX"	1.07	3.20	3.71	4.35
12/15-16/24	N/A	0.38	1.73	1.62	1.65
12/28-30/24	N/A	0.23	1.57	1.89	1.79
12/31/24-1/1/25	N/A	1.14	1.24	1.15	0.91
1/31-2/1/25	"AY"	0.23	1.47	1.40	1.35
2/06-07/25	N/A	N/A	N/A	0.49	0.45
2/12-14/25	"AZ"	N/A	N/A	1.47	1.38
2/15-16/25	"BA"	0.86	2.59	2.57	2.48
3/05-06/25	"BB"	0.71	2.46	2.53	1.89
3/16-17/25	N/A	0.74	1.07	1.34	1.16
3/20-21/25	N/A	0.58	1.12	0.95	0.66
3/31-4/1/25	N/A	1.37	2.01	1.77	1.52
4/4/25	N/A	0.18	0.23	0.22	0.27
4/7/25	N/A	0.46	0.69	0.70	0.80
4/11-12/25	"BC"	0.33	2.06	1.82	1.48

4/25-26/25	N/A	0.64	1.12	1.15	1.16
5/3-5/25	"BD"	1.09	2.29	1.95	1.21
5/8-9/25	N/A	0.56	1.14	1.14	1.22
5/13-15/25	N/A	1.19	6.15	5.78	5.50
5/16/25	N/A	0.51	0.56	0.48	0.24
5/21-22/25	N/A	0.81	1.98	2.35	2.05
6/10/25	N/A	0.38	0.38	0.90	1.37
6/16-17/25	N/A	0.53	2.44	3.01	2.74
6/18-19/25	N/A	1.91	3.33	3.60	3.58
6/19-20/25	N/A	1.80	1.85	1.42	1.42
6/25-26/25	N/A	0.33	0.33	0.34	0.72
6/26-27/25	"BE"	2.84	2.92	3.04	3.91
6/29-30/25	N/A	0.36	0.38	N/A	N/A
7/1-2/25	N/A	1.52	2.36	2.50	2.84
7/8-9/25	N/A	0.81	0.86	2.55	2.77
7/9-11/25	N/A	2.49	3.78	3.22	2.64
7/13-14/25	N/A	2.87	2.97	3.21	2.87
7/14-15/25	"BF"	1.32	1.37	1.22	1.21
7/16-17/25	N/A	0.51	0.74	0.77	1.09
7/19-20/25	N/A	0.99	1.32	1.79	2.79
7/25-26/25	N/A	0.69	0.71	1.43	2.26
7/27-28/25	"BG"	1.40	2.49	1.49	1.53
9/10-11/25	N/A	0.33	0.97	1.34	1.65
9/16-17/25	N/A	0.69	2.57	2.00	2.17
9/23-24/25	N/A	0.46	0.81	0.86	0.29
9/25-26/25	N/A	0.56	0.89	0.75	0.66

[1]Lettered (“A” through “BG”) events were also characterized for water quality (Tables E-4, E-5).

Table E-2. Event hydrologic data for PLBR. “Pilot study”, “early” development, “late” development, and “post” development events shaded in light orange, brown, blue, and green, respectively.

Storm date(s)	Storm ID[1]	Event runoff (cm)	Event peak runoff (cm h^{-1})	Event runoff ratio (-)	Event max new water (%)	Event old water (m)	Event new water (m)	Event baseflow runoff (m)	Event direct runoff (m)
12/9-11/19	"A"	0.390	0.037	0.151	59.5	0.0023	0.0016	0.0018	0.0021
1/25-26/20	"B"	0.910	0.155	0.230	75.5	0.0033	0.0058	0.0024	0.0067
2/06-08/20	"C"	0.559	0.052	0.202	64.2	0.0030	0.0026	0.0020	0.0035
3/13/20	N/A	0.125	0.008	0.197	48.2	0.0007	0.0001	0.0007	0.0006
3/14-15/20	N/A	0.135	0.007	0.161	47.1	0.0012	0.0002	0.0008	0.0005
3/18-19/20	N/A	0.187	0.026	0.123	31.7	0.0022	0.0001	0.0008	0.0011
3/23/20	N/A	0.070	0.005	0.092	N/A	N/A	N/A	0.0004	0.0003
3/25/20	N/A	0.077	0.008	0.119	35.3	0.0007	0.0001	0.0004	0.0004
3/28/20	N/A	0.317	0.058	0.142	68.4	0.0014	0.0018	0.0009	0.0023
4/12-14/20	N/A	1.525	0.175	0.245	85.4	0.0038	0.0114	0.0040	0.0112
4/23-24/20	N/A	0.280	0.025	0.131	54.4	0.0018	0.0010	0.0010	0.0018
4/26-27/20	N/A	0.186	0.016	0.152	50.0	0.0019	0.0007	0.0010	0.0008
4/30-5/1/20	"D"	0.746	0.080	0.242	74.0	0.0029	0.0045	0.0026	0.0049
5/03-04/20	N/A	0.125	0.011	0.160	27.6	0.0011	0.0001	0.0009	0.0004
5/06-07/20	N/A	0.136	0.010	0.129	48.3	0.0012	0.0002	0.0008	0.0005
5/08-09/20	N/A	0.118	0.010	0.172	N/A	N/A	N/A	0.0008	0.0004
5/22/20	N/A	0.071	0.010	0.073	39.2	0.0006	0.0001	0.0003	0.0004
5/23/20	N/A	0.045	0.005	0.119	23.9	0.0004	0.0000	0.0003	0.0001
5/28/20	N/A	0.032	0.003	0.097	43.1	0.0003	0.0000	0.0002	0.0001
6/4-5/20	N/A	0.127	0.013	0.048	N/A	N/A	N/A	0.0004	0.0008
6/10-11/20	N/A	0.153	0.030	0.101	53.1	0.0009	0.0006	0.0004	0.0011
6/20-21/20	N/A	0.889	0.030	0.265	95.0	0.0018	0.0071	0.0020	0.0068
6/22-23/20	N/A	2.460	1.011	0.391	93.5	0.0037	0.0209	0.0059	0.0187
6/30-7/01/20	N/A	0.135	0.020	0.083	59.5	0.0011	0.0003	0.0007	0.0007
7/10-11/20	N/A	0.087	0.009	0.150	72.0	0.0007	0.0001	0.0005	0.0004
7/22-23/20	N/A	0.060	0.004	0.061	50.7	0.0005	0.0001	0.0003	0.0003
7/30-31/20	"E"	0.402	0.109	0.129	88.3	0.0016	0.0024	0.0013	0.0027
8/3-4/20	"F"	1.689	0.301	0.213	87.0	0.0045	0.0124	0.0036	0.0133
8/12-13/20	N/A	0.867	0.273	0.236	88.5	0.0034	0.0052	0.0029	0.0058

8/14-15/20	N/A	1.861	0.664	0.297	86.1	0.0048	0.0135	0.0064	0.0122
8/28-29/20	N/A	0.170	0.025	0.082	N/A	N/A	N/A	0.0004	0.0013
9/03-04/20	N/A	0.324	0.090	0.440	N/A	N/A	N/A	0.0010	0.0022
9/10/20	N/A	0.043	0.010	0.058	73.4	0.0003	0.0001	0.0001	0.0003
9/29-30/20	"G"	0.441	0.096	0.185	78.1	0.0023	0.0021	0.0014	0.0030
10/11-12/20	"H"	0.437	0.061	0.146	53.5	0.0025	0.0018	0.0009	0.0035
10/29-30/20	"J"	1.563	0.232	0.299	77.6	0.0054	0.0102	0.0044	0.0112
11/11-12/20	"K"	1.455	0.148	0.278	67.2	0.0068	0.0077	0.0043	0.0102
11/30-12/1/20	N/A	1.729	0.244	0.398	86.8	0.0043	0.0130	0.0043	0.0130
12/24-25/20	"L"	2.322	0.291	0.548	83.1	0.0084	0.0148	0.0068	0.0164
1/1-2/21	N/A	1.146	0.187	0.373	78.6	0.0040	0.0072	0.0040	0.0075
2/15-16/21	"N"	1.088	0.141	0.404	N/A	N/A	N/A	0.0032	0.0077
3/24-25/21	N/A	1.369	0.260	0.350	N/A	N/A	N/A	0.0042	0.0095
3/31-4/1/21	"Q"	0.786	0.049	0.348	45.4	0.0058	0.0021	0.0031	0.0048
5/28-29/21	"R"	1.218	0.164	0.262	85.7	0.0049	0.0073	0.0036	0.0086
7/17-18/21	"S"	0.383	0.105	0.255	N/A	N/A	N/A	0.0011	0.0027
8/17-19/21	"T"	1.464	0.113	0.264	81.2	0.0072	0.0075	0.0047	0.0099
8/20/21	N/A	0.329	0.055	0.254	51.6	0.0024	0.0009	0.0011	0.0022
9/1/21	"U"	1.657	0.272	0.391	92.5	0.0057	0.0102	0.0032	0.0134
9/23/21	"V"	1.149	0.252	0.400	77.5	0.0052	0.0063	0.0024	0.0091
10/25-26/21	N/A	1.852	0.274	0.304	N/A	N/A	N/A	0.0052	0.0134
10/29-30/21	"W"	3.215	0.543	0.471	85.1	0.0083	0.0238	0.0092	0.0229
1/16-17/22	N/A	0.990	0.160	0.398	N/A	N/A	N/A	0.0020	0.0079
2/2-4/22	"X"	0.771	0.034	0.274	N/A	N/A	N/A	0.0019	0.0058
4/5-6/22	"Y"	0.876	0.116	0.295	N/A	N/A	N/A	0.0019	0.0069
4/18-19/22	N/A	0.671	0.095	0.273	N/A	N/A	N/A	0.0020	0.0047
5/6-8/22	"Z"	3.244	0.207	0.471	76.6	0.0126	0.0198	0.0107	0.0217
5/22-23/22	N/A	0.675	0.125	0.429	70.7	0.0034	0.0029	0.0020	0.0048
5/27-28/22	N/A	1.188	0.295	0.418	88.3	0.0040	0.0073	0.0034	0.0084
6/08-09/22	N/A	0.832	0.103	0.243	85.5	0.0038	0.0040	0.0021	0.0062
6/22-23/22	N/A	0.248	0.035	0.196	63.6	0.0018	0.0004	0.0005	0.0020
7/08-09/22	"AA"	0.376	0.028	0.296	48.2	0.0024	0.0007	0.0009	0.0029
7/18-19/22	N/A	0.157	0.019	0.248	64.4	0.0011	0.0002	0.0005	0.0011
7/31/-8/1/22	N/A	0.079	0.004	0.097	23.9	0.0005	0.0000	0.0003	0.0005
8/04-05/22	N/A	0.156	0.013	0.140	66.2	0.0009	0.0002	0.0004	0.0012
8/05-06/22	N/A	0.224	0.014	0.276	20.9	0.0015	0.0001	0.0007	0.0015

8/14-15/22	N/A	0.044	0.006	0.057	32.8	0.0003	0.0000	0.0001	0.0003
8/17-18/22	N/A	0.089	0.041	0.167	82.1	0.0003	0.0003	0.0002	0.0007
9/5-7/2022	N/A	1.423	0.234	0.227	84.0	0.0067	0.0069	0.0030	0.0112
9/11-12/22	N/A	0.610	0.067	0.296	81.3	0.0030	0.0023	0.0019	0.0042
9/30-10/1/22	N/A	0.361	0.032	0.165	74.9	0.0020	0.0012	0.0007	0.0029
10/02-04/22	N/A	1.492	0.121	0.321	73.6	0.0076	0.0074	0.0048	0.0101
10/04-05/22	N/A	0.353	0.013	0.817	29.2	0.0021	0.0004	0.0035	0.0000
10/13-14/22	N/A	0.540	0.047	0.312	63.9	0.0030	0.0019	0.0014	0.0040
10/17-18/22	N/A	0.222	0.012	0.583	65.2	0.0015	0.0004	0.0010	0.0012
11/11-12/22	"AB"	0.685	0.049	0.290	77.1	0.0037	0.0026	0.0026	0.0043
11/15/16/22	"AC"	1.010	0.133	0.379	70.5	0.0037	0.0058	0.0028	0.0073
11/27/22	N/A	0.094	0.010	0.186	53.7	0.0006	0.0001	0.0005	0.0005
11/30-12/01/22	N/A	0.213	0.011	0.271	47.0	0.0014	0.0004	0.0011	0.0010
12/03-04/22	N/A	0.428	0.036	0.383	65.0	0.0023	0.0015	0.0017	0.0026
12/15-16/22	"AD"	2.621	0.172	0.372	N/A	N/A	N/A	0.0077	0.0185
12/22-23/22	N/A	2.314	0.200	0.458	83.4	0.0064	0.0159	0.0059	0.0172
12/31/22-1/01/23	N/A	0.305	0.017	0.353	N/A	N/A	N/A	0.0013	0.0018
1/05-06/23	N/A	0.109	0.004	0.535	N/A	N/A	N/A	N/A	N/A
1/12-14-23	N/A	0.195	0.008	0.226	N/A	N/A	N/A	0.0011	0.0009
1/19-20/23	N/A	0.147	0.010	0.264	N/A	N/A	N/A	0.0007	0.0008
1/22-24/23	N/A	0.328	0.010	0.315	35.1	0.0027	0.0006	0.0016	0.0017
1/25-26/23	N/A	0.467	0.029	0.354	51.7	0.0031	0.0016	0.0019	0.0027
2/12-14/23	N/A	0.634	0.052	0.257	60.0	0.0035	0.0029	0.0024	0.0040
2/16-18/23	N/A	1.392	0.170	0.378	77.9	0.0056	0.0084	0.0046	0.0093
2/27-28/23	N/A	0.160	0.012	0.191	44.9	0.0013	0.0003	0.0006	0.0010
3/3-4/23	"AE"	0.469	0.059	0.260	61.8	0.0025	0.0022	0.0014	0.0033
3/10-11/23	N/A	0.079	0.004	0.184	30.8	0.0007	0.0001	0.0005	0.0003
3/23-26/23	N/A	0.327	0.015	0.179	64.0	0.0025	0.0008	0.0013	0.0019
4/01-02/23	N/A	0.082	0.005	0.112	26.4	0.0007	0.0001	0.0003	0.0005
4/15-16/23	N/A	0.456	0.089	0.249	85.1	0.0022	0.0024	0.0013	0.0033
4/22-23/23	"AF"	0.311	0.040	0.123	79.3	0.0018	0.0013	0.0009	0.0022
4/28-5/1/23	"AG"	2.692	0.143	0.395	78.7	0.0104	0.0166	0.0105	0.0164
5/13-14/23	N/A	0.192	0.013	0.210	39.8	0.0016	0.0003	0.0009	0.0010
5/20-21/23	N/A	0.098	0.008	0.184	N/A	N/A	N/A	0.0005	0.0005
6/21-24/23	N/A	0.539	0.029	0.241	53.5	0.0049	0.0005	0.0019	0.0035
6/27-28/23	"AH"	0.136	0.027	0.268	73.4	0.0010	0.0003	0.0007	0.0007

6/30-7/1/23	N/A	0.203	0.039	0.222	78.8	0.0015	0.0005	0.0005	0.0015
7/1/23	N/A	0.601	0.070	0.439	90.8	0.0046	0.0020	N/A	N/A
7/14-15/23	N/A	0.358	0.056	0.367	87.4	0.0024	0.0012	0.0016	0.0020
7/21-22/23	N/A	0.894	0.091	0.498	88.2	0.0060	0.0029	0.0033	0.0057
7/24-25/23	N/A	0.515	0.031	0.814	71.5	0.0040	0.0011	0.0030	0.0021
7/28-29/23	N/A	0.840	0.096	0.358	90.9	0.0046	0.0038	0.0033	0.0051
8/6-7/2023	N/A	0.443	0.035	0.238	78.4	0.0028	0.0017	0.0017	0.0027
8/7-8/2023	N/A	1.224	0.216	0.429	91.7	0.0041	0.0081	0.0043	0.0080
8/10-11/23	N/A	0.208	0.010	0.237	19.9	0.0019	0.0002	0.0018	0.0003
9/08-09/23	N/A	0.059	0.026	0.045	78.3	0.0016	0.0003	0.0002	0.0004
9/10-12/23	N/A	1.052	0.113	0.462	85.5	0.0079	0.0027	0.0034	0.0071
9/12-13/23	N/A	1.279	0.242	0.421	86.7	0.0045	0.0083	0.0051	0.0077
9/17-18/23	N/A	0.054	0.005	0.089	30.1	0.0005	0.0000	0.0002	0.0004
9/22-25/23	"AJ"	2.072	0.151	0.379	85.6	0.0089	0.0119	0.0062	0.0145
10/7/23	N/A	0.358	0.040	0.455	N/A	N/A	N/A	N/A	N/A
10/14-15/23	"AK"	0.259	0.033	0.175	78.7	0.0015	0.0011	0.0007	0.0019
11/10-11/23	N/A	0.188	0.009	0.277	38.6	0.0014	0.0002	0.0006	0.0013
11/21-22/23	"AL"	2.178	0.253	0.393	78.6	0.0069	0.0135	0.0057	0.0160
11/26-27/23	N/A	0.128	0.009	0.295	49.3	0.0011	0.0001	0.0007	0.0005
12/1-2/23	N/A	0.059	0.008	0.128	45.6	0.0010	0.0001	0.0003	0.0003
12/3-4/23	N/A	0.562	0.037	0.416	63.4	0.0037	0.0019	0.0021	0.0035
12/10-12/23	"AM"	2.749	0.166	0.584	75.1	0.0108	0.0167	0.0089	0.0186
12/17-18/23	N/A	3.730	0.515	0.479	90.2	0.0068	0.0305	0.0101	0.0272
12/27-28/23	N/A	1.672	0.154	0.509	65.2	0.0084	0.0083	0.0056	0.0111
1/6-7/24	N/A	1.313	0.133	0.579	61.3	0.0080	0.0051	0.0048	0.0084
1/9-10/24	N/A	3.681	0.537	0.551	71.4	0.0162	0.0207	0.0125	0.0243
1/12-13/24	N/A	0.659	0.078	0.402	32.4	0.0053	0.0013	0.0027	0.0039
1/24-27/24	"AN"	0.664	0.015	1.810	N/A	N/A	N/A	0.0024	0.0042
1/28-29/24	"AN"	1.582	0.234	0.451	60.2	0.0081	0.0077	0.0044	0.0114
2/12-14/24	"AO"	0.853	0.098	0.267	50.2	0.0055	0.0030	0.0023	0.0062
2/18-19/24	N/A	0.099	0.003	0.527	N/A	N/A	N/A	0.0010	0.0000
2/22-23/24	N/A	0.284	0.023	0.284	N/A	N/A	N/A	0.0010	0.0018
2/28-29/24	N/A	0.139	0.013	0.134	56.3	0.0012	0.0002	0.0006	0.0008
3/2-3/24	N/A	0.750	0.082	0.307	57.0	0.0043	0.0032	0.0024	0.0051
3/5/24	N/A	0.453	0.053	0.271	43.3	0.0029	0.0016	0.0012	0.0033
3/9-10/24	"AP"	1.138	0.183	0.350	72.5	0.0050	0.0064	0.0040	0.0074

3/23-24/24	"AQ"	0.899	0.124	0.252	69.4	0.0042	0.0048	0.0026	0.0064
3/27-28/24	N/A	0.395	0.036	0.269	41.2	0.0028	0.0011	0.0016	0.0023
4/1/24	N/A	0.880	0.122	0.350	74.5	0.0035	0.0053	0.0020	0.0068
4/2/24	N/A	2.044	0.492	0.473	80.4	0.0069	0.0136	0.0053	0.0151
4/3-4/2024	N/A	2.412	0.387	0.718	N/A	N/A	N/A	0.0122	0.0119
5/4-5/24	N/A	0.716	0.059	0.269	44.9	0.0049	0.0023	0.0018	0.0053
5/9-10/24	N/A	0.173	0.012	0.449	16.5	0.0015	0.0002	0.0009	0.0008
5/11-12/24	N/A	0.467	0.057	0.361	34.4	0.0036	0.0010	0.0017	0.0030
5/14-15/24	"AR"	0.289	0.014	0.317	24.3	0.0026	0.0003	0.0014	0.0015
5/27-28/24	"AS"	2.399	0.628	0.431	90.7	0.0060	0.0180	0.0074	0.0166
6/5-6/24	N/A	2.358	0.532	0.510	85.1	0.0083	0.0153	0.0083	0.0153
6/29-30/24	N/A	0.771	0.106	0.343	69.3	0.0048	0.0029	0.0023	0.0054
7/12-13/24	N/A	0.340	0.052	0.197	74.3	0.0026	0.0007	0.0011	0.0023
7/16-17/24	N/A	0.343	0.059	0.262	86.1	0.0022	0.0012	0.0013	0.0021
7/22-23/24	"AT"	0.036	0.003	0.091	6.5	0.0004	0.0000	0.0002	0.0001
7/29-30/24	N/A	0.030	0.007	0.043	20.0	0.0003	0.0000	0.0001	0.0002
7/30-31/24	"AU"	0.006	0.002	0.042	17.8	0.0001	0.0000	0.0000	0.0000
8/2-3/24	N/A	0.240	0.043	0.193	88.5	0.0015	0.0009	0.0005	0.0019
8/3-4/24	"AV"	0.501	0.097	0.332	76.8	0.0031	0.0019	0.0016	0.0034
8/6-7/24	N/A	0.035	0.005	0.068	18.3	0.0003	0.0000	0.0001	0.0003
8/7-10/24	N/A	2.498	0.334	0.331	77.3	0.0113	0.0137	0.0063	0.0187
8/16-17/24	N/A	0.003	0.000	0.012	N/A	N/A	N/A	0.0000	0.0000
8/17-18/24	N/A	0.072	0.021	0.111	N/A	N/A	N/A	0.0001	0.0006
8/18-19/24	N/A	1.927	0.344	0.345	88.1	0.0053	0.0141	0.0058	0.0134
9/17-18/24	N/A	0.013	0.001	0.032	N/A	N/A	N/A	0.0000	0.0001
9/21-22/24	N/A	0.176	0.035	0.162	82.3	0.0012	0.0005	0.0004	0.0014
9/25/24	N/A	0.025	0.003	0.045	29.4	0.0002	0.0000	0.0001	0.0002
9/26-27/24	N/A	1.025	0.194	0.307	78.4	0.0040	0.0061	0.0023	0.0080
9/27-29/24	N/A	0.112	0.013	0.117	45.7	0.0010	0.0002	0.0005	0.0006
9/30/24	N/A	0.037	0.005	0.076	N/A	N/A	N/A	0.0002	0.0002
10/1-2/24	N/A	0.127	0.011	0.139	N/A	N/A	N/A	0.0006	0.0007
11/10-11/24	"AW"	0.123	0.017	0.114	38.5	0.0012	0.0001	0.0003	0.0010
11/20-21/24	N/A	0.320	0.039	0.178	84.6	0.0021	0.0011	0.0008	0.0024
11/22-23/24	N/A	0.320	0.039	0.471	24.6	0.0006	0.0000	0.0032	0.0000
11/26/24	N/A	0.046	0.006	0.076	67.6	0.0004	0.0001	0.0001	0.0004
11/27-28/24	N/A	0.360	0.038	0.227	66.8	0.0023	0.0013	0.0007	0.0029

12/10-12/24	"AX"	0.941	0.096	0.253	67.2	0.0046	0.0048	0.0030	0.0064
12/15-16/24	N/A	0.493	0.046	0.304	54.7	0.0030	0.0019	0.0010	0.0039
12/28-30/24	N/A	0.515	0.022	0.272	24.5	0.0047	0.0004	0.0019	0.0033
12/31/24-1/1/25	N/A	0.511	0.074	0.444	84.0	0.0029	0.0022	0.0020	0.0031
1/31-2/1/25	"AY"	0.443	0.040	0.317	N/A	N/A	N/A	0.0012	0.0032
2/06-07/25	N/A	0.185	0.015	0.379	N/A	N/A	N/A	0.0008	0.0011
2/12-14/25	"AZ"	0.368	0.018	0.251	N/A	N/A	N/A	0.0015	0.0022
2/15-16/25	"BA"	1.158	0.104	0.451	61.7	0.0075	0.0041	0.0034	0.0082
3/05-06/25	"BB"	0.496	0.041	0.196	64.9	0.0038	0.0011	0.0017	0.0032
3/16-17/25	N/A	0.190	0.021	0.142	53.3	0.0016	0.0003	0.0006	0.0013
3/20-21/25	N/A	0.151	0.018	0.159	49.3	0.0013	0.0002	0.0006	0.0009
3/31-4/1/25	N/A	0.330	0.042	0.186	74.3	0.0023	0.0010	0.0010	0.0023
4/4/25	N/A	0.030	0.002	0.139	N/A	N/A	N/A	0.0002	0.0001
4/7/25	N/A	0.051	0.005	0.073	N/A	N/A	N/A	0.0002	0.0003
4/11-12/25	"BC"	0.249	0.014	0.136	N/A	N/A	N/A	0.0007	0.0018
4/25-26/25	N/A	0.113	0.010	0.099	N/A	N/A	N/A	0.0003	0.0009
5/3-5/25	"BD"	0.494	0.054	0.253	N/A	N/A	N/A	0.0014	0.0036
5/8-9/25	N/A	0.139	0.019	0.121	N/A	N/A	N/A	0.0003	0.0011
5/13-15/25	N/A	2.298	0.241	0.398	N/A	N/A	N/A	0.0068	0.0162
5/16/25	N/A	0.138	0.015	0.288	N/A	N/A	N/A	0.0014	0.0000
5/21-22/25	N/A	0.537	0.046	0.228	N/A	N/A	N/A	0.0018	0.0035
6/10/25	N/A	0.173	0.027	0.193	N/A	N/A	N/A	0.0006	0.0011
6/16-17/25	N/A	0.695	0.053	0.231	N/A	N/A	N/A	0.0024	0.0046
6/18-19/25	N/A	2.675	0.291	0.743	N/A	N/A	N/A	0.0086	0.0182
6/19-20/25	N/A	1.466	0.291	1.029	N/A	N/A	N/A	0.0077	0.0069
6/25-26/25	N/A	0.095	0.006	0.278	N/A	N/A	N/A	0.0002	0.0007
6/26-27/25	"BE"	1.258	0.330	0.414	91.3	0.0043	0.0086	0.0042	0.0084
6/29-30/25	N/A	0.194	0.013	0.508	N/A	N/A	N/A	0.0019	0.0001
7/1-2/25	N/A	0.677	0.066	0.270	84.4	0.0044	0.0024	0.0029	0.0039
7/8-9/25	N/A	0.302	0.043	0.119	N/A	N/A	N/A	0.0007	0.0023
7/9-11/25	N/A	1.596	0.254	0.496	83.9	0.0074	0.0091	0.0060	0.0099
7/13-14/25	N/A	2.743	0.932	0.855	90.7	0.0056	0.0214	0.0086	0.0189
7/14-15/25	"BF"	1.101	0.200	0.902	76.2	0.0061	0.0053	0.0075	0.0035
7/16-17/25	N/A	0.590	0.048	0.770	32.7	0.0051	0.0008	0.0053	0.0006
7/19-20/25	N/A	0.779	0.125	0.436	57.3	0.0049	0.0029	0.0039	0.0039
7/25-26/25	N/A	0.474	0.082	0.331	76.5	0.0030	0.0017	0.0021	0.0027

7/27-28/25	"BG"	0.640	0.055	0.430	72.5	0.0047	0.0017	0.0031	0.0033
9/10-11/25	N/A	0.070	0.014	0.052	36.9	0.0007	0.0000	0.0001	0.0006
9/16-17/25	N/A	0.686	0.080	0.344	74.7	0.0043	0.0026	0.0014	0.0054
9/23-24/25	N/A	0.104	0.024	0.120	62.7	0.0008	0.0002	0.0003	0.0007
9/25-26/25	N/A	0.086	0.019	0.114	69.2	0.0007	0.0002	0.0003	0.0005

[1]Lettered (“A” through “BG”) events were also characterized for water quality (Tables E-4, E-5).

Table E-3. Event hydrologic data for UTLP. “Pilot study”, “early” development, “late” development, and “post” development events shaded in light orange, brown, blue, and green, respectively.

Storm date(s)	Storm ID[1]	Event runoff (cm)	Event peak runoff (cm h^{-1})	Event runoff ratio (-)	Event max new water (%)	Event old water (m)	Event new water (m)	Event baseflow runoff (m)	Event direct runoff (m)
12/9-11/19	"A"	N/A	N/A	N/A	N/A	N/A	N/A	N/A	N/A
1/25-26/20	"B"	N/A	N/A	N/A	N/A	N/A	N/A	N/A	N/A
2/06-08/20	"C"	N/A	N/A	N/A	N/A	N/A	N/A	N/A	N/A
3/13/20	N/A	0.033	0.002	0.059	19.0	0.0002	0.0000	0.0002	0.0001
3/14-15/20	N/A	0.038	0.002	0.055	21.0	0.0004	0.0000	0.0003	0.0001
3/18-19/20	N/A	0.068	0.013	0.053	55.3	0.0006	0.0003	0.0003	0.0004
3/23/20	N/A	0.019	0.002	0.031	13.1	0.0002	0.0000	0.0001	0.0001
3/25/20	N/A	0.027	0.004	0.031	28.9	0.0002	0.0000	0.0001	0.0001
3/28/20	N/A	0.209	0.062	0.098	89.1	0.0006	0.0015	0.0004	0.0017
4/12-14/20	N/A	2.479	0.397	0.384	93.1	0.0038	0.0210	0.0034	0.0214
4/23-24/20	N/A	0.077	0.007	0.038	62.7	0.0005	0.0003	0.0004	0.0004
4/26-27/20	N/A	0.077	0.004	0.061	54.8	0.0009	0.0003	0.0003	0.0004
4/30-5/1/20	"D"	0.292	0.036	0.112	71.6	0.0013	0.0016	0.0010	0.0019
5/03-04/20	N/A	0.072	0.003	0.120	27.6	0.0007	0.0000	0.0006	0.0001
5/06-07/20	N/A	0.078	0.003	0.093	29.6	0.0007	0.0001	0.0006	0.0002
5/08-09/20	N/A	0.072	0.004	0.115	29.1	0.0007	0.0001	0.0006	0.0002
5/22/20	N/A	0.033	0.003	0.040	24.4	0.0003	0.0000	0.0002	0.0002
5/23/20	N/A	0.032	0.002	0.074	13.5	0.0003	0.0000	0.0002	0.0001
5/28/20	N/A	0.030	0.001	0.198	3.4	0.0003	0.0000	0.0002	0.0001
6/4-5/20	N/A	0.076	0.004	0.043	31.8	0.0007	0.0001	0.0005	0.0003
6/10-11/20	N/A	0.069	0.005	0.047	49.4	0.0005	0.0002	0.0003	0.0004
6/20-21/20	N/A	0.093	0.005	0.040	69.5	0.0005	0.0004	0.0004	0.0006
6/22-23/20	N/A	2.648	1.371	0.483	90.3	0.0046	0.0219	0.0044	0.0221
6/30-7/01/20	N/A	0.151	0.021	0.095	N/A	N/A	N/A	0.0008	0.0007
7/10-11/20	N/A	0.066	0.003	0.447	N/A	N/A	N/A	0.0005	0.0002
7/22-23/20	N/A	0.071	0.005	0.101	4.2	0.0007	0.0000	0.0004	0.0003
7/30-31/20	"E"	0.181	0.018	0.058	43.3	0.0014	0.0004	0.0005	0.0013
8/3-4/20	"F"	1.187	0.325	0.150	90.0	0.0036	0.0083	0.0019	0.0100
8/12-13/20	N/A	1.115	0.701	0.287	88.7	0.0030	0.0079	0.0029	0.0083

8/14-15/20	N/A	1.756	0.889	0.219	N/A	N/A	N/A	0.0044	0.0132
8/28-29/20	N/A	0.121	0.007	0.057	N/A	N/A	N/A	0.0007	0.0005
9/03-04/20	N/A	0.101	0.026	0.133	N/A	N/A	N/A	0.0004	0.0006
9/10/20	N/A	0.012	0.001	0.044	N/A	N/A	N/A	0.0001	0.0000
9/29-30/20	"G"	0.027	0.002	0.011	16.5	0.0003	0.0000	0.0001	0.0001
10/11-12/20	"H"	0.123	0.033	0.043	50.4	0.0009	0.0004	0.0002	0.0010
10/29-30/20	"J"	0.604	0.154	0.138	74.5	0.0025	0.0035	0.0012	0.0048
11/11-12/20	"K"	0.504	0.072	0.099	74.6	0.0024	0.0026	0.0010	0.0041
11/30-12/1/20	N/A	1.439	0.540	0.385	93.4	0.0032	0.0112	0.0023	0.0121
12/24-25/20	"L"	1.800	0.777	0.472	74.1	0.0072	0.0108	0.0032	0.0148
1/1-2/21	N/A	0.671	0.170	0.232	74.7	0.0028	0.0037	0.0019	0.0048
2/15-16/21	"N"	0.591	0.103	0.230	N/A	N/A	N/A	0.0013	0.0046
3/24-25/21	N/A	0.490	0.086	0.160	N/A	N/A	N/A	0.0015	0.0034
3/31-4/1/21	"Q"	0.329	0.020	0.138	22.7	0.0032	0.0001	0.0014	0.0019
5/28-29/21	"R"	0.420	0.054	0.098	64.2	0.0026	0.0016	0.0010	0.0032
7/17-18/21	"S"	0.660	0.218	0.234	N/A	N/A	N/A	0.0013	0.0053
8/17-19/21	"T"	0.368	0.035	0.070	49.5	0.0023	0.0016	0.0009	0.0028
8/20/21	N/A	0.057	0.014	0.050	37.3	0.0005	0.0001	0.0002	0.0003
9/1/21	"U"	0.495	0.155	0.134	85.1	0.0023	0.0030	0.0006	0.0043
9/23/21	"V"	0.644	0.279	0.220	86.1	0.0021	0.0043	0.0009	0.0056
10/25-26/21	N/A	1.092	0.295	0.165	N/A	N/A	N/A	0.0023	0.0086
10/29-30/21	"W"	3.381	1.067	0.500	92.1	0.0043	0.0295	0.0052	0.0286
1/16-17/22	N/A	0.527	0.116	0.212	N/A	N/A	N/A	0.0012	0.0041
2/2-4/22	"X"	0.279	0.012	0.114	N/A	N/A	N/A	0.0009	0.0018
4/5-6/22	"Y"	0.400	0.075	0.143	47.5	0.0027	0.0013	0.0009	0.0031
4/18-19/22	N/A	0.251	0.031	0.107	55.8	0.0018	0.0008	0.0010	0.0016
5/6-8/22	"Z"	1.209	0.129	0.193	86.0	0.0042	0.0079	0.0036	0.0085
5/22-23/22	N/A	0.249	0.045	0.134	73.4	0.0015	0.0009	0.0011	0.0014
5/27-28/22	N/A	1.294	0.614	0.421	94.1	0.0024	0.0106	0.0031	0.0098
6/08-09/22	N/A	0.243	0.040	0.071	63.3	0.0016	0.0009	0.0010	0.0014
6/22-23/22	N/A	0.088	0.005	0.062	22.1	0.0008	0.0001	0.0006	0.0003
7/08-09/22	"AA"	0.074	0.004	0.068	24.5	0.0007	0.0001	0.0004	0.0004
7/18-19/22	N/A	0.052	0.002	0.147	6.9	0.0005	0.0000	0.0004	0.0001
7/31/-8/1/22	N/A	0.036	0.001	0.042	4.7	0.0004	0.0000	0.0002	0.0001
8/04-05/22	N/A	0.039	0.003	0.040	11.6	0.0003	0.0000	0.0003	0.0001
8/05-06/22	N/A	0.070	0.017	0.067	41.4	0.0006	0.0002	0.0003	0.0004

8/14-15/22	N/A	0.015	0.001	0.023	3.7	0.0002	0.0000	0.0001	0.0000
8/17-18/22	N/A	0.025	0.001	0.076	4.1	0.0003	0.0000	0.0002	0.0000
9/5-7/2022	N/A	0.524	0.202	0.086	N/A	N/A	N/A	0.0011	0.0041
9/11-12/22	N/A	0.165	0.014	0.071	N/A	N/A	N/A	0.0008	0.0008
9/30-10/1/22	N/A	0.063	0.005	0.032	41.0	0.0005	0.0001	0.0003	0.0003
10/02-04/22	N/A	0.270	0.045	0.062	N/A	N/A	N/A	0.0008	0.0019
10/04-05/22	N/A	0.071	0.003	0.216	N/A	N/A	N/A	0.0005	0.0002
10/13-14/22	N/A	0.137	0.015	0.059	64.4	0.0009	0.0001	0.0006	0.0008
10/17-18/22	N/A	0.107	0.008	0.233	32.0	0.0009	0.0001	0.0007	0.0004
11/11-12/22	"AB"	0.150	0.021	0.067	46.0	0.0011	0.0004	0.0008	0.0007
11/15/16/22	"AC"	0.306	0.056	0.114	79.3	0.0013	0.0018	0.0011	0.0020
11/27/22	N/A	0.049	0.003	0.096	3.9	0.0005	0.0000	0.0003	0.0001
11/30-12/01/22	N/A	0.113	0.005	0.153	17.9	0.0011	0.0001	0.0007	0.0004
12/03-04/22	N/A	0.152	0.014	0.127	51.9	0.0012	0.0003	0.0008	0.0007
12/15-16/22	"AD"	1.003	0.096	0.155	66.9	0.0044	0.0057	0.0024	0.0076
12/22-23/22	N/A	1.036	0.155	0.227	86.2	0.0029	0.0075	0.0023	0.0080
12/31/22-1/01/23	N/A	0.126	0.004	0.160	N/A	N/A	N/A	0.0010	0.0003
1/05-06/23	N/A	0.091	0.002	0.720	N/A	N/A	N/A	N/A	N/A
1/12-14-23	N/A	0.147	0.003	0.214	N/A	N/A	N/A	0.0011	0.0004
1/19-20/23	N/A	0.100	0.004	0.172	N/A	N/A	N/A	0.0007	0.0003
1/22-24/23	N/A	0.178	0.004	0.195	17.1	0.0017	0.0001	0.0011	0.0006
1/25-26/23	N/A	0.164	0.007	0.124	35.1	0.0014	0.0003	0.0009	0.0008
2/12-14/23	N/A	0.245	0.017	0.107	61.3	0.0018	0.0007	0.0013	0.0011
2/16-18/23	N/A	0.648	0.181	0.170	80.2	0.0030	0.0035	0.0023	0.0041
2/27-28/23	N/A	0.127	0.004	0.152	22.3	0.0012	0.0001	0.0011	0.0002
3/3-4/23	"AE"	0.272	0.054	0.129	70.9	0.0016	0.0011	0.0012	0.0015
3/10-11/23	N/A	0.127	0.003	0.417	6.1	0.0012	0.0000	0.0011	0.0002
3/23-26/23	N/A	0.294	0.006	0.173	34.8	0.0026	0.0003	0.0019	0.0010
4/01-02/23	N/A	0.117	0.003	0.128	6.9	0.0011	0.0000	0.0009	0.0003
4/15-16/23	N/A	0.148	0.016	0.080	N/A	N/A	N/A	0.0009	0.0006
4/22-23/23	"AF"	0.093	0.012	0.055	45.7	0.0011	0.0002	0.0006	0.0003
4/28-5/1/23	"AG"	0.691	0.034	0.107	N/A	N/A	N/A	0.0028	0.0041
5/13-14/23	N/A	0.115	0.005	0.129	N/A	N/A	N/A	0.0009	0.0003
5/20-21/23	N/A	0.092	0.005	0.173	N/A	N/A	N/A	0.0008	0.0002
6/21-24/23	N/A	0.080	0.002	0.036	N/A	N/A	N/A	0.0005	0.0003
6/27-28/23	"AH"	0.021	0.001	0.116	N/A	N/A	N/A	0.0002	0.0000

6/30-7/1/23	N/A	0.029	0.004	0.031	N/A	N/A	N/A	0.0001	0.0002
7/1/23	N/A	0.027	0.004	0.026	N/A	N/A	N/A	0.0001	0.0001
7/14-15/23	N/A	0.018	0.001	0.032	N/A	N/A	N/A	0.0002	0.0000
7/21-22/23	N/A	0.030	0.007	0.021	54.3	0.0002	0.0001	0.0001	0.0002
7/24-25/23	N/A	0.023	0.002	0.042	28.6	0.0002	0.0000	0.0001	0.0001
7/28-29/23	N/A	0.080	0.032	0.030	70.2	0.0004	0.0004	0.0002	0.0006
8/6-7/2023	N/A	0.031	0.003	0.016	42.0	0.0003	0.0001	0.0001	0.0002
8/7-8/2023	N/A	0.189	0.110	0.060	80.6	0.0007	0.0012	0.0005	0.0014
8/10-11/23	N/A	0.027	0.001	0.029	5.5	0.0003	0.0000	0.0003	0.0000
9/08-09/23	N/A	0.021	0.001	0.028	9.4	0.0002	0.0000	0.0001	0.0001
9/10-12/23	N/A	0.619	0.196	0.167	82.8	0.0018	0.0043	0.0013	0.0049
9/12-13/23	N/A	0.488	0.202	0.157	86.5	0.0016	0.0034	0.0019	0.0029
9/17-18/23	N/A	0.050	0.001	0.082	3.0	0.0005	0.0000	0.0004	0.0001
9/22-25/23	"AJ"	0.379	0.061	0.073	70.8	0.0020	0.0018	0.0013	0.0025
10/7/23	N/A	0.107	0.030	0.086	N/A	N/A	N/A	N/A	N/A
10/14-15/23	"AK"	0.076	0.005	0.056	N/A	N/A	N/A	0.0005	0.0003
11/10-11/23	N/A	0.231	0.006	0.333	N/A	N/A	N/A	0.0017	0.0006
11/21-22/23	"AL"	0.677	0.177	0.123	89.6	0.0019	0.0046	0.0016	0.0051
11/26-27/23	N/A	0.067	0.001	0.159	N/A	N/A	N/A	0.0007	0.0000
12/1-2/23	N/A	0.032	0.002	0.075	N/A	N/A	N/A	0.0003	0.0000
12/3-4/23	N/A	0.151	0.009	0.110	52.8	0.0009	0.0003	0.0008	0.0007
12/10-12/23	"AM"	0.569	0.057	0.131	73.8	0.0025	0.0032	0.0017	0.0040
12/17-18/23	N/A	5.173	1.083	0.672	94.0	0.0054	0.0463	0.0086	0.0431
12/27-28/23	N/A	0.507	0.078	0.178	84.3	0.0023	0.0028	0.0018	0.0032
1/6-7/24	N/A	0.452	0.060	0.191	66.1	0.0026	0.0019	0.0019	0.0026
1/9-10/24	N/A	3.965	1.111	0.638	93.8	0.0066	0.0331	0.0068	0.0328
1/12-13/24	N/A	0.317	0.052	0.179	84.2	0.0020	0.0011	0.0021	0.0011
1/24-27/24	"AN"	0.264	0.004	0.766	N/A	N/A	N/A	0.0017	0.0009
1/28-29/24	"AN"	0.966	0.211	0.285	65.4	0.0067	0.0029	0.0023	0.0074
2/12-14/24	"AO"	0.407	0.049	0.133	36.9	0.0032	0.0008	0.0018	0.0022
2/18-19/24	N/A	0.099	0.002	0.572	N/A	N/A	N/A	0.0009	0.0000
2/22-23/24	N/A	0.126	0.007	0.123	N/A	N/A	N/A	0.0009	0.0004
2/28-29/24	N/A	0.098	0.004	0.116	N/A	N/A	N/A	0.0008	0.0002
3/2-3/24	N/A	0.277	0.032	0.120	N/A	N/A	N/A	0.0011	0.0017
3/5/24	N/A	0.146	0.018	0.092	34.2	0.0012	0.0003	0.0006	0.0008
3/9-10/24	"AP"	0.732	0.205	0.211	69.2	0.0036	0.0038	0.0023	0.0050

3/23-24/24	"AQ"	0.358	0.003	0.124	62.0	0.0021	0.0014	0.0014	0.0021
3/27-28/24	N/A	0.162	0.009	0.145	35.9	0.0014	0.0002	0.0012	0.0004
4/1/24	N/A	0.391	0.096	0.171	70.6	0.0018	0.0021	0.0009	0.0030
4/2/24	N/A	2.351	1.250	0.512	85.0	0.0053	0.0182	0.0035	0.0200
4/3-4/2024	N/A	1.673	0.591	0.652	82.3	0.0051	0.0105	0.0067	0.0100
5/4-5/24	N/A	0.178	0.012	0.085	40.0	0.0015	0.0003	0.0009	0.0009
5/9-10/24	N/A	0.112	0.003	0.240	3.9	0.0011	0.0000	0.0010	0.0001
5/11-12/24	N/A	0.140	0.017	0.121	41.8	0.0012	0.0002	0.0010	0.0004
5/14-15/24	"AR"	0.104	0.003	0.128	11.9	0.0010	0.0000	0.0009	0.0001
5/27-28/24	"AS"	1.270	0.844	0.279	81.0	0.0037	0.0090	0.0024	0.0103
6/5-6/24	N/A	1.926	0.818	0.356	87.0	0.0044	0.0148	0.0032	0.0161
6/29-30/24	N/A	0.094	0.021	0.053	59.6	0.0006	0.0003	0.0004	0.0006
7/12-13/24	N/A	0.054	0.011	0.024	48.7	0.0004	0.0001	0.0002	0.0003
7/16-17/24	N/A	0.017	0.001	0.020	3.4	0.0002	0.0000	0.0002	0.0000
7/22-23/24	"AT"	0.019	0.000	0.069	1.9	0.0002	0.0000	0.0002	0.0000
7/29-30/24	N/A	0.019	0.002	0.026	13.1	0.0001	0.0000	0.0001	0.0001
7/30-31/24	"AU"	0.017	0.001	2.253	13.9	0.0001	0.0000	0.0001	0.0001
8/2-3/24	N/A	0.052	0.025	0.044	61.0	0.0003	0.0002	0.0001	0.0004
8/3-4/24	"AV"	0.127	0.059	0.067	88.2	0.0004	0.0007	0.0004	0.0009
8/6-7/24	N/A	0.051	0.004	0.057	39.6	0.0004	0.0001	0.0003	0.0002
8/7-10/24	N/A	1.204	0.505	0.148	89.9	0.0031	0.0089	0.0020	0.0101
8/16-17/24	N/A	0.034	0.001	0.124	N/A	N/A	N/A	0.0003	0.0001
8/17-18/24	N/A	0.023	0.001	0.112	N/A	N/A	N/A	0.0000	0.0002
8/18-19/24	N/A	0.235	0.065	0.068	78.9	0.0011	0.0014	0.0007	0.0017
9/17-18/24	N/A	0.015	0.000	0.043	N/A	N/A	N/A	0.0001	0.0000
9/21-22/24	N/A	0.027	0.003	0.026	N/A	N/A	N/A	0.0001	0.0001
9/25/24	N/A	0.020	0.001	0.056	N/A	N/A	N/A	0.0001	0.0001
9/26-27/24	N/A	0.338	0.124	0.085	79.5	0.0013	0.0022	0.0007	0.0027
9/27-29/24	N/A	0.080	0.003	0.097	17.6	0.0006	0.0000	0.0006	0.0002
9/30/24	N/A	0.030	0.001	0.079	N/A	N/A	N/A	0.0003	0.0000
10/1-2/24	N/A	0.070	0.003	0.068	15.7	0.0007	0.0000	0.0005	0.0002
11/10-11/24	"AW"	0.092	0.006	0.084	4.7	0.0009	0.0000	0.0005	0.0004
11/20-21/24	N/A	0.124	0.022	0.090	33.7	0.0010	0.0002	0.0006	0.0007
11/22-23/24	N/A	0.074	0.002	0.109	11.7	0.0007	0.0000	0.0006	0.0001
11/26/24	N/A	0.034	0.002	0.052	7.0	0.0003	0.0000	0.0003	0.0001
11/27-28/24	N/A	0.128	0.017	0.085	43.3	0.0010	0.0003	0.0006	0.0007

12/10-12/24	"AX"	0.595	0.305	0.137	80.6	0.0024	0.0035	0.0014	0.0045
12/15-16/24	N/A	0.119	0.011	0.072	56.5	0.0009	0.0003	0.0007	0.0005
12/28-30/24	N/A	0.135	0.005	0.075	14.6	0.0013	0.0001	0.0007	0.0006
12/31/24-1/1/25	N/A	0.128	0.021	0.141	50.5	0.0010	0.0003	0.0006	0.0007
1/31-2/1/25	"AY"	0.144	0.013	0.106	N/A	N/A	N/A	0.0007	0.0008
2/06-07/25	N/A	0.100	0.006	0.220	N/A	N/A	N/A	0.0007	0.0003
2/12-14/25	"AZ"	0.153	0.008	0.111	N/A	N/A	N/A	0.0009	0.0006
2/15-16/25	"BA"	0.368	0.108	0.149	N/A	N/A	N/A	0.0010	0.0027
3/05-06/25	"BB"	0.137	0.011	0.072	23.4	0.0013	0.0001	0.0007	0.0007
3/16-17/25	N/A	0.076	0.002	0.066	4.2	0.0008	0.0000	0.0006	0.0002
3/20-21/25	N/A	0.072	0.004	0.109	9.3	0.0007	0.0000	0.0006	0.0002
3/31-4/1/25	N/A	0.088	0.011	0.058	35.1	0.0008	0.0001	0.0005	0.0004
4/4/25	N/A	0.030	0.002	0.113	3.5	0.0003	0.0000	0.0002	0.0001
4/7/25	N/A	0.028	0.002	0.035	4.9	0.0003	0.0000	0.0002	0.0001
4/11-12/25	"BC"	0.059	0.002	0.040	13.7	0.0006	0.0000	0.0004	0.0002
4/25-26/25	N/A	0.050	0.003	0.043	N/A	N/A	N/A	0.0003	0.0002
5/3-5/25	"BD"	0.069	0.004	0.057	N/A	N/A	N/A	0.0004	0.0003
5/8-9/25	N/A	0.046	0.003	0.038	N/A	N/A	N/A	0.0003	0.0001
5/13-15/25	N/A	0.728	0.274	0.132	N/A	N/A	N/A	0.0015	0.0058
5/16/25	N/A	0.033	0.002	0.137	N/A	N/A	N/A	N/A	N/A
5/21-22/25	N/A	0.075	0.006	0.037	N/A	N/A	N/A	0.0005	0.0003
6/10/25	N/A	0.028	0.004	0.021	21.4	0.0003	0.0000	0.0002	0.0001
6/16-17/25	N/A	0.078	0.008	0.028	49.4	0.0006	0.0002	0.0003	0.0004
6/18-19/25	N/A	0.497	0.214	0.139	73.9	0.0019	0.0030	0.0010	0.0039
6/19-20/25	N/A	0.350	0.193	0.247	76.4	0.0017	0.0020	0.0014	0.0021
6/25-26/25	N/A	0.036	0.001	0.050	7.7	0.0002	0.0000	0.0000	0.0003
6/26-27/25	"BE"	1.607	1.012	0.411	86.6	0.0034	0.0128	0.0028	0.0133
6/29-30/25	N/A	0.072	0.002	0.190	N/A	N/A	N/A	0.0003	0.0004
7/1-2/25	N/A	0.170	0.034	0.060	64.7	0.0012	0.0005	0.0008	0.0009
7/8-9/25	N/A	0.068	0.007	0.024	35.9	0.0005	0.0001	0.0002	0.0005
7/9-11/25	N/A	0.467	0.130	0.177	79.1	0.0021	0.0026	0.0016	0.0031
7/13-14/25	N/A	1.334	0.747	0.465	87.5	0.0029	0.0104	0.0031	0.0103
7/14-15/25	"BF"	0.364	0.133	0.301	73.2	0.0018	0.0015	0.0027	0.0010
7/16-17/25	N/A	0.158	0.010	0.145	33.4	0.0014	0.0002	0.0015	0.0001
7/19-20/25	N/A	0.317	0.114	0.114	75.0	0.0018	0.0014	0.0015	0.0016
7/25-26/25	N/A	0.146	0.045	0.064	65.4	0.0010	0.0005	0.0008	0.0006

7/27-28/25	"BG"	0.152	0.021	0.100	55.9	0.0012	0.0003	0.0009	0.0006
9/10-11/25	N/A	0.042	0.004	0.025	15.9	0.0004	0.0000	0.0003	0.0002
9/16-17/25	N/A	0.153	0.018	0.070	68.1	0.0009	0.0007	0.0004	0.0011
9/23-24/25	N/A	0.042	0.001	0.144	N/A	N/A	N/A	0.0004	0.0001
9/25-26/25	N/A	0.053	0.001	0.080	4.4	0.0005	0.0000	0.0004	0.0002

[1]Lettered ("A" through "BG") events were also characterized for water quality (Tables E-4, E-5).

Table E-4. *EMC* results for PLBR. "Pilot study", "early" development, "late" development, and "post" development events shaded in light orange, brown, blue, and green, respectively.

Storm date (beginning)	Storm ID	TSS (mg/L)	SC (µS)	Cl (mg/L)	IC-NO_3-N (mg/L)	SO_4 (mg/L)	TP (mg/L)	TN (mg/L)	TDP (mg/L)	TDN (mg/L)
12/9/2019	A	22.28	292.28	51.73	0.59	10.96	0.11	0.97	0.05	0.89
1/25/2020	B	133.37	166.56	29.87	0.45	4.07	0.19	0.96	0.06	0.77
2/5/2020	C	37.34	278.80	46.91	0.57	8.59	0.09	1.00	0.03	0.91
4/30/2020	D	42.32	190.25	24.13	0.27	4.92	0.14	1.23	0.04	0.85
7/30/2020	E	204.42	189.89	29.27	0.64	6.78	0.75	2.21	0.10	1.25
8/3/2020	F	80.35	130.23	14.52	0.37	3.64	0.22	1.09	0.10	0.82
9/29/2020	G	57.30	267.41	41.29	0.43	6.13	0.35	1.17	0.05	0.74
10/11/2020	H	30.98	343.86	53.37	0.30	7.88	0.21	0.78	0.05	0.59
10/29/2020	J	89.68	186.39	25.28	0.40	4.73	0.41	1.30	0.14	0.92
11/11/2020	K	21.33	236.24	32.50	0.18	6.37	0.17	0.94	0.10	0.73
12/24/2020	L	116.05	197.40	34.15	0.38	4.52	0.20	1.18	0.05	0.63
2/15/2021	N	101.03	711.79	180.94	0.67	8.46	0.16	1.49	0.02	1.03
3/31/2021	Q	18.38	409.12	75.26	0.51	9.92	0.06	1.15	0.03	1.06
5/28/2021	R	66.08	200.61	30.49	0.25	3.94	0.17	1.15	0.05	0.76
7/17/2021	S	187.92	314.04	59.28	0.51	8.80	0.47	1.75	0.05	1.04
8/17/2021	T	13.75	243.30	35.87	0.38	5.63	0.12	0.84	0.07	0.74
9/1/2021	U	42.77	157.64	22.78	0.66	5.74	0.24	1.44	0.13	1.22
9/23/2021	V	86.60	160.25	22.33	0.42	4.36	0.27	1.22	0.12	0.96
10/29/2021	W	96.06	105.44	12.79	0.45	3.49	0.32	1.32	0.16	0.94
2/2/2022	X	12.63	797.00	204.64	0.85	13.12	0.07	1.40	0.04	1.25
4/5/2022	Y	83.44	269.75	48.96	0.38	6.21	0.16	1.30	0.05	0.99
5/6/2022	Z	65.15	194.13	25.81	0.27	4.54	0.14	1.06	0.05	0.84
7/9/2022	AA	16.47	407.28	69.73	0.50	7.78	0.11	1.01	0.05	0.92
11/11/2022	AB	31.97	280.84	46.98	0.22	14.44	0.22	0.95	0.12	0.64
11/15/2022	AC	90.85	188.22	28.70	0.47	8.43	0.32	1.29	0.11	0.92
12/15/2022	AD	60.89	182.11	29.35	0.52	5.99	0.21	1.13	0.08	0.88
3/3/2023	AE	52.47	274.50	41.45	0.68	9.53	0.15	1.49	0.04	1.27
4/22/2023	AF	72.32	295.64	44.86	0.56	9.58	0.48	2.84	0.15	1.61
4/28/2023	AG	57.01	194.17	23.24	0.27	5.59	0.19	1.20	0.06	0.80
6/27/2023	AH	22.58	286.27	41.68	0.49	8.57	0.13	1.18	0.04	0.89
9/23/2023	AJ	13.00	250.70	25.94	0.32	28.64	0.11	0.89	0.07	0.82

10/14/2023	AK	26.82	359.23	55.06	0.65	22.57	0.12	1.12	0.06	1.00
11/21/2023	AL	161.92	196.43	24.56	0.46	14.33	0.48	1.50	0.16	0.93
12/10/2023	AM	40.46	183.72	21.54	0.33	11.63	0.18	1.05	0.10	0.87
1/28/2024	AN	104.93	452.25	105.93	0.43	7.90	0.20	1.07	0.05	0.81
2/12/2024	AO	59.63	322.64	62.33	0.47	9.28	0.15	1.07	0.04	0.80
3/9/2024	AP	97.30	220.39	33.18	0.36	6.70	0.22	1.14	0.05	0.76
3/23/2024	AQ	55.14	238.64	38.44	0.40	7.53	0.16	1.11	0.05	0.84
5/14/2024	AR	7.63	492.30	83.45	0.73	14.87	0.06	1.21	0.03	1.11
5/27/2024	AS	264.07	117.90	14.31	0.32	3.16	0.45	1.64	0.08	0.81
7/22/2024	AT	12.91	549.88	88.80	0.70	9.61	0.11	1.08	0.02	0.96
7/30/2024	AU	14.13	479.83	75.57	0.77	11.66	0.09	1.38	0.03	1.17
8/3/2024	AV	111.87	264.84	37.44	0.32	9.47	0.44	1.40	0.07	0.97
11/10/2024	AW	5.83	515.55	90.77	0.42	19.64	0.13	0.91	0.08	0.81
12/11/2024	AX	73.06	232.18	32.73	0.44	10.24	0.33	1.21	0.06	0.84
1/31/2025	AY	30.08	1321.75	345.29	0.80	14.32	0.12	1.48	0.03	1.33
2/12/2025	AZ	4.28	1190.23	287.64	0.91	18.37	0.03	1.18	0.02	1.15
3/5/2025	BB	44.51	431.57	80.54	0.61	12.27	0.12	1.31	0.03	1.09
4/11/2025	BC	4.60	481.10	81.10	0.60	13.36	0.05	0.94	0.02	0.88
5/3/2025	BD	30.41	360.55	55.88	0.20	6.69	0.15	1.00	0.04	0.64
6/26/2025	BE	232.51	171.54	23.23	0.45	4.43	0.58	1.57	0.06	0.99
7/27/2025	BG	38.91	314.34	47.02	0.37	6.25	0.20	0.97	0.06	0.77

Table E-4 (continued).

Storm date (beginning)	Storm ID	PP (mg/L)	PN (mg/L)	PO_4-P (mg/L)	NH_4-N (mg/L)	NO_2-N (mg/L)	FIA-NO_3-N (mg/L)	DON (mg/L)	SOC-P (mg/L)	Turbidity (NTU)
12/9/2019	A	0.06	0.08	0.04	0.02	0.01	0.60	0.26	0.01	N/A
1/25/2020	B	0.12	0.20	0.05	0.03	0.01	0.44	0.29	0.02	N/A
2/5/2020	C	0.06	0.10	0.02	0.02	0.01	0.60	0.29	0.01	N/A
4/30/2020	D	0.10	0.38	0.02	0.02	0.00	0.29	0.53	0.02	N/A
7/30/2020	E	0.65	0.96	0.10	0.12	0.04	0.67	0.42	0.01	N/A
8/3/2020	F	0.13	0.26	0.09	0.02	0.01	0.36	0.43	0.01	N/A
9/29/2020	G	0.29	0.43	0.03	0.01	0.01	0.44	0.28	0.02	N/A
10/11/2020	H	0.16	0.18	0.03	0.00	0.00	0.29	0.30	0.01	N/A
10/29/2020	J	0.26	0.39	0.11	0.01	0.01	0.38	0.51	0.03	N/A
11/11/2020	K	0.07	0.21	0.08	0.01	0.00	0.20	0.52	0.02	N/A
12/24/2020	L	0.14	0.44	0.04	0.01	0.01	0.38	0.27	0.01	N/A
2/15/2021	N	0.14	0.47	0.01	0.05	0.01	0.72	0.25	0.01	N/A
3/31/2021	Q	0.03	0.09	0.02	0.03	0.01	0.53	0.50	0.01	N/A
5/28/2021	R	0.12	0.39	0.03	0.01	0.01	0.29	0.46	0.02	N/A
7/17/2021	S	0.41	0.71	0.03	0.07	0.04	0.50	0.44	0.02	N/A
8/17/2021	T	0.05	0.10	0.04	0.01	0.01	0.21	0.51	0.02	N/A
9/1/2021	U	0.11	0.22	0.11	0.06	0.02	0.60	0.54	0.02	N/A
9/23/2021	V	0.15	0.26	0.10	0.03	0.01	0.41	0.51	0.02	N/A
10/29/2021	W	0.16	0.38	0.13	0.01	0.01	0.44	0.49	0.03	N/A
2/2/2022	X	0.03	0.15	0.03	0.08	0.01	0.83	0.33	0.01	N/A
4/5/2022	Y	0.12	0.31	0.04	0.06	0.01	0.38	0.54	0.01	N/A
5/6/2022	Z	0.09	0.22	0.03	0.04	0.01	0.27	0.53	0.02	N/A
7/9/2022	AA	0.06	0.09	0.03	0.06	0.01	0.49	0.36	0.02	N/A
11/11/2022	AB	0.11	0.31	0.11	0.01	0.00	0.21	0.42	0.01	N/A
11/15/2022	AC	0.22	0.37	0.10	0.02	0.01	0.46	0.43	0.01	N/A
12/15/2022	AD	0.13	0.26	0.08	0.03	0.01	0.49	0.35	0.01	N/A
3/3/2023	AE	0.11	0.21	0.03	0.10	0.01	0.70	0.47	0.01	N/A
4/22/2023	AF	0.33	1.24	0.10	0.08	0.02	0.55	0.96	0.05	N/A
4/28/2023	AG	0.14	0.40	0.03	0.02	0.01	0.28	0.49	0.02	N/A
6/27/2023	AH	0.08	0.30	0.03	0.01	0.01	0.50	0.36	0.02	N/A
9/23/2023	AJ	0.03	0.06	0.06	0.02	0.00	0.34	0.46	0.02	N/A
10/14/2023	AK	0.06	0.12	0.05	0.02	0.01	0.73	0.25	0.01	N/A

11/21/2023	AL	0.32	0.57	0.14	0.01	0.00	0.47	0.45	0.02	121.0
12/10/2023	AM	0.09	0.18	0.08	0.02	0.01	0.34	0.51	0.02	35.2
1/28/2024	AN	0.15	0.28	0.03	0.03	0.01	0.44	0.33	0.01	128.6
2/12/2024	AO	0.10	0.28	0.02	0.03	0.01	0.48	0.28	0.02	58.9
3/9/2024	AP	0.17	0.38	0.03	0.03	0.01	0.38	0.35	0.02	115.8
3/23/2024	AQ	0.11	0.28	0.03	0.03	0.01	0.41	0.39	0.02	51.7
5/14/2024	AR	0.03	0.10	0.01	0.05	0.01	0.80	0.26	0.01	8.3
5/27/2024	AS	0.37	0.83	0.06	0.04	0.01	0.34	0.41	0.02	247.1
7/22/2024	AT	0.09	0.13	0.01	0.02	0.01	0.69	0.24	0.01	12.5
7/30/2024	AU	0.07	0.21	0.02	0.01	0.01	0.89	0.26	0.01	13.2
8/3/2024	AV	0.36	0.42	0.04	0.02	0.02	0.47	0.46	0.03	91.9
11/10/2024	AW	0.05	0.10	0.07	0.01	0.01	0.49	0.31	0.01	8.3
12/11/2024	AX	0.26	0.37	0.05	0.02	0.01	0.47	0.35	0.01	86.5
1/31/2025	AY	0.08	0.14	0.02	0.14	0.01	0.87	0.31	0.01	34.4
2/12/2025	AZ	0.02	0.03	0.01	0.03	0.01	0.95	0.17	0.01	6.1
3/5/2025	BB	0.09	0.22	0.02	0.04	0.01	0.69	0.35	0.02	36.8
4/11/2025	BC	0.03	0.06	0.01	0.01	0.00	0.60	0.27	0.01	7.1
5/3/2025	BD	0.11	0.36	0.02	0.03	0.01	0.22	0.39	0.02	24.7
6/26/2025	BE	0.52	0.58	0.04	0.09	0.02	0.44	0.45	0.02	241.0
7/27/2025	BG	0.14	0.19	0.03	0.03	0.01	0.40	0.34	0.03	32.4

Table E-5. *EMC* results for UTLP. "Pilot study", "early" development, "late" development, and "post" development events shaded in light orange, brown, blue, and green, respectively.

Storm date (beginning)	Storm ID	TSS (mg/L)	SC (µS)	Cl (mg/L)	IC-NO_3-N (mg/L)	SO_4 (mg/L)	TP (mg/L)	TN (mg/L)	TDP (mg/L)	TDN (mg/L)
12/9/2019	A	N/A	N/A	N/A	N/A	N/A	N/A	N/A	N/A	N/A
1/25/2020	B	N/A	N/A	N/A	N/A	N/A	N/A	N/A	N/A	N/A
2/5/2020	C	N/A	N/A	N/A	N/A	N/A	N/A	N/A	N/A	N/A
4/30/2020	D	312.37	203.01	27.89	0.38	6.94	0.16	1.52	0.03	0.92
7/30/2020	E	59.59	433.18	72.77	1.03	13.66	0.08	1.67	0.01	1.41
8/3/2020	F	589.37	182.22	24.82	0.66	6.52	0.33	1.75	0.08	1.12
9/29/2020	G	26.73	399.41	61.35	0.82	12.81	0.07	1.28	0.02	1.10
10/11/2020	H	199.15	252.59	36.90	0.83	8.76	0.19	1.97	0.09	1.41
10/29/2020	J	94.45	272.52	40.77	0.54	9.19	0.15	1.54	0.07	1.31
11/11/2020	K	185.09	225.37	42.02	0.50	4.78	0.19	1.37	0.05	0.78
12/24/2020	L	31.21	493.92	105.60	0.71	10.95	0.06	1.37	0.03	1.26
2/15/2021	N	167.41	295.82	51.34	0.75	7.42	0.18	1.92	0.05	1.38
3/31/2021	Q	75.45	311.21	51.49	0.74	8.97	0.16	1.65	0.10	1.49
5/28/2021	R	279.25	192.72	26.66	1.92	6.16	0.47	3.42	0.21	2.69
7/17/2021	S	417.19	236.70	30.52	1.08	7.19	0.24	2.27	0.13	1.98
8/17/2021	T	187.85	107.42	12.27	0.44	3.31	0.29	1.50	0.13	1.02
9/1/2021	U	162.93	360.00	71.92	0.73	8.46	0.16	1.73	0.04	1.29
9/23/2021	V	174.70	248.30	38.47	0.59	8.41	0.22	1.88	0.05	1.35
10/29/2021	W	4.25	501.75	97.10	1.20	16.05	0.03	1.34	0.02	1.33
2/2/2022	X	52.76	409.29	61.24	0.61	11.35	0.16	1.41	0.05	1.10
4/5/2022	Y	37.11	234.19	37.43	0.75	10.11	0.20	2.22	0.13	2.04
5/6/2022	Z	49.25	214.72	38.85	0.75	5.86	0.17	1.42	0.09	1.19
7/9/2022	AA	133.26	316.06	54.90	0.90	11.15	0.18	1.85	0.03	1.32
11/11/2022	AB	55.69	278.87	39.64	0.59	8.41	0.14	1.65	0.04	1.27
11/15/2022	AC	56.09	239.77	28.26	0.46	9.12	0.19	1.39	0.10	1.14
12/15/2022	AD	3.24	560.18	103.48	1.15	16.67	0.02	1.35	0.01	1.28
3/3/2023	AE	126.53	781.04	237.80	0.91	7.88	0.12	1.71	0.03	1.36
4/22/2023	AF	1211.76	148.95	19.57	1.10	5.55	0.79	3.36	0.07	1.66
4/28/2023	AG	26.36	808.77	209.51	1.10	13.51	0.06	1.62	0.03	1.50
6/27/2023	AH	14.99	437.53	74.22	0.89	13.80	0.09	1.81	0.02	1.49
9/23/2023	AJ	N/A	N/A	N/A	N/A	N/A	N/A	N/A	N/A	N/A

10/14/2023	AK	2.95	554.98	102.33	0.97	15.06	0.02	1.19	0.01	1.18
11/21/2023	AL	117.71	216.92	31.60	0.84	7.70	0.30	1.94	0.10	1.36
12/10/2023	AM	32.03	213.75	29.16	0.47	7.31	0.15	1.40	0.08	1.10
1/28/2024	AN	54.03	417.47	90.96	0.63	8.22	0.12	1.26	0.04	0.99
2/12/2024	AO	363.01	219.84	35.82	0.40	4.69	0.36	1.85	0.05	0.95
3/9/2024	AP	66.31	282.47	48.99	0.65	8.01	0.15	1.83	0.04	1.43
3/23/2024	AQ	2.24	500.83	91.51	1.12	17.36	0.02	1.39	0.01	1.35
5/14/2024	AR	1045.85	158.14	19.99	0.94	5.09	0.85	3.54	0.05	1.52
5/27/2024	AS	1.83	556.28	101.97	1.20	17.47	0.02	1.45	0.01	1.43
7/22/2024	AT	119.25	198.40	23.60	1.69	6.58	0.31	2.97	0.12	2.46
7/30/2024	AU	3.64	549.22	98.12	0.66	17.55	0.03	1.00	0.01	0.89
8/3/2024	AV	245.02	344.78	55.36	1.13	10.84	0.42	2.89	0.07	1.71
11/10/2024	AW	34.66	523.85	106.23	0.99	13.66	0.06	1.61	0.02	1.50
12/11/2024	AX	2.61	544.12	98.13	1.03	16.60	0.02	1.32	0.01	1.30
1/31/2025	AY	213.76	138.26	14.24	0.82	4.21	0.34	2.10	0.15	1.55
2/12/2025	AZ	31.17	353.60	57.85	1.11	11.54	0.12	1.77	0.06	1.59
3/5/2025	BB	242.15	452.42	109.30	0.39	5.36	0.21	1.29	0.05	0.81
4/11/2025	BC	22.73	949.30	233.61	1.11	14.34	0.06	1.73	0.02	1.59
5/3/2025	BD	4.05	2368.67	660.76	1.16	18.42	0.02	1.49	0.01	1.46
6/26/2025	BE	0.94	506.36	90.20	0.88	15.76	0.02	1.17	0.01	1.16
7/27/2025	BG	4.65	536.17	95.26	0.75	14.74	0.02	1.06	0.01	0.99

Table E-5 (continued).

Storm date (beginning)	Storm ID	PP (mg/L)	PN (mg/L)	PO_4-P (mg/L)	NH_4-N (mg/L)	NO_2-N (mg/L)	FIA-NO_3-N (mg/L)	DON (mg/L)	SOC-P (mg/L)	Turbidity (NTU)
12/9/2019	A	N/A	N/A	N/A	N/A	N/A	N/A	N/A	N/A	N/A
1/25/2020	B	N/A	N/A	N/A	N/A	N/A	N/A	N/A	N/A	N/A
2/5/2020	C	N/A	N/A	N/A	N/A	N/A	N/A	N/A	N/A	N/A
4/30/2020	D	0.13	0.60	0.03	0.03	0.01	0.40	0.49	0.01	N/A
7/30/2020	E	0.07	0.26	0.01	0.03	0.01	1.14	0.23	0.01	N/A
8/3/2020	F	0.25	0.63	0.07	0.02	0.01	0.67	0.42	0.01	N/A
9/29/2020	G	0.05	0.19	0.02	0.00	0.00	0.83	0.26	0.01	N/A
10/11/2020	H	0.10	0.56	0.07	0.01	0.01	0.84	0.55	0.02	N/A
10/29/2020	J	0.08	0.23	0.05	0.01	0.01	0.63	0.66	0.02	N/A
11/11/2020	K	0.15	0.59	0.04	0.02	0.01	0.50	0.32	0.01	N/A
12/24/2020	L	0.04	0.10	0.01	0.01	0.01	0.73	0.52	0.02	N/A
2/15/2021	N	0.13	0.54	0.03	0.01	0.01	0.78	0.57	0.02	N/A
3/31/2021	Q	0.07	0.16	0.07	0.02	0.01	0.65	0.81	0.03	N/A
5/28/2021	R	0.26	0.73	0.19	0.13	0.02	1.76	0.79	0.02	N/A
7/17/2021	S	0.11	0.29	0.11	0.02	0.01	1.13	0.82	0.02	N/A
8/17/2021	T	0.16	0.47	0.10	0.01	0.01	0.45	0.56	0.03	N/A
9/1/2021	U	0.12	0.44	0.03	0.04	0.01	0.71	0.54	0.01	N/A
9/23/2021	V	0.17	0.53	0.02	0.06	0.01	0.57	0.72	0.03	N/A
10/29/2021	W	0.01	0.01	0.01	0.01	0.00	1.11	0.20	0.01	N/A
2/2/2022	X	0.11	0.31	0.04	0.01	0.00	0.62	0.46	0.01	N/A
4/5/2022	Y	0.07	0.18	0.12	0.07	0.01	0.75	1.22	0.01	N/A
5/6/2022	Z	0.08	0.23	0.08	0.02	0.01	0.70	0.46	0.01	N/A
7/9/2022	AA	0.15	0.53	0.02	0.04	0.01	0.87	0.41	0.01	N/A
11/11/2022	AB	0.10	0.37	0.02	0.03	0.01	0.61	0.62	0.02	N/A
11/15/2022	AC	0.09	0.25	0.07	0.01	0.01	0.49	0.64	0.03	N/A
12/15/2022	AD	0.01	0.07	0.01	0.00	0.00	1.23	0.05	0.01	N/A
3/3/2023	AE	0.09	0.35	0.02	0.06	0.01	1.04	0.26	0.01	N/A
4/22/2023	AF	0.72	1.69	0.05	0.03	0.03	1.09	0.51	0.02	N/A
4/28/2023	AG	0.04	0.12	0.01	0.03	0.01	1.09	0.38	0.01	N/A
6/27/2023	AH	0.07	0.31	0.00	0.11	0.02	0.93	0.43	0.01	N/A
9/23/2023	AJ	N/A	N/A	N/A	N/A	N/A	N/A	N/A	N/A	N/A
10/14/2023	AK	0.01	0.02	0.01	0.01	0.00	1.02	0.15	0.01	N/A

11/21/2023	AL	0.20	0.58	0.08	0.01	0.01	0.85	0.50	0.02	111.1
12/10/2023	AM	0.06	0.30	0.06	0.01	0.01	0.48	0.60	0.02	33.9
1/28/2024	AN	0.09	0.27	0.02	0.03	0.01	0.63	0.33	0.02	59.0
2/12/2024	AO	0.32	0.90	0.03	0.05	0.01	0.42	0.48	0.02	318.5
3/9/2024	AP	0.11	0.40	0.03	0.06	0.01	0.67	0.69	0.02	64.5
3/23/2024	AQ	0.01	0.05	0.00	0.01	0.01	1.23	0.10	0.01	2.4
5/14/2024	AR	0.80	2.02	0.03	0.02	0.02	1.00	0.49	0.01	920.4
5/27/2024	AS	0.01	0.02	0.01	0.01	0.00	1.36	0.05	0.01	1.5
7/22/2024	AT	0.19	0.51	0.11	0.02	0.01	1.98	0.45	0.01	111.7
7/30/2024	AU	0.02	0.11	0.01	0.01	0.00	0.74	0.14	0.01	2.8
8/3/2024	AV	0.36	1.18	0.05	0.01	0.01	1.23	0.46	0.01	153.5
11/10/2024	AW	0.04	0.10	0.00	0.02	0.01	1.14	0.34	0.01	49.2
12/11/2024	AX	0.01	0.02	0.00	0.01	0.00	1.04	0.25	0.01	4.34
1/31/2025	AY	0.19	0.54	0.12	0.06	0.02	0.78	0.69	0.02	157.5
2/12/2025	AZ	0.06	0.18	0.05	0.02	0.01	1.22	0.34	0.01	28.1
3/5/2025	BB	0.16	0.48	0.03	0.03	0.01	0.41	0.37	0.02	222.6
4/11/2025	BC	0.04	0.14	0.01	0.05	0.01	1.19	0.34	0.01	30.1
5/3/2025	BD	0.01	0.03	0.00	0.02	0.01	1.24	0.20	0.01	4.3
6/26/2025	BE	0.01	0.02	0.01	0.02	0.00	1.00	0.14	0.01	1.1
7/27/2025	BG	0.01	0.07	0.00	0.01	0.01	0.80	0.18	0.01	4.5